Università degli Studi di Padova

Head Office: Università degli Studi di Padova

Department: Surgical, Oncological and Gastroenterological Sciences

Ph.D. COURSE IN: CLINICAL AND EXPERIMENTAL ONCOLOGY AND IMMUNONOLGY

SERIES: XXII

THESIS TITLE

DISSECTION OF THE MICROENVIRONMENT ROLE IN T-LARGE GRANULAR LYMPHOCYTE LEUKEMIA

Coordinator: Prof. Paola Zanovello

Supervisor: Prof. Gianpietro Semenzato

Co-Supervisors: Dr. Renato Zambello and Dr. Antonella Teramo

Ph.D. student : Cristina Vicenzetto

a.a. 2018/2019

Table of Contents

I List of Tables

II List of Figures

III List of Abbreviations

ADAM17: ADAM metallopeptidase domain 17

AICD: Activation-Induced Cell Death

ANC: Absolute Neutrophil Count

ANKL: Aggressive NK Leukemia

APC: Antigen Presenting Cells

AU: Arbitrary Units

BM: Bone Marrow

CCL: C-C Motif Chemokine Ligand

CCR: C-C Motif Chemokine Receptor

CD: Cluster of Differentiation

cDNA: complementary DNA

CLPD-NK: Chronic Lymphoproliferative Disorders of NK cells

CMML: Chronic Myelomonocytic Leukemia

CTL: Cytotoxic T Lymphocyte

CTX: Cyclophosphamide

CXCR: C-X-C Motif Chemokine Receptor

CyA: Cyclosporine A

DBD: DNA Binding Domain

DC: Dendritic Cells

ddCt: delta-delta threshold Cycle

DNA: Deoxyribonucleic Acid

EAE: Experimental Autoimmune Encephalomyelitis

ELISA: Enzyme-Linked Immunosorbent Assay

Erk: Extracellular signal–Regulated Kinases

FACS: Fluorescently Activated Cell Sorter

FasL: Fas Ligand

FcγR: Fcγ Receptor

FI: Fold Increase

FMO: Fluorescence Minus One

FoxP3: Factor forkhead box P3

GM-CSF: Granulocytes-Macrophage Colony Stimulating Factor

HC: Healthy Controls

IFN: Interferon

IgG: Immunoglobulin G

IL: Interleukin

IL-R: Interleukin Receptor

IQR: Interquartile Range

IRF: Interferon Regulatory Factor

LGL: Large Granular Lymphocytes

LGLL: Large Granular Lymphocytes Leukemia

LPS: Lipopolysaccharide

mAb: monoclonal Antibody

MHC: Major Histocompatibility Complex

mRNA: messenger RNA

MSC: Mesenchymal Stromal Cells

NFkB: kappa-light-chain-enhancer of activated B cells

NK: Natural Killer

p: protein

PB: Peripheral Blood

PBMC: Peripheral Blood Mononuclear Cells

PCR: Polymerase Chain Reaction

PDGF: Platelet-Derived Growth Factor

Pts: Patients

RA: Rheumatoid Arthritis

RORγT: RAR-related Orphan Receptor gamma T

RNA: Ribonucleic Acid

rpm: rotations per minute

RT: room temperature

RT-qPCR: Reverse Transcriptase-Quantitative PCR

S: Serine

SASP: Senescence Associated Secretory Phenotype

SLE: Systemic Lupus Erythematosus

STAT: Signal Transducer and Activator of Transcription

T: Threonine

TCR: T Cell Receptor

Tg: Transgenic

TGF: Tissue Growth Factor

Th17: T helper 17

TLR: Toll Like Receptor

TNF: Tumour Necrosis Factor

TME: Tumour Microenvironment

Treg: T regulatory

u-: unphosphorylated

WB: Western Blot

WBC: White Blood Cells

WHO: World Health Organization

w/o: without

wt: wild type

Y: Tyrosine

1 Abstract

T Large granular lymphocytes leukemia (T-LGLL) is a rare lymphoproliferative disorder characterized by the clonal expansion of T-LGL. According to the expression on the leukemic clone of CD8- (CD8+ T-LGLL) and CD4-related determinants (CD4+ T-LGLL) two main groups of patients are identified. Somatic mutations are involved in T-LGLL pathogenesis; they have been identified in genes that are central for the survival of the leukemic clone and are differently distributed among the patients. *STAT3* mutations characterize CD8+ T-LGLL cases with a discrete immunophenotype (i.e. $CD16^{+}/CD56^{-}$) and correlate with neutropenia, which represents the most relevant clinical manifestation in T-LGLL. On the other hand, *STAT5b* mutations can be observed in CD4+ patients, usually characterized by an indolent disease. The leukemic clone survival is mediated by several deregulated pathways that are likely under the control of external stimuli. Indeed, several pro-inflammatory cytokines are increased in patients' plasma, including CCL5 and IL-6. This latter cytokine has been demonstrated to sustain LGL survival *via* STAT3 activation.

The role of soluble factors have been described in the pathogenesis of T-LGLL, but no data are up to now available on the cellular compartment of the microenvironment. For this reason we studied the involvement of tumour microenvironment (TME) cells and we found that: a) monocytes are central for leukemic LGL survival; b) leukemic cells belonging to CD8+ and CD4+ T-LGLL patients take advantage from different TME-mediated survival mechanisms.

In CD8+ patients, particularly in cases with severe neutropenia, monocytes were altered in their population distribution, with an increase of intermediate and non-classical monocytes; in addition Th17/Treg ratio was found to be higher than in healthy controls, due to an increased Th17 cells percentage. Since these two features were associated with a high pro-inflammatory stimulus and correlated with the presence of concurrent autoimmune diseases, which are often reported in T-LGLL, we suggest that a strong peripheral blood inflammation is ongoing in CD8+ neutropenic patients. All these data taking together, we propose that a network takes place between LGL, monocytes and Th17 cells in CD8+ neutropenic patients. In detail, we identified that the CCL5 produced by the leukemic clone specifically stimulates the expression of IL-6 in monocytes, a cytokine that in turn is mandatory for the survival of the leukemic clone and for Th17 cells differentiation. We also reported that the above described alterations of cell subsets were partially reverted after immunosuppressive therapy, suggesting a putative role of these drugs as TME modifiers.

A pro-inflammatory environment with different features was present in CD4+-LGLL patients, who were characterized by an indolent course of the disease. Similarly to CD8+ patients, they expressed a high Th17/Treg ratio, but the imbalance in this setting is sustained by a reduction of Treg cells. CD4+ LGLL patients were also found to be characterized by a peculiar over-activation of Erk in monocytes, which was reported to

be indicative of Senescence Associated Secretory Phenotype (SASP), mostly composed of pro-inflammatory cytokines. Our data obtained through cytokines arrays demonstrated an overall higher level of plasma soluble factors in CD4+ patients than healthy controls, in particular soluble CD14 and Lymphotactin, which could account for TME cellular imbalances of these cases.

This study emphasizes the role of inflammatory background occurring in the TME of T-LGLL patients pointing to newly reported differences between T-LGLL sub-types. In particular in symptomatic patients, we identified a putative network between TME cells and leukemic LGL, which could help defining new targets to design innovative strategies.

2 Introduction

2.1 Peripheral blood mononuclear cells

2.1.1 Large Granular Lymphocytes

Large Granular Lymphocytes (LGL) belong to the lymphoid lineage of hematopoietic cells and are mature post-thymic lymphocytes. In normal adults, LGL account for 5% to 15% of peripheral blood mononuclear cells (PBMC) and their normal absolute count is around 0.2-0.4 $x10^9/L$[1]. These cells are characterized by a distinct morphology (fig. 1): large size (15-18 µm), round or reniform nucleus and an abundant cytoplasm with typical azurophilic granules. The granules contain cytolytic components, such as perforin and granzymes B, a cytotoxic equipment that allows LGL to provide cytotoxic functions and, therefore, to play a central role in cell-mediated immune response[2].

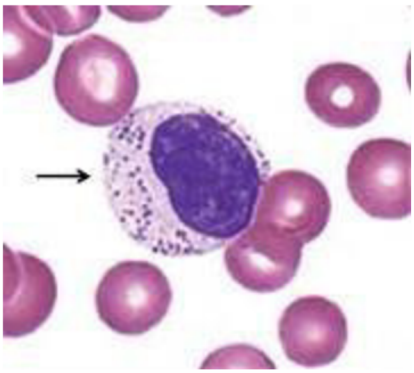

Figure 1: LGL morphology. The arrow points a LGL stained with ematoxilin-eosin from a blood smear.

LGL are divided into two different lineages, based on the expression of cluster of differentiation (CD)3, the co-receptor of the T cell receptor (TCR): CD3+ cells, i.e. cytotoxic T lymphocytes and CD3- cells, i.e. natural killer cells [3,4]. Physiologically, 85% of LGL in peripheral blood (PB) belong to the NK lineage, which represents the main component of innate immune system and mediates the major histocompatibility complex (MHC) not-restricted cytotoxicity. The remaining 15% are cytotoxic T lymphocytes (CTL), which are the cytotoxic cells of the adaptive immune system and mediate MHC-restricted cytotoxicity after TCR stimulation[5]. LGL activation depends on antigen recognition, which leads to an approximately 50,000-fold increase of proliferation of these cells. They exert their cytotoxic action by the release of the granules: perforin can generate holes in the plasma membrane of the target cell and granzyme B is able to induce apoptosis by cleaving cytoplasmatic caspases. Moreover, activated LGL express Fas-ligand (L), which binds the ubiquitous expressed Fas and induces their apoptosis[6]. In physiological conditions, upon antigen clearance, activated LGL are then eliminated through a process known as activation-induced cell death (AICD), which represents an important mechanism for the maintenance of immune

homeostasis. Since LGL do not undergo apoptosis efficiently, an impairment of AICD process allows the maintenance of cytotoxic clones, leading to the development of a malignant condition, referred to as Large Granular Lymphocytes Leukemia[7].

2.1.2 Monocytes

Monocytes were firstly introduced in the mid-nineteenth century by Paul Ehrlich, who defined the cells with a kidney shaped nucleus as "transitional cell". The term "monocyte" was proposed in 1910 and till the 70s it was thought that most of the resident macrophages differentiate from circulating monocytes. Technological advances, such as single-cell transcriptomics, subsequently pointed out that most resident macrophages are able of self-renewal and do not derive from circulating monocytes[8].

2.1.2.1 Monocytes classification

The advent of flow cytometric analyses contributed to disentangle monocytes heterogeneity. Monocytes can be phenotypically classified in three categories: classic, intermediate and non-classical[9].

This classification is based on the surface expression of the lipopolysaccharide (LPS) receptor CD14, also known as Toll-like receptor (TLR) 4, and CD16, the low-affinity immunoglobulin (Ig)G receptor Fcγ III involved in the antibody-dependent cellular cytotoxicity[10]. Classic monocytes are the most frequent type, up to 90% of the total monocytes, and they are defined by a high surface expression of CD14 and the absence of CD16 ($CD14^{++}/CD16^{-}$)[11]. The remaining 10% is shared between the intermediate and non-classical monocytes, characterized by high CD14 and low CD16 expression ($CD14^{++}/CD16^{+}$), and by a low/negative CD14 and a high CD16 expression ($CD14^{\pm}/CD16^{++}$), respectively[12].

Recently, it has been proposed to update the classification based on surface marker expression to a continuum of monocyte phenotypes, a definition already well accepted for macrophages[13]. These hypotheses are also supported by the gene expression profile analysis, because the intermediate monocytes are proposed as a continuum of maturation between classic and non-classical[11]. Moreover, by human *in-vivo* deuterium labelling, it has been demonstrated that classic monocytes are released from the bone marrow (BM) and remain in the blood stream up to 24 hours before they die, or migrate or differentiate in intermediate monocytes, since their deuterium integration is detected after 72 hours of injection. In the end, intermediate monocytes might differentiate in non-classical monocytes because their deuterium peak is reached at 7 days post-injection. This different potential has been also demonstrated in a xenograft model of human classical monocytes into humanized mice[14].

The three categories of monocytes were also proven to be highly heterogeneous. RNA sequencing evidenced that intermediate monocytes are the most heterogeneous[15]. Therefore, different molecular features can be exploited to identify and characterize the

three monocytes subtypes named above (fig.2).

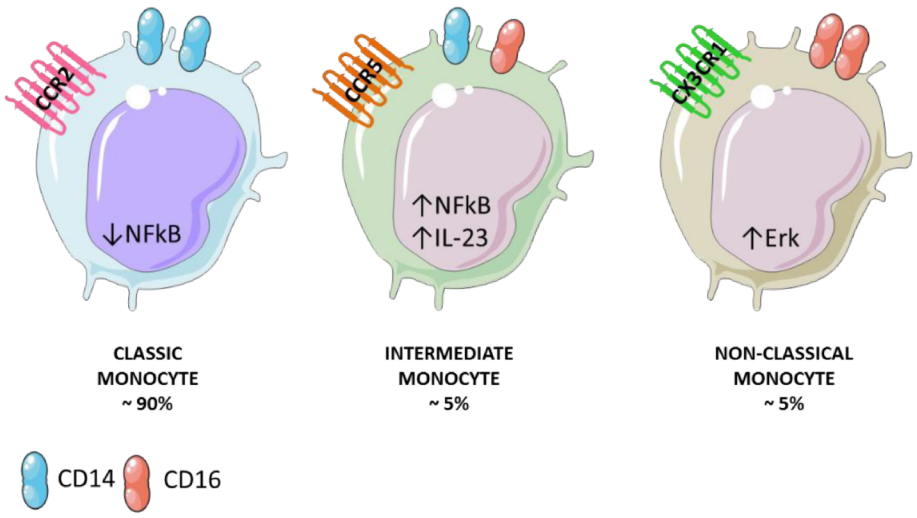

Figure 2: Three different classes of monocytes. The cartoon reports the three classes of monocytes with their respective biological peculiarities regarding surface receptors expression, signaling activation and percentage.

2.1.2.1.1 Classic monocytes

Classic monocytes are transient cells that remain in the blood stream approximately 24 hours after the release from the bone marrow and then they can repopulate a fraction of resident macrophages in several body districts, as demonstrated in several mouse models, or they can convert in non-classical monocytes[16]. Moreover, Classical monocytes are defined as the principal source of dendritic cells (DC)[12].

From the phenotypical point of view classic monocytes differ from the other two subtypes for the specific expression of C-C domain chemokine receptor type (CCR)2[17], which is mandatory for BM egression[18], C-X-C domain chemokine receptor type (CXCR)1, CXCR2 and interleukin-13 receptor α1 (IL-13R α1)[11]. Moreover, they also express the highest level of sensing receptor genes and genes involved in tissue repair and immune response. Classical monocytes are the "less differentiated and most proliferative" among the three types because their expression profile is enriched in anti-apoptotic genes.[11] They are also different for their cytokine secretion and differential potential: upon TLRs stimulation, they have been reported to be the best tumour necrosis factor (TNF) α, IL-6 and IL-1β producers. This aspect however is still controversial, because also non-classical monocytes have been reported to strongly induce IL-1β and TNFα expression. These discrepancies are likely to be related to different methods and reagents used[11,12,19].

It has been demonstrated that heterogeneity is present within classical monocytes by single-cell expression profiling: a sub-group results less activated due to the lower expression of nuclear factor kappa-light-chain-enhancer of activated B cells (NFkB) complex, interferon regulatory factor (IRF) 8 and several cytokines, including IL-1β,

IL-12A, IL-15 and IL-23A[20].
Taking together, these features underline that classic monocytes are involved in inflammation after infection, antibacterial activity and phagocytosis, which are confirmed also by the generation of a transcriptomic network and proteomic studies[21,22].

2.1.2.1.2 Intermediate monocytes

Intermediate monocytes are proposed to be the intersectional link from classic to non-classical monocytes and they are indeed the most heterogeneous subgroup[11,15]. They have an enriched expression of MHC II processing genes, a high expression of CD40 and co-stimulatory factors, underlining a strong potential of antigen presentation and a major T lymphocytes stimulatory function[11,20]. Moreover, their exclusive expression of CCR5 makes intermediate monocytes also recruiters of DCs[20]. A high expression of IRF5, IRF8, NFkB1 and protein (p)65, all involved in NFkB signaling, have also been detected in this monocytes class, as compared to other monocytes. Moreover, some cytokines are more produced by this group of monocytes, including IL-1β, IL-12A, IL-18 and IL-23A; therefore intermediate monocytes contribute to Th1 and Th17 differentiation.
The expression profile of the intermediate monocytes is closer to the non-classical profile than to the classic one[19]. Despite this similarity, and in contrast with non-classical monocytes which produce TNFα, when intermediate monocytes are stimulated by LPS, they induce IL-10 underlining an anti-inflammatory potential[19].

2.1.2.1.3 Non-classical monocytes

Non-classical monocytes are the most differentiated and less proliferative cells as demonstrated by the high expression of pro-apoptotic genes and Cyclin-dependent kinase inhibitor 1C (CDNK1C), a potent cell cycle inhibitor[11]. They patrol vasculature[23] responding to viral infection and to damaged cells and they are the best cytokines producers in these settings[21]. Moreover, an enrichment of genes involved in cytoskeleton rearrangement and of genes linked to the complement activation and adhesion, such as Integrin alpha L (ITGAL) and Siglec10, has been identified[11]. Non-classical monocytes do not express CCR2 and down-modulate typical classic monocytes markers, the receptor more sensitive to migratory stimuli being CX3CR1[11,21]. An upregulation of a metalloprotease, referred to ADAM metallopeptidase domain 17 (ADAM17), has been identified, which is involved in the processing of TNF, which is, in turn, also upregulated[20].
The inflammatory behaviour of the non-classical monocytes is also mediated by cellular senescence and these cells are the most important producers of the senescence-associated secretory phenotype SASP, which defines the secretion of pro-inflammatory cytokines by senescent cells, via the activation of NFkB[24]. This category has the highest

expression of micro-RNA (mir)146a and Erk activation, the lowest expression of the protein expressed by proliferating cells Ki67, the shortest telomere length and an impairment in the respiratory chain[24].

2.1.2.2 Alteration of the monocytes physiology

An altered distribution of monocytes can be found in several pathological conditions. It has been reported that CD16+ monocytes reach a peak after the acute myocardial infarction, being a negative prediction of myocardial salvage. Increased CD16+ monocytes are also associated with atherosclerosis, as they correlate with dyslipidemia and they can be induced by statin treatment[25]. Moreover, the induction of CD16 on monocytes is related to cardiovascular risk in diabetes[26].
Deregulation in monocytes distribution has been evidenced in several autoimmune diseases, which are indeed often correlated with chronic inflammatory stimuli. For instance, in rheumatoid arthritis (RA) the increase of the intermediate monocytes correlates with the high level of IL-17 in plasma. Since Th17 lymphocytes are important for RA pathogenesis, also a role for intermediate monocytes has been postulated in this disease[27] and their high presence during methotrexate treatment has been proposed as a negative predictor[25]. On the other hand, the clinical impact of the monocyte physiology is controversial. An example rests on the role of non-classical monocytes in systemic lupus erythematosus (SLE), since they are reported to be reduced and less functional, but they can also harbour a deregulated pattern of expression in genes linked to chronic immune stimulation, feature even identified in classical monocytes.

Classic monocytes can be altered in different conditions: in chronic myelomonocytic leukemia (CMML) the increased percentage of classical monocytes is a useful tool to discriminate between CMML, reactive monocytosis and myeloid malignancies in patients with a borderline monocyte count. Furthermore, classic monocytes have aberrant expression of CD56, CD62L and CD115 and a down-regulation of Human Leukocyte Antigen-DR isotype (HLA-DR)[28].

Upon aging, people become more susceptible to infection, less responsive to vaccines and have a higher incidence of cancer and cardiovascular diseases; this phenomenon is associated to an age-associated decline of the immune system, defined as immunosenescence which is associated to a low-grade inflammation[29]. In this context, the three categories of monocytes do not present a different transcriptional signature, but they have a lower cytokines expression than young subjects [interferon (IFN)-α for classic and IFN-γ for non-classical monocytes], upon TLRs stimulation[19]. This reduction might lead to an impaired migration of the immune cells towards the infection site, explaining the worse outcome for old patients[19]. Moreover, non-classical monocytes derived from old subjects show a higher CX3CR1 expression, leading to a potential increased recruitment to inflamed sites, which can be a risk factor for the development of chronic inflammatory disease for this category of people[19]. In elderly,

the absolute count of non-classical monocytes is higher as compared to young subjects and they have been also demonstrated to secrete a higher basal level of SASP, as TNFα and IL-8[24].

2.1.3 Th17 lymphocytes and T regulatory cells

2.1.3.1 Th17 cells

Th17 lymphocytes were firstly evidenced in mouse model of autoimmune encephalomyelitis and type II collagen-induced arthritis, two diseases associated to Th17 CD4+ lymphocytes dysfunction, where they were identified as the autoimmune pathogenetic cause and named IL17-producing CD4+ lymphocytes induced by IL-23[30].

Subsequently, this new population was demonstrated to differentiate independently from Th1, even if they share the cytokine receptor IL-12Rβ2, which binds IL-23 for Th17 or IL-12 for Th1. In presence of INFγ, the Th17 differentiation is blocked and, indeed, upon INFγ blockade and availability of IL-23, it is possible to induce Th17 without Th1 or Th2 master regulator transcription factors activaton[31]. *In-vitro* and *in-vivo* studies have confirmed that differentiation of IL-17-producing effector T cells is independent from the mechanisms required for Th1 or Th2 cell development. The tissue inflammatory action of Th17 lymphocytes has been further clarified: they secrete IL-6 and several chemokines, such as C-C Motif Chemokine Ligand (CCL)2, CCL7, CXCL1 and CCL20 and they induce neutrophils recruitment toward lungs[32].

Nowadays, Th17 CD4+ lymphocytes are well accepted as a further CD4+ lineage differentiation and their maturation pathway has been defined. Under physiological conditions, CD4+ *näive* cells differentiate in the thymus towards Th17 lineage only if they express the lineage precursor marker CD161, a glycoprotein that induces Th17 cells to migrate[33]. Moreover, on the cell membrane Th17 precursors are equipped with the receptors necessary to sense the proper differentiative cytokines cocktails, i.e. IL-23R, transforming growth factor (TGF)-βR, IL-6R, IL-21R and IL-1R, necessary to bind IL-23, TGF-β1 and IL-6[33].

Th17 cells produce different cytokines and chemokines that are active on both non-immune and immune cells. IL-17A and IL-17F induce epithelial cells, endothelial cells and fibroblasts to produce CXCL8, which is crucial for recruitment of neutrophil granulocytes. A similar effect is induced by IL-22 and IL-26 on epithelial cells. Th17 cells are also able to recruit neutrophils through the activation of monocytes by the combined activity of IL-17A, IL-17F and granulocytes-macrophage colony stimulating factor (GM-CSF), as well as the direct production of CXCL8 and GM-CSF. IL-17A, IL-17F, IL-22 and IL-26 also stimulate epithelial cells to produce CCL20, that results in the recruitment of Th17 cells themselves. IL-21 activates NK cells and CD8+ cytotoxic T cells, is a powerful B cell stimulatory factor and also provides an autocrine amplification loop for Th17 cells themselves.

The transcription factor known as the “master regulator” of Th17 differentiation is

RAR-related orphan receptor gamma T (RORγT), but others regulators are similarly crucial: Signal transducer and activator of transcription 3 (STAT3), Transcription factor Maf (c-Maf), Basic leucine zipper transcription factor, ATF-like (BATF) and IRF4 access to similar loci. On the contrary, Fosl2 is a negative regulator, because its occupancy overlaps with BATF and IRF4. Moreover, RORγ is not the prototypical regulator, because it does not "lock" the lineage program, since it can be easily switched[34]. Taken together, Th17 cells have a great plastic capacity and are sensitive to different external stimuli either in physiological and pathological conditions.

2.1.3.1.1 Th17 cells role in pathological condition

The direct pathogenetic involvement of Th17 cells has been reported in many autoimmune disorders. One of the most studied, used as a model to study Th17 plasticity, is experimental autoimmune encephalomyelitis (EAE). Pathological Th17 cells are induced by IL-23, IL-6 and TGF-β3, which, differently from TGF-β1, blocks c-Maf and Aryl-hydrocarbon Receptor (Ahr), notably the genes responsible for the regulatory phenotype of Th17 lymhocytes[35]. IL-23 is mandatory for the pathogenicity because it blocks the production of IL-10, an immunomodulatory cytokine, and induces GM-CSF and TGF-β3 as an autocrine self-maintenance[36]. Moreover, activation of T-box transcription factor (T-bet) induces the expression of IFNγ, an important pathogenetic mediator. This kind of Th17 involvement in autoimmune diseases can be extended to many other pathological conditions such as allergic reactions and others autoimmune diseases[37].

2.1.3.2 T regulatory lymphocytes

The importance of thymus in establishing and maintaining the self-tolerance was firstly evidenced fifty years ago. Forty years later a subset of CD4+ T lymphocytes has been identified expressing high amounts of CD25 and capable of suppressing disease in models of autoimmunity[38].

Treg cells differentiate mainly in the thymus medulla where CD4+ lymphocytes undergo high-avidity interactions with self-peptide/MHC class II complexes and IL-2R signaling and are responsible for the systemic self-tolerance[38]. Moreover, Treg can differentiate in the secondary lymphoid organs giving rise to the peripheral Treg, which are responsible for the maintenance of the tolerance to commensal microbiota[39]. They develop from *näive* T-cell precursors upon exposure to antigenic stimulation under tolerogenic conditions, i.e. strong TCR signaling, suboptimal co-stimulation and high amounts of TGF-β1 and retinoic acid[38]. Moreover, it has recently been shown that a small subpopulation of Treg cells express CCR6, which is associated with T cells that possess an effector-memory phenotype and their development is boosted by IL-35[40].

To gain the induction of Treg lineage the expression of the transcription factor forkhead

box P3 (FoxP3) is mandatory, which is considered the "master regulator" for Treg development. A peculiarity of Treg is an overall DNA hypomethylation, which makes a cell poised for expressing not only Foxp3 but also other Treg cell function-associated molecules and contribute to the stability of cell lineages that are critical for long-term immune tolerance[41]. Among these other factors, Forkhead box protein O1 (Foxo1) inhibits the expression of the inflammatory cytokine IFNγ[42].

Treg lymphocytes are central to maintain the self-tolerance and, indeed, their depletion in mouse models leads to acute autoimmunity[43]. Upon FoxP3 stimulation, Treg cells express Cytotoxic T-Lymphocyte Antigen 4 (CTLA4), IL-10, IL-10Rα, CD5 and Fas. On the other hand FoxP3 blocks the expression of pro-inflammatory cytokines including IL-2, TNFα, IFNγ, IL-17 and IL-4[43]. The immunomodulatory action of the regulatory lymphocytes can be subdivided according to different functions: inhibitory cytokines release, cytolysis and metabolic disruption. The first one refers to the secretion of the above listed cytokines (IL-10, TGF-β and IL-35). The cytolytic action is mediated by the secretion of Granzime A and Perforin and the expression of FasL and Galectin1, which all induce T cells apoptosis. Treg cells block effector lymphocytes also through the depletion of important metabolites: their higher expression of CD25 impounds IL-2, a cytokine necessary for lymphocytes survival; concurrent expression of the ectoenzymes CD39 and CD73 was shown to generate pericellular adenosine, which suppresses effector T-cell function and enhances the generation of induced Treg cells by inhibiting IL-6 expression while promoting TGFβ secretion. Eventually, Treg cells suppress effector T-cell function directly by transferring the potent inhibitory second messenger cyclic AMP (cAMP) into effector T cells through membrane gap junctions[40].

2.1.3.2.1 Treg cells role in pathological condition

The major pathogenic role of Treg cells deals with tumorigenesis. As far as lymphomas are concerned, Treg cells have been categorized in four types, accordingly to their role:

- Suppressors Treg cells: they favour the immune evasion of the lymphoma cells by blocking CTL;
- Malignant Treg cells: they favour the tumours proliferation, as for adult T lymphocyte leukemia;
- Killer Treg cells: they induce the apoptosis of cancerous cells;
- Incompetent Treg cells: they result less active and are reduced in numbers[44].

2.1.3.3 Th17/Treg ratio and its implication in pathological condition

TGF-β is an important player for differentiation and growth of both Th17 and Treg cells. It induces the expression of the transcription factors RORγT and FoxP3 and the differentiation towards one or another type of lymphocytes based on the cytokine microenvironment. A period of co-signal transduction for both cell type differentiation

has been reported: FoxP3 directly bounds to RORγT promoter, blocking Th17 differentiation. Treg cells develop in presence of low levels of pro-inflammatory cytokines and TGF-β empowers FoxP3 expression. On the other hand, in presence of IL-6 and other pro-inflammatory cytokines, STAT3 activation leads to the release of RORγT from FoxP3 blockade and induces IL-23R expression ending with Th17 cells differentiation[37]. Alternatively, Th17 cells can also differentiate even in absence of IL-6, but in presence of IL-21[45]. The differentiation from T *naïve* lymphocytes to Treg or Th17 cells is then a mutually exclusive process[46] (fig. 3).

The importance of the homeostasis between Th17 and Treg to maintain a functional immune system is likely to be reasonable[37]. An unbalanced Th17/Treg ratio has been proposed as one of the causes for RA progression[47]. Moreover, for several autoimmune diseases, i.e. RA and multiple sclerosis, a reduction in Treg cells numbers and in their functionality has been demonstrated to correlate with disease severity[46]. Many other diseases are also influenced by an altered Th17/Treg ratio including ankylosing spondylitis, psoriasis and psoriatic arthritis, SLE, inflammatory bowel disease, as well as Crohn's disease[48].

Drugs designed to modify Treg- and, in particular, Th17-responses have already proved efficacy and received approval for the treatment of certain autoimmune diseases, while others are currently being tested in clinical trials. Drugs are thought to be multidirectional and comprise direct targeting of Th17-related cytokines, cytokine receptors, intracellular signaling pathways, as well as inhibiting Th17- and enhancing Treg-specific transcription factors[48].

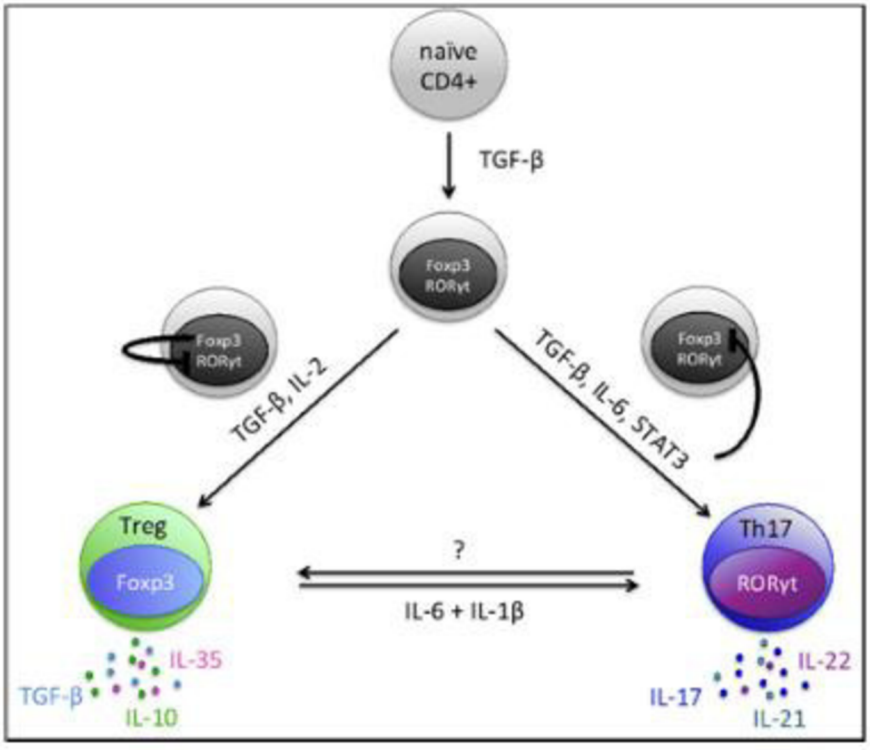

Figure 3: Schematic representation of the plasticity of Th17 and Treg cells differentiation[46].

2.2 T-Large granular lymphocytes leukemia

2.2.1 LGLL classification

Large Granular Lymphocyte Leukemia (LGLL) is a rare chronic lymphoproliferative disorder characterized by the clonal expansion of LGL[49].

The 2016 World Health Organization (WHO) classification identifies two main chronic lymphoproliferations among LGLL: T-LGLL, which defines a CTL clonal expansion and represents the most frequent variant up to 85% of total LGLL cases, and NK cells neoplasm, which can be further subdivided in the provisional entity of Chronic Lymphoproliferative Disorders of NK cells (CLPD-NK, ~10% of cases) and the Aggressive NK Leukemia (ANKL, <5% of cases and with the highest prevalence in Asia)[50].

Epidemiological studies have estimated that LGL proliferations account for 2%–5% of chronic lymphoproliferative disorders in North America and Europe and for 5%–6% in Asia[51]. Recently, the incidence of LGLL has been published from the Dutch and the American registry, which reported 0.72 cases and 0.2 cases per 1 million individuals per year respectively[52,53]. T-LGLL and CLPD-NK are commonly diagnosed in elderly patients, the median age at diagnosis being 66.5 years with females likely to be diagnosed at 3 years earlier compared with males[53].

T-LGLL and CLPD-NK share an indolent and chronic nature, with similar clinical and biological features[54]. The discovery of the same genetic lesions, both in leukemic T-LGLs and NK cells, might suggest a common pathogenetic mechanism, despite they arise from different cell lineages[55]. In contrast, ANKL is characterized by a highly aggressive clinical behavior[56] and it has been suggested to represent a separate clinico-pathologic entity within NK cells proliferations.

Apart from the LGLL variants listed in the WHO classification, LGLL has represented a matter of controversy, because LGL proliferations include a large spectrum of disorders ranging from polyclonal, usually self-limiting lymphocytosis, to indolent clonal expansions, until symptomatic treatment requiring aggressive diseases[57,58]. This thesis is focused on the study of T-LGLL.

2.2.2 T-LGLL diagnosis

The diagnosis of T-LGLL requires the demonstration of a clonal lymphocytosis lasting more than six months and must be differentiated from transient lymphocytosis that can be often detected in patients affected by viral infections, autoimmune diseases, solid tumours or after organ transplantation[4]. Moreover also chronic polyclonal LGL expansions are described, but they are referred as benign expansions[4]. The threshold for LGL lymphocytosis was set at 2×10^9/L. However, since several patients can present lower clonal expansion of LGL and are typically associated with cytopenias or

autoimmune conditions, a threshold of 0.5×10^9/L is now generally accepted[59].

A T-LGL lymphoproliferation must be properly identified using the expression of the cytotoxic markers CD16, CD57 and CD56[57]. Moreover, leukemic T-LGL show terminal effector memory phenotype, i.e. $CD3^+/CD4^-/CD5^{dim}/CD8^+/CD27^-/CD28^-/CD62L^-/CD45RA^+/CD122^+/CCR7^{-}$[60]. In addition, T-LGL can also express cytotoxic NK cell markers and receptors as killer immunoglobulin–like receptor (KIR) and C-type lectin receptor, as the CD94/NKG2 heterodimer[61]. A rare subset of leukemic T-LGL, characterized by the typical immunophenotype $CD3^+/CD8^+/CD56^+$, denotes an aggressive form of T-LGLL with a poor outcome and a younger age of incidence[62].
T-LGL are usually CD8+, but CD4+ chronic T-LGL proliferations have been described, with or without the co-expression of CD8, resulting more indolent than the classical CD8+ form[63]. Despite the expression of CD4, which usually defines T helper cells, both CD8 and CD4 LGL are classified as cytotoxic T lymphocytes and are to some extent associated to cytomegalovirus infection[64,65].

T-LGLL typically harbours an αβTCR, but a few, uncommon, clonal T-LGL can express a γδTCR and display a Vδ1/2 and Vδ9 profile[66]. Patients affected by γδTCR-LGLL show similar clinical and biological features to the αβTCR form[67].

To define the diagnosis of T-LGLL, the clonal nature of T-LGL expansion has to be assessed by detection of TCRγ gene rearrangement[60]. Moreover, deep sequencing of TCR has demonstrated a restricted diversity of TCR repertoire[68]. Flow cytometry analysis with monoclonal antibodies against the Vβ repertoire of the TCR can be used as a surrogate for clonality by showing the preferential use of one or two TCR-Vβ segments[57,69], strongly associated with monoclonal CDR3 region. It is worth mentioning that fluctuations in clonal dominance, referred to as clonal drift, are described up to one third of cases[57,70].

Bone marrow aspirate and/or biopsy is not recommended for T-LGLL diagnosis and are not routinely performed as a part of the initial diagnostic work-up. However, in some cases in whom the diagnosis is not specified or the etiology of cytopenias is not clear, a BM evaluation is needed to exclude other bone marrow failure syndromes frequently associated to LGLL such as Myelodysplastic Syndrome (MDS), Aplastic Anemia and Paroxysmal Nocturnal Hemoglobinuria[57].

2.2.3 Clinical features

Patients affected by T-LGLL have usually an indolent course with an overall survival of 14.5 years[71]. Approximately one-third of patients are asymptomatic at diagnosis, whereas two-thirds of patients will become symptomatic during the course of the disease[2]. Clinical manifestations include mainly cytopenias and neutropenia is the most frequent feature. Neutropenia is defined by an absolute neutrophil count (ANC) lower than 1,500/mm^3 and about 25% of neutropenic patients develop also severe neutropenia

(ANC<500/mm^3)[72]. Infections derived by chronic neutropenia affect from 15% to 39% of patients, involving primarily skin, oropharynx, and the perirectal area[73]. Moreover, severe septic complications may occur in about 5% of patients, representing the primary cause of T-LGLL related death[59].
Concerning other cytopenias, transfusion-dependent anemia affects between 6% and 22% of patients according to different series, whereas pure red cell aplasia occurs in 8% to 19% of cases. Thrombocytopenia is less severe and has been described in less than 20% of cases. A quarter of patients harbours splenomegaly, with T-LGLL infiltration; on the contrary, hepatomegaly or lymphadenopathy are rarely observed[74]. B symptoms and fatigue are rare and they are observed in only 20%-30% of cases[59]. As mentioned, when T-LGLL is sustained by a clone CD3$^+$/CD8$^+$/CD56$^+$, the disease is associated with very high LGL count, hepatosplenomegaly, lymphadenopathy, severe anaemia and thrombocytopenia and presents with an aggressive course of the disease similar to ANKL[62].

T- LGLL is commonly associated with autoimmune diseases, reported in about 15% to 40% of patients. RA is the most frequent disorder that is present in about 15% of the cases. Autoimmune cytopenias are reported in approximately 10% of patients, including pure red cells aplasia, immune thrombocytopenia and haemolytic anemia. SLE, Sjögren's syndrome, autoimmune thyroid disorders, coagulopathy, vasculitis with cryoglobulinemia, pulmonary artery hypertension and inclusion body myositis have occasionally been reported[59].
Besides autoimmune diseases, T-LGLL can correlate also with other haematological malignancies. Defects in downregulation of immunoglobulin secretion in LGL leukemia might lead to the development of autoantibodies and clonal B-cell malignancies observed in this disease, monoclonal gammopathy of undetermined significance being the most frequent (10%–20%)[59]. Chronic lymphoid leukemia, follicular lymphoma, mantle cell lymphoma, Hodgkin lymphoma, myelodysplastic syndromes and aplastic anaemia can be also associated with LGLL[75–77].

2.2.4 T-LGLL pathogenesis

The etiology of T-LGLL has not been clarified yet, but accumulating evidence suggests that a chronic antigenic stimulation, mediated either by auto- or viral-antigen, might lead to a polyclonal T-LGL expansion in the bone marrow[57,78]. Indeed, many chronic viral infections have been documented, including Hepatitis C virus, Cytomegalovirus, Epstein-Barr virus or Human T-lymphotropic virus[79–81]. Moreover, the discovery of a direct interaction between DC, which are antigen presenting cells (APC), and LGL in patients' bone marrow suggests that this site represents the place where the lymphoproliferation begins[82].

Even if T-LGLL pathogenesis is not to date completely understood, the hypothesis has been proposed that a multi-step process drives to T-LGLL development, as shown in

figure 4. The first event, namely the chronic antigenic stimulation (described above), triggers T-LGL activation. The second step is represented by a proper pro-inflammatory environment (described in section 2.2.6) that promotes a polyclonal expansion. The monoclonal expansion is obtained when somatic mutations in key genes or deregulation of cellular pathways lead to the resistance to apoptosis[57].

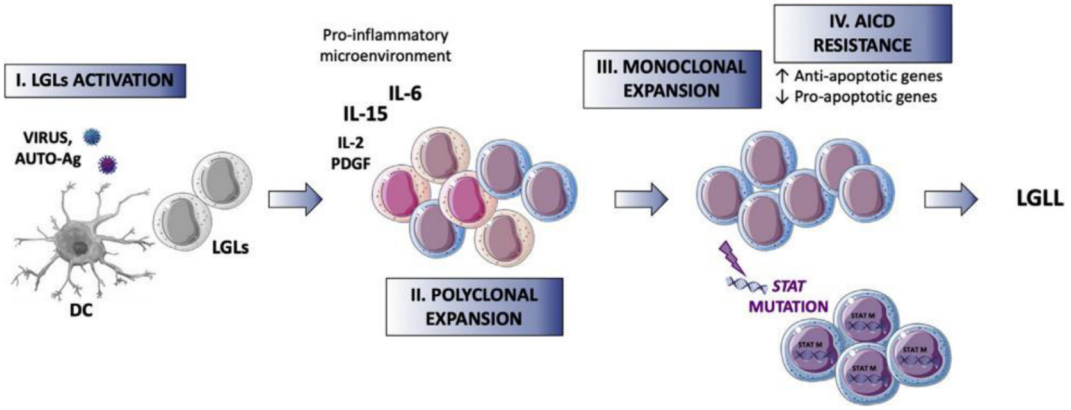

Figure 4: LGLL pathogenetic scheme[57].

The chronic expansion is initially consequent to a failure in the apoptotic machinery that induces leukemic LGL to become resistant to AICD[6]. Several mechanisms can be considered: the abundant and constitutive expression of Fas and FasL present on clonal T-LGL surface[83]; on the other hand, patients' sera contain elevated levels of the soluble form of Fas (sFas), which may act as a decoy receptor for FasL[84]. These two features result in the Fas-resistant phenotype of leukemic LGL[84]. This resistance can also be partly ascribed to the impaired death-inducing signaling complex (DISC) formation. In normal conditions, DISC assembly is the immediate downstream event of Fas–FasL cross-linking and is a prerequisite for Fas-mediated apoptosis. However, in leukemic LGLs, the overexpression of the DISC inhibitory Cellular FLICE-like Inhibitory Protein (c-FLIP) is thought to impair DISC formation and thus prevent Fas-mediated apoptosis[85].

The resistance to the apoptosis induction is also followed by constitutive activation of pro-survival pathways. In particular, the Ras–Mitogen-activated protein kinase1 (MEK1)–extracellular signal–regulated kinases (ERK) pathway is constitutively active and contributes to the resistance of Fas-mediated apoptosis[86]. The activation of Ras triggers an over-stimulation of Phosphoinositide 3-kinases (PI3K)-protein kinase B and Akt axis, leading to an activation of the NFkB machinery, which ultimately ends to the expression of anti-apoptotic proteins as B-cell lymphoma 2 (Bcl2) and induced myeloid leukemia cell differentiation protein 1 (Mcl1)[87]. Moreover, Akt can further trigger the already constitutively active Janus kinase (JAK)/STAT pathway, which is defined as the hallmark of T-LGLL development, since its inhibition leads to cell death via the ablation of Mcl1[88,89]. The central role of the JAK/STAT pathways is also underlined by the presence in patients' plasma of cytokines that further activate this pathway and by

the identification of activating somatic mutations, so far reported as a minor criteria in the 2016 WHO classification[50].

2.2.5 *STAT* mutations

2.2.5.1 *STAT3* mutations

The presence of *STAT3* mutations has been documented in 11–73% of patients and the most frequent are Y640F and D661Y, located in the SH2 domain, which promotes the dimerization, phosphorylation and localization in the nucleus of STAT3 proteins[90] (fig. 5). Activating *STAT3* mutations can be also detected in the coiled-coil and DNA binding domains (DBD). Phenotypically, no difference has been observed between patients with somatic mutations in the SH2 domain as compared to those with mutations in the DBD and in the coiled-coil domains[91]. The activating action of the mutations was related both to a stronger STAT3 phosphorylation, ending with a higher downstream anti-apoptotic proteins expression and also to a higher transcription of the target genes[90].

Despite their high mutational frequency, it has been demonstrated that the presence of *STAT3* mutations are insufficient to induce LGLL in mice models, therefore it has been suggested that *STAT3* mutations do not play a causal role in development of T-LGL leukemia, but additional mutations or deregulation of pro-survival pathways are necessary to develop the disease[92]. Consistently, the demonstration has been recently provided that *STAT* mutation represents a secondary event arising either within an already pre-expanded clonotype, or simultaneously with the clonal expansion of the immunodominant TCR Vβ clonotype[57,93].
As already stated, STAT3, even in its unmutated form, is constitutively activated in leukemic LGL. Moreover, patients, that resulted wild type (wt) for *STAT3*, can present mutations in other genes directly related with JAK/STAT pathway, leading as well to T cell activation[94,95].
In terms of clinical impact of *STAT* mutations, a significant correlation between the presence of *STAT3* mutations and neutropenia/symptomatic disease or rheumatoid arthritis has been highlighted in several studies[72,96,97]. In particular, it has been found that neutropenic patients, mostly *STAT3* mutated, are associated to a peculiar immunophenotype, i.e. CD3+/CD8+/CD16+/CD56-[72].

2.2.5.2 *STAT5b* mutations

STAT5b mutations have been identified in a small subset (2%) of T-LGLL patients, with a distinctive immunophenotype ($CD3^+/CD8^+/CD56^+$) and a clinically aggressive disease, with a poor prognosis[98] (fig. 4). Then, *STAT5b* mutations were detected also in 55% of CD4+ T-LGLL patients, underlining that *STAT5b* mutations characterize, but not exclusively, the CD4+ phenotype rather than the CD8+ phenotype[99]. Clinically, *STAT5b* mutated CD4+ T-LGLL patients show an indolent and asymptomatic disease,

in contrast to the aggressive disease observed in CD8+ T-LGLL patients harbouring these genetic lesions[99]. Consistently, we have identified *STAT5b* mutations in indolent CD4+ T-LGLL patients in our center, but in a lower percentage (15.2%), possibly as a consequence of the different numbers of patients that have been evaluated. In *STAT5b* mutated cases an immunophenotypic signature has not been identified. CD4+ T-LGLL is characterized by two immunophenotypes and *STAT5b* mutated patients are all equipped with the most frequent one (i.e. $CD4^+/CD16^-/CD56^+/CD57^+$)[72]. The most recurrent STAT5b genetic lesions hitherto reported are Y665F and N642H (fig. 5).
It has been hypothesized that the biological role of the mutations relies on the stabilization of the dimeric structure, leading to a more stable DNA interaction and therefore a higher downstream signaling activation[98].

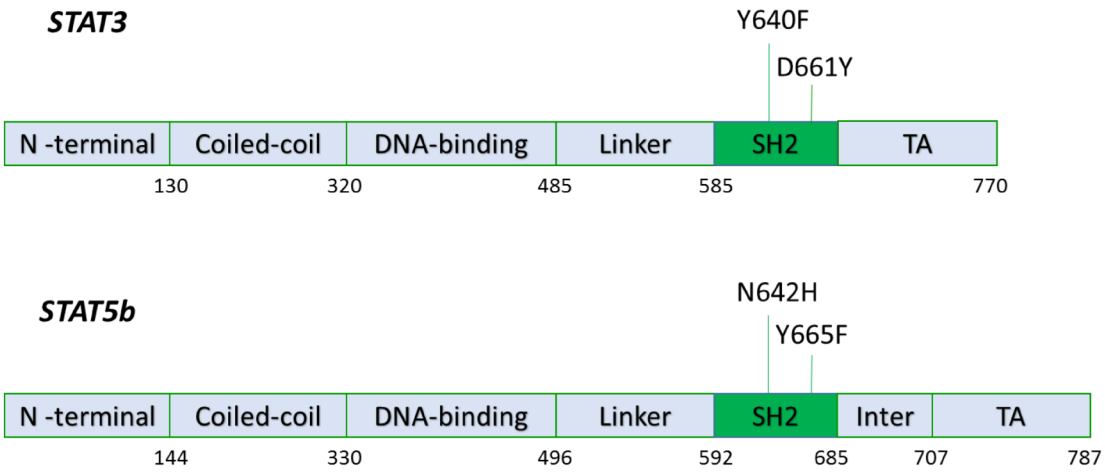

Figure 5: Graphical representation of *STAT3* and *STAT5b* genes. *STAT3* and *STAT5b* genes reporting the most frequent mutations described in T-LGLL.

2.2.6 T-LGLL microenvironment

2.2.6.1 T-LGLL microenvironment in peripheral blood

The pathogenesis of LGLL is driven not only by somatic mutations in key genes, as *STAT3* or *STAT5b*, but also by external pro-inflammatory stimuli. Several pro-inflammatory cytokines have been found at high level in patients' plasma and they provide pro-survival action on leukemic LGL. A system biology computational approach, which integrates the survival signals of a normal CTL with the known deregulated pathways in T-LGLL, has identified the crucial events[100]. In particular, leukemic LGL need an antigen priming, but a chronic stimulation mediated by IL-15 and Platelet-Derived Growth Factor (PDGF) is necessary to maintain the persistence of the deregulated pathways[100]. PDGF exists as homo- or heterodimers and the homodimer PDGF-BB is significantly higher in patients' plasma compared to healthy controls.

IL-15 stimulates LGL proliferative and cytotoxic capacity *in-vitro*, as IL-2 does[101,102]. The IL-15 membrane form has been detected on LGL surface as well as the expression of the specific receptor IL-15Rα, suggesting the capability of specific response on LGL, also confirmed by the presence of the other two receptors necessary for the signaling, i.e. IL-2/IL-15Rβ (CD122) and the common γ-chain (CD132)[101]. The expression of the soluble cytokine might be related to monocytes, since IL-15 mRNA expression correlates also with CD14 production[101]. IL-15 mediated survival is induced by proteasomal degradation of the pro-apoptotic protein Bid and this effect can be reverted upon Bortezomib (Bz, a proteasome inhibitor) treatment, leading to leukemic LGL apoptosis[103]. Chronic *in-vitro* IL-15 stimulation induces chromosomal aberrations and hyper-methylation, through the repression of miR-29b, which is responsible of the DNA Methyltransferase 3 Beta (DNMT3B) down-modulation. Moreover, myc and NFkB activation leads to DNMT3B activation and this effect can be reverted *in-vitro* by Bz treatment[104].

The pathogenetic role of IL-15 has been also demonstrated *in-vivo*: transgenic (tg) mice overexpressing murine IL-15, under MHC class I promoter control in order to lead a higher efficiency of expression, developed an early lymphocytosis with lethal accumulation of NK cells and CD8+ clonal T-lymphocytes in peripheral blood, several lymphoid and other organs[105]. Since the above mentioned *in-vitro* effects of Bortezomib, its liposomal formulation was tested *in-vivo* leading to a reduction of the leukemic burden in IL-15tg mice[104,106]. On the other hand, mice overexpressing recombinant human IL-15 develop a benign and non-clonal NK and CD8+ T lymphocytes expansion, which is then followed by an acute expansion of CD8+ T lymphocytes, defined as terminal stage. CD8+ terminal stage cells are transplantable in syngeneic mice causing a secondary leukemia. The leukemic cells have constitutive STAT5b activation and they grow *ex-vivo* only supplemented by IL-15, indicating the crucial role of this cytokine for the leukemogenesis. Moreover, leukemic cells co-express the specific receptor IL-15Rα that is mandatory for the development of the terminal stage, underlying the importance of the *in cis* activation. Double transgenic mouse IL-15Rα$^{-/-}$IL-15Tg maintained a controlled CD8+ lymphocytes expansion. The specific expression of IL-15Rα on leukemic cells can be attributed to a reduced methylation of its promoter in comparison to healthy CD8+ lymphocytes[107].

The importance of specific IL-15 receptor has also been demonstrated in patients. A higher concentration of the soluble form of IL-15Rα has been detected in comparison to healthy controls and this correlates with the incidence of neutropenia. The expression of IL-15Rα was detected on monocytes and, for some patients, on LGL; this underlines a high sensitivity even to a low dose of IL-15 for LGL mediated by *in cis* activation also thanks to the IL-15Rα shedding from monocytes, which in turn is induced by the metalloprotease ADAM17[108]. A further proof of the *in cis* action of IL-15 comes from clinics: a phase I clinical trial has been performed using a monoclonal murine antibody against CD122, which blocks the *in trans* activation of the trimeric receptors. The

biological drug has been demonstrated to be safe but only a little and transient increase of the neutrophils has been detected in some patients[109]. On the contrary, the *in-vitro* chemical inhibition of CD132 with the peptide BNZ-1 in *ex-vivo* T-LGLL PBMC and *in-vivo* models effectively decreases the IL-15, IL-2 and IL-9 mediated survival[110].

A microarray analysis on purified LGL underlies a disease specific higher expression of IL-1β in comparison to healthy controls, which has been also confirmed by the high presence of this cytokine in the patients' plasma. The steepest difference has been detected in patients affected also by RA, a common co-morbidity for LGLL, due to the pathogenetic role of IL-1β in this disease[111]. Consistently, another study has underlined the higher mRNA expression of IL-1β and IL-1Rα, but confirmed the higher presence in patients' plasma only for IL-1Rα[112]. Moreover, IL-18 (also connected to RA), CCL5, CCL4, IFNγ and IL-8 are constitutively expressed and found at higher concentrations in patients' plasma than in healthy subjects; this allows to observe an overall proliferative Type I lymphokine profile in T-LGLL, a pattern of secretion that can be also linked to anti-viral response, since these chemokines can stimulate CD8+ lymphocytes after infection[112].

Other cytokines related to RA are demonstrated to play a role in T-LGLL: *in-vitro* IL-6 treatment contributes to LGL survival through the phosphorylation of STAT3 inducing the expression of the anti-apoptotic protein Mcl1. Moreover, when IL-6 is neutralized by a monoclonal antibody (mAb), the survival of LGL is clearly reduced. IL-6 and the soluble form of its specific receptor IL-6Rα are detectable in the non-leukemic fraction of PBMC, speculating that monocytes might be the cellular source. Moreover, plasma levels of IL-6 and IL-6Rα are notably higher in LGLL patients as compared to healthy controls. Anyway, IL-6 treatment fails in inducing the STAT3 mediated SOCS3 expression, i.e. the negative feed-back of STAT3 activation. It has been demonstrated that SOCS3 is epigenetically silenced and its STAT3 inhibiting role is restored upon treatment with demethylating agents[113].

Monocytes might also secrete IL-8/CXCL8, since a high expression of these cytokines has been identified in the non-leukemic fraction of PBMC. Only leukemic T-LGL overexpress CXCR1 and to a less extent they are positive for the receptors of these cytokines (CXCR3 and CXCR4). Taken together, these findings allow to suggest a specific LGL chemotaxis in presence of IL-8/CXCL8[114]. Consistently, late inflammation CCRs, namely CXCR1 and CXCR2, are overexpressed in T-LGLL, indicating that leukemic T-LGL behave as terminally differentiated inflammatory cells. Furthermore, an inverse correlation between the CCR5 expression and neutropenia or lymphocytosis has been described[115]. On the contrary, another study did not identify a differential expression among patients, with exception of CCR7 down-modulation for patients' LGL. A correlation between CCR5 and CXCR3 expression has been identified, together with an increased presence of their ligands in patients' plasma (CXCL10 and CXCL9), further underlining the heterogeneity of T-LGLL[116].

2.2.6.2 Bone marrow features

The analysis of leukemic LGL infiltration in the bone marrow is not routinely performed to assess the diagnosis of LGLL. Aspirates and biopsies sometimes are found ipercellular and the infiltrates represent small groups of LGL with small, minimally irregular nuclei and sparse cytoplasm. The bone marrow involvement recognizes two patterns: a) an interstitial clusterization of CD8+, CD57+, granzyme B+ and TIA1 Cytotoxic Granule Associated RNA Binding Protein + (TIA-1) lymphocytes; b) a linear arrangement of cells with the same immunophenotype representing the LGL accumulation in microvascular stuctures[117,118]. Some lymphoid aggregates of CD20+ and non-cytotoxic CD3+ lymphocytes which are common to infective reaction and autoimmune diseases can be observed[117]. Moreover, an increased amount of erythroid precursors leads occasionally, i.e. around the 30% of the cases, to a decreased M:E ratio (the ratio between myeloid and erythroid precursors). Reticulin deposit has been identified in BM biopsies of T-LGLL patients, evidencing a fibrosis status which is more evident close to the lymphoid aggregates[119].

2.2.6.2.1 Bone marrow T-LGLL microenvironment

Mesenchymal stromal cells (MSC) play a role in cytopenia development in bone marrow of T-LGLL patients: they are demonstrated to be less in number, to grow slowly, to be more senescent and to deposit more collagen type I, III and V than MSC derived from healthy controls. All these findings lead to a reduced growth of hematopoietic precursors. MSC express less fibroblast growth factors (FGF) and, upon treatment with this cytokine, MSC become less senescent and deposit less collagen, leading to a higher hematopoietic precursor growth. In CD8+ T-LGLL cases, a strong reduction of CD4+ lymphocytes with a parallel enrichment in CD8+ takes places. It has been postulated that this phenomenon could represent an underappreciated part of the pathogenesis in which leukemic cells act not directly on hematopoietic precursors but on BM microenvironment[119].

The direct role of MSC is still to be defined, but it has been proved that bone marrow derived DC induce the proliferation of either leukemic T-LGL or NK cells. A direct connection between DCs and LGL or NK cells found in patients' BM biopsies has been demonstrated, suggesting that DC pulsed with a particular antigen, which is still to be defined, might be the potential inciting agent responsible of LGL proliferation[82].

2.2.7 Treatment for T-LGLL

Patients require treatment when affected by symptomatic neutropenia, severe neutropenia, symptomatic or transfusion dependent anaemia or in presence of concomitant symptomatic autoimmune diseases. Standard treatment of T-LGLL is based on immunosuppressive therapy, although the evidence supporting this approach is limited due to the lack of perspective clinical trials. A minimum of 4–6 months of therapy is mandatory to assess the response. A treatment algorithm is reported in figure 6[57]. First-line therapy relies on single immunosuppressive oral agents: methotrexate (MTX, 10 mg/m2 per week) or cyclophosphamide (CTX, 100 mg/d)[120,121]. Treatment efficiency is reported by several retrospective series, but only few prospective trials are available[59].

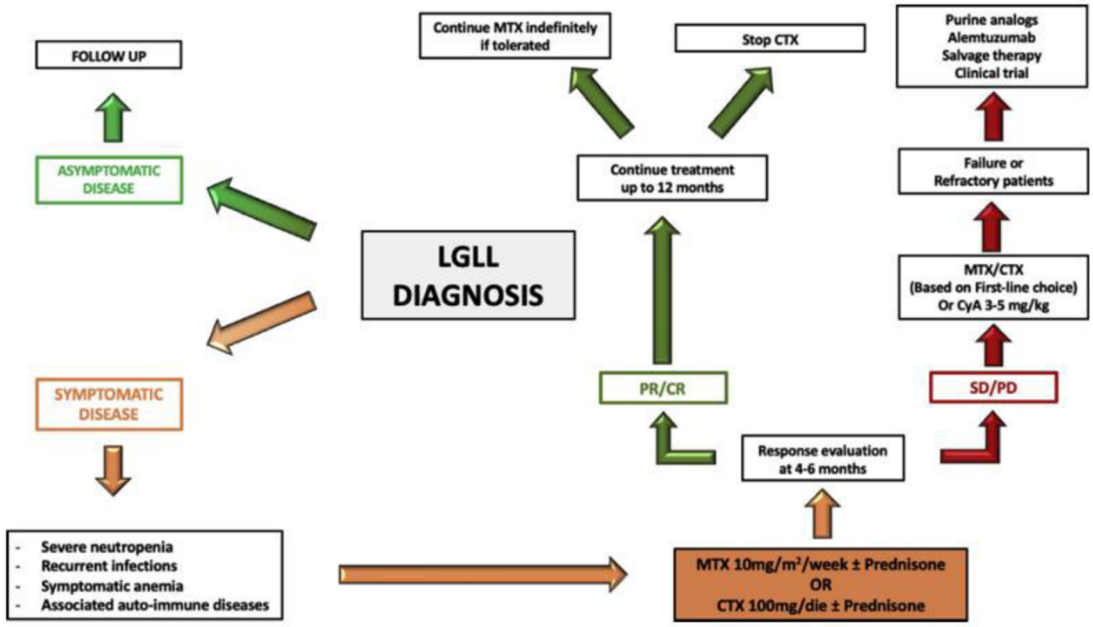

Figure 6: Treatment algorithm up to date accepted in LGLL[57]. MTX: Methotrexate. CTX: Cyclophosphamide. CyA: Cyclosporin A. CR: complete response. SD: stable disease. PD: progressive disease.

MTX oral therapy can be considered partially effective: in two separated studies an overall response rate (ORR) of 40–50% has been evidenced[122,123]. Oral CTX as first line therapy showed efficacy in a retrospective French-Italian-American experience of 45 patients, with 71% ORR and 47% CR, with 3 patients obtaining a molecular response[121]. Deep sequencing analyses of LGL clones after treatment demonstrated that CTX provides a durable response, whereas MTX and cyclosporine A (Cy-A) treatment are associated with the persistence of leukemic clones[96]. Moreover, a contradictory predictive role of incidence of *STAT3* mutation and response to MTX must be emphasized: it has been claimed that *STAT3* Y640F mutation might predict MTX response, with an ORR of 73%, but the longest time of response has been identified in patients *STAT3* wt[124,125]. Treatment should be continued no more than 9-12 months to

avoid potential Myelodysplastic Syndrome/Acute Myeloid Leukemia complications[57]. The results of the first perspective trial of immunosuppressive therapy in LGLL have been recently reported: 55 patients underwent MTX as first line therapy, with 38% ORR; non-responding patients switched to CTX therapy with 64% ORR[125]. A randomized trial (NCT01976182) investigating the first line therapy with MTX vs CTX is on-going in France aiming to determine the best first line choice of therapy in this setting.
CyA (3-5 mg/kg) is usually preferred in patients with severe anemia or as a second line, for which the ORR is variable (21-100%) and the duration of treatment is undefined, since the disease usually relapses[126]. Many other options have been proposed as salvage-therapy: Alemtuzumab (anti-CD52) reaches an ORR of 74% and a complete response of 47%, but toxicities limit its use; purine analogs (fludarabine, cladadrine, pentostatine or bendamustine) have been experienced in few patients and the ORR is promising (70-80%)[127–129].

Considering the poor response of the approved drugs, the role described of *STAT* mutations and microenvironment in T-LGL survival, and the concurrence of autoimmune diseases prompted the application of drugs directed towards these targets. Rituximab (anti-CD20) has been used in few T-LGLL patients with concurrent RA and LGLL, with unexpected responses; authors suggested that the elimination of B cell expansion and auto-antigens is responsible for LGL clone suppression[130]. Tofacitinib, a JAK3 inhibitor, approved for the treatment of refractory RA, was tested in 9 patients (4 carrying *STAT3* mutations) affected by concomitant refractory LGLL and RA, with hematological response in 6 patients and neutropenia improvement in 5 out 7 patients[131].

3 Aim of the study

T-LGLL is a chronic and heterogeneous lymphoproliferative disorder; cells proliferation is sustained by both deregulated pathways within the leukemic clone and by external pro-inflammatory stimuli. In particular, NFkB and JAK/STAT axes are reported to be constitutively active in leukemic clone. The abnormal STAT activation is also strengthened by somatic, mutually exclusive mutations in *STAT3* or *STAT5b* genes, specifically detected in CD8+ and CD4+ T-LGLL respectively. The intracellular deregulations are also affected by external stimulation. In fact, some pro-inflammatory cytokines are increased in T-LGLL patients' plasma including IL-6 and CCL5. Moreover, one of its receptors, CCR5 is less expressed on leukemic LGL surface.

With the above background, this study has been designed to evaluate the microenvironment in T-LGLL focusing on two main topics: the role of monocytes in LGLL and the distribution of T cell subsets, notably Th17 and Treg. The first issue addresses the role of monocytes in leukemic T-LGL survival, characterizing putative relationships between monocytes and LGL, particularly mediated by IL-6 and CCL5. Since three classes of monocytes are recognized, namely classic, intermediate and non-classical and since their distribution can be altered in several autoimmune diseases, conditions often associated to T-LGLL, we evaluated the distribution of monocytes subsets and their molecular features in peripheral blood of T-LGLL patients.

Regarding the second topic, since nothing is actually known on the putative pro-leukemic role of other subsets of the immune system in T-LGLL, i.e. residual T lymphocytes, we planned to evaluate Th17 and Treg lymphoid populations in patients' peripheral blood.

Eventually, to better characterize the inflammatory environment in peripheral blood of patients, our study also aims to provide a preliminary evaluation of the patients' secretome in order to identify possible new pathogenetic cytokines taking place in the TME. In a few symptomatic patients requiring treatment, we also evaluated whether therapy would impact on TME cells.

4 Material and Methods

4.1 Cellular biology

4.1.1 Mononuclear cells isolation

Mononuclear cells were obtained by density gradient separation using a polymeric saccharide with hydrophilic properties (Lymphosep, Cedarlane, Burlington, Canada). Blood samples were properly diluted (peripheral blood 1:3 and Buffy coat 1:6) in physiological solution (sodium chloride 0,9%; Monico Spa, Italy) and subsequently the polymeric solution was stratified underneath the diluted blood. The gradient separation was performed by centrifugation at 2200 rotations per minutes (rpm), at 20°C for 20' without brake. At the end, the different blood cells were stratified according to their density: erythrocytes first, granulocytes are found under the polymeric solution, PBMC are stratified at the polymer-supernatant interface and platelets are also found in the supernatant (fig. 7). MC were collected and washed twice with physiological solution and centrifuged at 1600 rpm, 20°C for 10' to rinse PBMC from the platelets and, in the end, the cells were diluted in a proper volume of physiological solution to be counted with a *Neubauer* chamber and further processed.

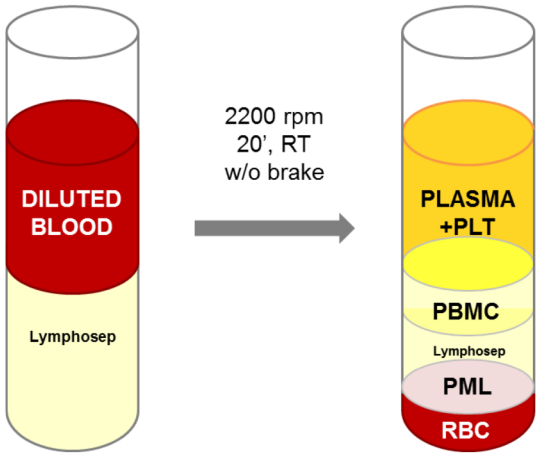

Figure 7: Schematic representation of mononuclear cells isolation. rpm: rotations per minutes, RT: room temperature; w/o without; PLT: platelets; PBMC: peripheral blood mononuclear cells; PML: polymorphonuclear cells; RBC: red blood cells.

4.1.2 Immuno-magnetical LGL and monocytes purification

LGL and/or monocytes were purified from PBMC with monoclonal antibodies (mAb) conjugated to magnetic microbeads (Miltenyi Biotec, Germany), anti-CD57 for LGL or anti-CD14 for monocytes. Purification was performed separately, but, when necessary, a double purification was carried out firstly to isolate monocytes and, subsequently, the negative fraction was used to extract LGL.
The defined number of cells was centrifuged at 1200 rpm, 20°C for 10' and then incubated for 15' at 4°C with the proper amount of purification buffer (PBS 1X, BSA 0,5%, EDTA 2 mM) and antibodies, in a ratio 5:1. At the end of the incubation time, the cells were washed from the antibody excess with purification buffer and centrifuged at 1200 rmp, 4°C for 10'. In the meantime, the proper magnetic column was placed in the MACS separator (Miltenyi Biotec, Bergisch Gladbach, Germany) and equilibrated with purification buffer. The cells were then resuspended in 500 µl of purification buffer and poured into the column, leading the binding of the cells magnetically labelled to the column and the collection of the unlabelled cells in the flow through. The column was rinsed 3 times with purification buffer and then removed from the separator and placed in another tube and the labelled cells were flushed out by pushing the plunger into the column. Both fractions were centrifuged at 1200 rpm, 20°C for 10' and, in the end, the cells were resuspended in the proper amount of physiological solution to be counted with a *Neubauer* chamber and further processed after the purity check performed by flow cytometry.

4.1.3 Cell culture

Cells were cultured $2x10^6$ cells/mL in RPMI 1640 (Euroclone, Milan, Italy) enriched with 10% Fetal Calf Serum (FCS; Euroclone, Milan, Italy), 1% penicillin + streptomycin (Gibco Laboratories, Dublin, Ireland) at 37°C and 5% CO2.

4.1.3.1 Cytokines stimulation

To perform cytokines stimulation, monocytes and LGL were purified from the same subjects. The two populations were obtained through a double immune-magnetic purification.
Monocytes were stimulated with recombinant human (rh) CCL5 (R&D Systems, Minneapolis, USA) 100ng/ml. LGL and negative counterpart were stimulated with rh-CCL5 100 ng/ml or rh-IL-6 (SIGMA; Saint Louis, USA) 20 ng/ml.
The cells were incubated for 12 hours at 37°C and 5% CO_2, after that, the cells and supernatant were harvested and further processed.

4.1.4 Cryopreservation

4.1.4.1 Vital cryopreservation

The volume of cells needed for the freezing was precipitated at 1600 rpm for 9' at 20°C and then resuspended with cold freezing medium (complete RPMI with the addition of

50% FCS and 7% Dimethyl sulfoxide, DMSO), to avoid the cytotoxicity of the DMSO. 1 mL of the resulting cell suspension was transferred into the cryovials and the tubes were put into the freezing-aid ("Mr. Frosty"). This device was half-filled with absolute isopropanol, which ensured a slow cooling rate of the cell suspension of 1 C/min to avoid cell damage. The freezing apparatus was stored up to 5 days at -80°C. The cryovials were transferred for long term storage in a liquid nitrogen tank (-196 C).

4.1.4.2 Cryopreservation for molecular analyses

- To extract RNA the cells were preserved in lysis buffer (RNeasy Mini Kit, Qiagen, Hilden, Germany) added with 1% β-mercaptoethanol (β-ME). The proper number of cells were aliquoted and centrifuged at 5000 rpm, 4°C for 5'. The supernatant was discarded or cryopreserved for further analysis. The cells were lysed and the lysate was kept at -80°C till the RNA extraction.
- To extract protein or DNA the cells were processed as for RNA extraction but the cells are frozen as pellet and kept at -80°C till the extraction.
- Plasma and cell culture supernatants were preserved at -80°C for serological evaluation.

4.2 Molecular biology

4.2.1 Mutational analysis

4.2.1.1 DNA extraction

DNA was extracted from patients' PBMC, approximately 1-20 million total cells. The "Puregene Cell and Tissue Kit" (Qiagen, Minneapolis, USA) was used. Firstly, the cells were lysed through 1 hour incubation with Cell lysis solution at 37°C, after shaking it firmly with a vortex. Then, RNA was degraded through treatment with RNase A solution for 1 hour at 37°C and subsequent cooling of the cell lysate in ice (5'). Protein was precipitated by adding Protein precipitation solution to the lysate and vortexing; the sample was centrifuged at 13000 rpm for 3' at room temperature (RT), after which the DNA containing supernatant was transferred into a new tube. 100% was added and DNA was precipitated gently inverting the tube several times until a white precipitate appeared. The sample was centrifuged at 13000 rpm for 2' at RT and the supernatant was discarded. The DNA precipitated was washed with ethanol 70% in order to eliminate alcohol contamination and centrifuge at 12000 rpm for 1 minute, after which the supernatant is discarded. DNA was endingly hydrated by adding DNA hydration solution to the DNA pellet, once it was completely dry, and incubated overnight at room temperature. The concentration of the RNA was assessed by evaluating the 260 nm absorbance with Nanodrop 2000 (ThermoFisher Scientific, Waltham, Massachusetts, USA) and the quality was evaluated considering the 260nm/280nm ratio more than 1.80 and the 260/230 ratio over 2.20. DNA samples were stored at 4°C for short-term usage or at -20° for longer storage time.

4.2.1.2 PCR

Polymerase chain reaction (PCR) was used in the present study as the first step of DNA sequencing for two main purposes: the screening of patients' mutational status on *STAT3/STAT5b*. Primers used for the amplification of *STAT3* and *STAT5b* hotspot regions (table 1) derived from literature and were specific for exon 21 of *STAT3* gene[90] and for exon 16 of *STAT5b* gene[98], respectively.

Table 1: Primers used for *STAT3* and *STAT5b* mutational screening; bp= base pairs.

Target region	Forward primer (5'-3')	Reverse primer (5'-3')	Amplicon length
STAT3 exon 21	TCCCATCGGTCACCCCAACA	CAGGCCACTGAACAGGGTG	523 bp
STAT5b exon 16	TGTTGGGGTTTTAAGATTTC	CAAATCAGAATGCGAACATTG	266 bp

A standard PCR protocol available in the lab was used, being this analysis a routine procedure on LGLL patients. The PCR reaction mixture with the reagents (Applied Biosystems, Weiterstadt, Germany) listed in table 2 was prepared on ice under a UV-sterilized hood, then DNA (200 ng/tube) was added outside the hood, up to a final volume of 25 µl. A negative control with no DNA was always present in the PCR to exclude the presence of contaminants.

Table 2: Components of the PCR mix and respective final concentrations.

Reagent	Volume (µl)	Final concentration
10X PCR Gold Buffer	2.5	1X
25 mM $MgCl_2$	1.5	1.5 mM
10 mM dNTPs	2	0.4 mM
20 µM forward primer	2	0.8 µM
20 µM reverse primer	2	0.8 µM
AmpliTaq Gold 5U/µL	0.25	1.25 U/25 µL
Sterile water	up to 25 µL	

Thermal cycling conditions used for standard PCR reactions are reported in table 3.

Table 3: Standard PCR program.

	Enzyme activation	**PCR (35 cycles)**			**Final extension**
Step		*Denaturation*	*Annealing*	*Extension*	
Temperature	94°C	94°C	Depending on the primers	72°C	72°C
Time	10’	30’’	1’30’’	1’	7’

4.2.1.3 Analysis of PCR products by gel electrophoresis

PCR products were run in a 2% agarose electrophoresis gel for the evaluation of the results. The gel was prepared dissolving agarose powder (Euroclone S.p.A, Milano, Italy) in 1X TAE buffer (TRIS 2M, glacial acetic acid 1M, EDTA 0.5M, pH 8.0; Sigma-Aldrich, St. Louis, USA) and adding 5% EuroSafe Nucleic Acid Staining Solution 20,000x (Euroclone S.p.A, Milan, Italy). The PCR reaction was mixed with 5 µL of 6X Loading Buffer (Qiagen, Minneapolis, USA) and entirely loaded in the gel; a 100bp DNA Ladder (Invitrogen, Milan, Italy) was loaded in the first well to discriminate the size of the amplicons analyzed. The result of the electrophoresis was analyzed using a ChemiDoc Gel Imaging System (Bio-Rad, California, USA).
As the PCR products were needed for Sanger sequencing, DNA was recovered from the agarose gel by excising the bands and extracting the DNA with the kit QIAquick Gel Extraction Kit 250 (Qiagen). Gel slices were dissolved in a buffer containing a pH indicator and the mixture was applied to the QIAquick spin column, which contains a silica membrane to which nucleic acids adsorb in high-salt conditions. Agarose and other impurities were washed away and DNA was eluted in 30 µl of the low-salt DNA Elution Buffer provided by the kit. DNA concentration after the gel extraction was measured with Nanodrop 2000.

4.2.1.4 Sanger sequencing

This technique has been the gold standard targeted approach for detecting single nucleotide variants (SNV), as well as insertions and deletions; in the present study, indeed, it was employed for the mutational screening of *STAT3/STAT5b* genes.

4.2.1.4.1 Cycle sequencing

Gel-extracted PCR products were prepared for Sanger sequencing with BigDye terminator v3.1 Cycle Sequencing Kit (Applied Biosystems, Weiterstadt, Germany). Cycle sequencing is a particular amplification reaction based on the same principles of a standard PCR; except for the presence in the reaction mix of fluorescently labelled ddNTPs, which stop the DNA elongation whenever they are randomly incorporated by the DNA polymerase. Two separate reaction mixtures were prepared for each sample,

one containing 1 µL of 3.2 µM forward primer and the other one with 1 µL of 3.2 µM reverse primer. Both reactions required 4 µL of the BigDye Terminator 3.1 Ready Reaction Mix provided by the kit, containing dNTPs, the four different fluorescent ddNTPs, AmpliTaq DNA polymerase, $MgCl_2$ and Tris-HCl buffer. 50 ng of purified amplicon per reaction was added. Sterile water was added to the reaction tube up to a final volume of 10 µL and samples were moved to the thermal cycler where the following amplification program was used (table 4).

Table 4: Thermal cycling conditions for cycle sequencing reaction.

Parameters	**Steps**			
	25 cycles			
	Denaturation	*Annealing*	*Extension*	Hold
Temperature	96°C	50°C	60°C	4°C
Time	10''	5''	4''	∞

4.2.1.4.2 Capillary sequencing

Cycle sequencing reactions were purified with DyeEx 2.0 Spin Kit (Qiagen) according to the manufacturer's protocol to remove unincorporated dye terminators and excess primers. After this step, 2 µL of each reaction was loaded onto an ABI PRISM 3130 Genetic Analyzer (Applied Biosystems, Weiterstadt, Germany) capillary sequencer, in which DNA samples were separated by size through a 4-capillary electrophoretic system injected with POP7 (Applied Biosystems, Weiterstadt, Germany) semi-liquid polymer. An electric field was applied to force the negatively charged DNA fragments into the capillaries and, shortly before reaching the positive electrode, a laser beam excited the flouorescently-labelled ddNTPs. When each dye was excited by the laser emitted light at a different wavelength, the four bases being in this way detected and distinguished in one capillary injection.
Sequencing output was provided in *.ab1 format files and analysed with ChromasPro data analysis software that converted raw fluorescence signals into a chromatogram (fig. 8). The nucleotide sequence containing the mutation site was searched in the chromatogram to check if the mutation was present.

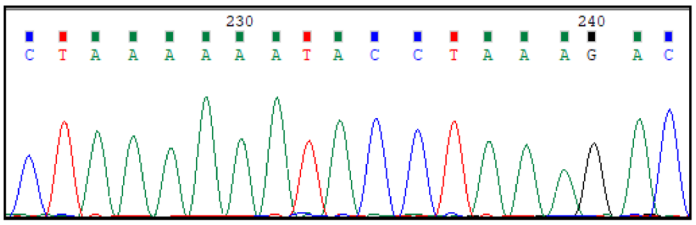

Figure 8: **Example of a chromatogram.** Sequencing output in the form of a chromatogram as it is visualized in ChromasPro software. The colour of each peaks represents the base called for that peak.

4.2.2 Expression analysis

4.2.2.1 RNA extraction

The isolation was carried out using columns and buffers included in RNeasy Mini Kit (Qiagen, Minneapolis, USA).

The lysates were thawed on ice and then mixed with 70 % ethanol in a ratio 1:1 to give the proper condition for the binding of RNA to the column. The columns were centrifuged at 10000 rpm, RT for 20'' to induce RNA binding and the supernatant was discarded. The columns were then washed one time with 350 µl of RW1 buffer and centrifuged at 10000 rpm, RT for 20'' and the supernatant was discarded. Afterwards, to gain a complete DNA digestion, the columns were incubated 15' at RT with 80 µl of DNase previously diluted 1:8 with RDD buffer. The enzyme was then discarded with the second washing step with 350 µl of RW1 buffer. To get salts removed, one washing step was performed with 500 µl of RPE buffer pouring it around the column wall and the columns were centrifuged at 10000 rpm, RT for 20''. The washing step was repeated and the columns centrifuged at 12800 rpm, RT for 2'. To remove all the remaining liquid from the column, the columns were re-centrifuged at 12800 rpm, RT for 2'. The columns were then transferred in 1,5 ml RNase-free tubes and 30 µl of RNase-free water was added directly on the membrane and incubated for 3' at RT. The RNA was eluted by centrifugation at 11000 rpm, RT for 1'. The RNA just purified was analyzed quantitatively and qualitatively using the spectrophotometer NanoDrop200 (ThermoFisher Scientific, Waltham, Massachusetts, USA). The concentration of the RNA was assessed by evaluating the 260 nm absorbance and the quality was evaluated considering the 260nm/280nm ratio more than 1.80 and the 260/230 ratio over 2.20.

4.2.2.2 cDNA synthesis

The RNA extracted was retrotranscribed using the Reverse Transcription System (Promega Corporation; Madison, WI, USA). 9,9 µL of RNAse free water containing 1 µg of RNA was first denaturated at 70°C for 5' and then cooled down for 5' at 4°C. Subsequently 10,1 µl of amplification mix was added for each sample and it was composed as follow: 2 µL of Reverse Transcriptase Buffer 10X, 4 µL $MgCl_2$ 25 mM, 2 µL nucleotides mix 10 mM, 0.5 µL RNAse inhibitor 40 U/µL, 0.6 µL AMV Retrotranscriptase 25 U/µL and 1 µL of oligo-timidine (dT) primer 0.5 mg/mL, which

were used to anneal with the poli-A (adenine) tail, in order to retrotrascribe only mRNA. The retranscription reaction was performed in the thermocyclator GeneAmp PCR System 2700 (Applied Biosystems, Weiterstadt, Germany) and the program was 42°C for 15', 95°C for 5' and then the reaction was stopped and kept at 4°C till the the sample were cryopreserved at –80°C for long-time storage.

4.2.2.3 Quantitative PCR

4.2.2.3.1 Primer design

The primers were generated with the Primer Express software version 3.0 (Applied Biosystems, Weiterstadt, Germany). They were designed to anneal two exons (one of them at the splicing junction) in order to be sure that only the cDNA of interest was amplified. The optimal length for single-stranded primers is about 15–20 bases, and the G/C content should be between 40% and 60%. They were also optimized in order to have a specific melting point which should not differ by more than 1–2°C between the two primers, with minimum and maximum Tm of 58°C and 60°C[132]. The primer used for this thesis project are reported in table 5.

Table 5: List of the primers used for expression analysis.

Primer	Forward	Reverse
GAPDH	AATGGAAATCCCATCACCATCT	CGCCCCACTTGATTTTGG
IL-6	GGCACTGGCAGAAAACAACCTG	TCACCAGGCAAGTCTCCTCATTGAAT
CCL5	TCTGCCTCCCCATATTCCTCGG	GGCGGTTCTTTCGGGTGACAAAG
CCR5	CAAAAAGAAGGTCTTCATTAC	CCTGTGCCTCTTCTTCTCATTT
p65	CCCCACGAGCTTGTAGGAAAG	CCAGGTTCTGGAAACTGTGGAT
NFkB1	CAAATAGACGAGCTCCGAGACA	GAGACTCGGTAAAGCTGAGTTTGC
IRF8	TGGACATTTCCGAGCCATACA	GCCTAGTTTGCATTTTTGCTCTTC
IL-23A	TCAGTGCCAGCAGCTTTCAC	TCTTAGATCCATGTGTCCCACTAGTG
TNF-α	CCCAGGCAGTCAGATCATCTTC	GGTTTGCTACAACATGGGCTACA
IL-10	CCCTAAACAGATGAAGTGCTCCTT	GGTGGTCGGAGATTCGTAGCT
ADAM17	ACACTGTAAAATGGCAGGACTTCTT	ATGTGGGCTAGAACCCTAGAGTCA

Every primer designed was tested for the specificity and for efficiency. The first aspect was evaluated by PCR and the amplification product was analysed in agarose gel to exclude non-specific amplification, the two techniques were described at sections 4.2.1.2 on page 28 and 4.2.1.3 on page 29. The primers were then analysed by q-PCR to derive their efficiency from a standard curve as described in the following section.

4.2.2.3.2 Quantitative PCR

The method used for detection exploited the fluorescent intercalating agent SyberGreen. It has a strong and measurable fluorescence emission when bound to a double standed (ds) DNA which increased in an exponential way every cycle of amplification, due to the duplication of the amplicon. The signal recorded, anyway, is not sequence specific, therefore the measurement of the SybrGreen amount was linked to the melting peak analysis, because the melting temperature is sequence specific allowing the identification of the amplicon from potential artefacts. The mix of reaction is reported in the table 6.

Table 6: Components for qPCR.

Reagents	Quantity
RNase free water	4,2 µL
5 µM forward primer	0,9 µL
5 µM reverse primer	0,9 µL
SYBR Green PCR Master Mix 2X (Roche, Basel, Switzerland) and NEB (Ipswich, USA)	7,5 µL

The reaction of amplification was carried out in the instruments 7000 Sequence Detection System (Applied Biosystems, Weiterstadt, Germany) or Quant Studio5 (ThermoFisher Scientific, Waltham, Massachusetts, USA) with the following steps:

- An initial step when Uracil N-glycosylase (UNG) was activated at 50°C for 2' to degrade any contamination of RNA left by cDNA synthesis, because it could detect uracil instead of timidine.
- A second step at 95°C for 10' to inactivate UNG and to denaturate the template cDNA.
- The third step consisted in the polymerase reaction. 40 cycles in which there was an alternation of a denaturation step at 95°C for 15'' and an annealing of primers and elongation od the amplicon at 60°C for 1'.
- The polymerase reaction can be further subdivided in 3 phases:
  - Initial phase in which the fluorescence intensity is below the baseline.
  - Exponential phase in which the quantity of the amplicon is related to the cycle number according to the equation: $[DNA_n] = [DNA_i] \times (1+\text{efficiency})^n$.
  - *Plateu* phase in which the reagents run out and the enzyme loses efficiency.

4.2.2.4 Expression evaluation

- Absolute quantification: this approach was exploited for the evaluation of the primer efficiency. The amplification reaction was carried out using scalar dilutions (1:5). The Ct (threshold cycles: indicated the fractional cycle number at which the amount of amplified target reaches a fixed threshold) obtained were plotted in a 2D diagram reporting the template quantity in the x axis and the relative Ct in the y axis. From the equation describing the curve it was possible to derive the slope (m) of the curve and the R^2. Efficient primers should give m=-3.32 and R^2>0.99, which meant 100% efficiency.
- Relative quantification: to evaluate the relative expression of target genes the ddCt method was used[133]. The average Ct of the target gene was normalized to a reference gene (a housekeeping gene, as GAPDH) by subtracting its average Ct to the target gene obtaining the delta-Ct (dCt). Once obtained DCT for every sample, they were further normalized in order to compare different experiment and different patients: the dCt of the calibrator was subtracted to the dCt for every sample, deriving the delta-delta Ct (ddCt). In the end it was possible to define the relative quantity of the expression, defined in arbitrary units (AU) as $AU=2^{-ddCt}$, because the primer used had 100% efficiency.

4.3 Biochemical analysis

4.3.1 Extraction of total cellular proteins

To obtain total cellular protein, monocytes, harvested after *in-vitro* culture or freshly purified, were washed in PBS, centrifuged at 5000 rpm for 5' at 4°C. The obtained pellet was lysed in a buffer containing: Tris-HCl (pH 7.5) 20mM, NaCl 150mM, EDTA 2mM, EGTA 2mM, Triton X-100 0.5% (v/v), dithiothreitol (DTT) 1mM (Amhersham Biosciences, UK), proteases inhibitors cocktail diluted 1:100, okadaic acid 1µM (Sigma-Aldrich, Steinheim, Germany), phenylmethylsulfonyl fluoride (PMSF) 1mM (Sigma-Aldrich, Steinheim, Germany), phosphatase inhibitors cocktail diluted 1:100 (Halt™ Phosphatase Inhibitor Cocktail, Pierce Biotechnology, Rockford, USA). The lysis was performed for 30' on ice, vortexing cells every 10'. Cells were then centrifuged at 13000 rpm for 10' at 4°C. The supernatant, containing cell protein extract, was collected and the proteins concentration was determined with the Bradford method.

4.3.2 Bradford method for protein quantification

The colorimetric system of Bradford (Sigma Aldrich, Steinheim, Germany) was used to establish proteins concentration. This method exploits the Comassie Brilliant Blue staining, which has the ability to bind proteins and to change their absorbance wavelength from 280 to 595nm, bringing the acquisition in the range of visible. In this way, the content of proteins is quantified with high sensitivity if it is in the range of 1-5µg/ml. A calibration curve was built by reading the absorbance at 595 nm with Bio

Photometer D30 (eppendorf, Milan, Italy) of different concentrations (0.5, 1, 2, 4, 8, 16 μg/ml) of the reference protein Bovine Serum Albumin (BSA; Sigma Aldrich, Steinheim, Germany). The absorbance values were plotted against the concentration of the reference protein in a Cartesian graph to obtain the calibration curve and its equation. From the equation, the coefficient of molar extinction ε was calculated. The knowledge of the coefficient of molar extinction is essential to define the protein concentration, indeed it can be obtained thanks to the Lambert-Beer law, $A=\varepsilon c\lambda$ (where A is the absorbance, c is the proteins concentration of the sample and λ is the length of the optic path). The tare of the spectrophotometer was obtained using, as blank, a solution of Bradford staining diluted 1:1 in milliQ water, then 1μL of protein extract was added to 1mL of Bradford reagent dilution and, in the end, the proteins concentration of the sample was determined reading the absorbance at λ=595nm and using the Lambert-Beer law.

4.3.3 Western Blotting (WB)

Firstly, a defined amount of extracted proteins was resuspended in a loading buffer containing 0.4 M Tris, 5% SDS, 0,25% Bromophenol Blue, 1.5% DTT, 5% β-mercaptoethanol. The protein suspension was heated at 100°C for 5'. The sample was then loaded in 10% poly-acrylamide gel and the electrophoresis run was performed at 25mA using a Tris-Glycine based running buffer TGS (Tris 25mM, glycine 192mM, SDS 0.1%, pH 8.3). The SeeBlue Plus2 Prestained Standard (Invitrogen, Carlsbad, CA) was used as molecular weight (MW).

After the electrophoretic separation, proteins were electro-transferred on a methanol activated PVDF membrane at 350mA for 2 hours, at 4°C in a buffer made of Tris 25 mM, glycine 192 mM (pH 8.3) and methanol 20%.

Subsequently, the membrane was saturated in TBS (0.137M Sodium Chloride, 0.0027M Potassium Chloride and 0.025M Tris)-Tween 0.1% (TBST), addicted with 5% w/V milk for 1 hour to block aspecific sites and then was incubated with the primary antibody in agitation overnight at 4°C.

The day after the membrane was washed for 30' in TBST followed by incubation with the secondary antibody for 1 hour. The secondary antibody dilution was: 1:5000 (anti-rabbit, made in goat, Cell Signaling Technology, USA) or 1:20000 (anti-mouse made in goat, KPL, USA) in TBST addicted with 5% of milk. After washing for 30' the membrane was ready to be developed.

Secondary Ab were conjugated with horseradish peroxidase (HRP), which converts luminol [LiteAblot ® PLUS and LiteAblot ® EXTEND (EuroClone, Milan Italy)] in a luminescent compound. The chemiluminescence measurement was performed using the Image Quant LAS 500 machine (GE Healthcare, USA) and the densitometric analysis of the bands was performed with the Image Quant TL software (GE Healthcare, USA).

The same membrane, after the "stripping" (a treatment that remove primary Ab bounded to the membrane) has been incubated with others different primary Ab. Stripping was obtained by the incubation of the membrane with the Restore Western

Blot Stripping Buffer (Pierce Biotechnology, USA) at 37°C under agitation.

4.3.3.1 Primary antibodies

For this study the following antibodies have been used: anti-phospho-STAT3(Y705), anti-STAT3, anti-phospho-p65(S536), anti-phospho-Erk (T202/Y204), anti-Erk, anti-phospho-p38(Y180/182), anti-p38, anti-GAPDH (Cell Signaling, USA) and anti-p65 (Santa Cruz Biotechnology, USA).

4.3.4 ELISA analysis for IL-6

The enzyme-linked immunosorbent assay (ELISA) was used to measure the IL-6 secretion in the culture supernatant by using Instant ELISA kit (Thermo Fisher, USA). Before starting, cell culture supernatants were centrifuged at 13000 rpm, 4°C for 10' to remove cellular debris. The microplate, already functionalized with the antibodies necessary for detection of IL-6, and the reference strips, used for the generation of the calibration curve, were prepared accordingly manufacturer instructions. Supernatant were then aliquoted in duplicate, the plate was covered and incubated for 3 hours at RT on a microplate shaker at 400 rpm.

At the end of the incubation, the microwell strips were washed 6 times with approximately 400 µl of Wash Buffer per well. The microwell plate was then dried prior the incubation with the substrate solution. The plate was subsequently incubated at RT for about 10', avoiding direct exposure to intense light, to allow the colour development through enzymatic reaction.

After 10' the colour development was monitored on a microplate reader (VictorX5 2030, Perkin Elmer, Milan, Italy) at 620 nm and the Stop Solution was added when the most concentrated standard sample reached an OD of 0.9-0.95.

The evaluation of the absorbance at 450 nm was measured by the microplate reader, which was used as the primary wavelength, whereas the absorbance at 620 nm was used as the reference wavelength.

The quantification was derived by the generation of a standard curve, using the reference strip, which were commercially available in the kit and contained a defined amount of IL-6. The absorbance value was plotted on a cartesian graph against the relative amount of IL-6 and the equation of the interpolated linear curve derived was used to derive the concentration of IL-6 in the culture supernatant.

4.3.5 Cytokines array

To determine the pattern of cytokines expression in T-LGLL, a Human Cytokine Antibody Array (Series 2000, RayBiotech, USA) was used to analyse 170 human cytokines related to angiogenesis, immunity and tumour proliferation pathways. Plasma of patients were analysed according to the manufacturer's instructions. Briefly, microarray nitrocellulose membranes were saturated in blocking buffer for 30' and subsequently incubated with 1:5 diluted samples under gentle agitation overnight at 4°C. Slides were washed in appropriate buffer and incubated with a biotin-conjugated

cocktail of antibodies for 2 hours at RT. After further washing, horseradish peroxidase (HRP)-conjugated streptavidin was incubated for 2 hours at RT. To visualise bound antibodies, samples were incubated for 5 minutes with the detection buffer and signal intensity was assessed with the chemiluminescence detector Amersham™ Imager 600 (GE Healthcare, USA). Densitometric analysis was performed by Image Quant TL software (GE Healthcare, USA). The data obtained were normalized for the mean optical density (OD) of the positive controls that were spotted in each array. The mean value of relative OD for each cytokine was then compared between patients.

4.4 Flow Cytometry

4.4.1 LGLL immunophenotype

For the immunophenotypical characterization of the patients, an immunostaining with fluorescently labelled monoclonal antibodies (BD, Becton Dickinson Europe, Milan, Italy) was performed, as reported in the table 7. For every tube 250,000 cells were stained and incubated at RT 10' in the dark. The excess of the unbound mAbs was washed with red blood cells lysis solution to get rid of eventual erythrocytes contamination, which could negatively influence the flow cytometric analysis. The cells were subsequently centrifuged for 5' at 1300 rpm at RT. The supernatant was discarded and the cells were resuspended in PBS 1X (ThermoFisher Scientific, Waltham, Massachusetts, USA). In the end, the immunophenotype was recorded in a FACS Canto II (BD, Becton Dickinson Europe, Milan, Italy) and the data processed by the Diva Software.

Table 7: Panel in use for the immunophenotypical characterization of T-LGLL patients.

Tube	FITC	PE	PE-Cy5 or PerCP-Cy5.5	APC
1	CD4	CD3	CD8	/
2	CD57	CD3	CD16	CD56
3	TCR γδ	CD3	HLA-DR	CD8
4	CD5	/	CD19	/

4.4.2 Annexin V staining

Apoptosis is a process characterized by a variety of morphological features. The translocation of the membrane phospholipid phosphatidylserine (PS) from the inner to the outer leaflet of the plasma membrane is one of the earliest indications of apoptosis.
Once exposed to the extracellular environment, binding sites on PS become available for Annexin V, which is a 35-36 kDa, Ca2+-dependent, phospholipid binding protein with a high affinity for PS. Annexin V can be conjugated to a fluorochrome, and used for the flow cytometric identification of cells in the early stages of apoptosis.

The activation of LGL apoptosis was evaluated after *in-vitro* culture of patients derived PBMC or PBMC without autologous monocytes for 1, 2, 3 and 5 days.
The staining was performed for $0.2x10^6$ cells, which were firstly harvested, washed with PBS to remove the medium and centrifuged at 1300 rpm for 5' at RT. The supernatant was then discarded and the cells were incubated for 10' in the darkness at RT with FITC-anti-human CD57. Cells then underwent a wash step with PBS and centrifuged at 1300 rpm for 5'. Subsequently the supernatant was discarded and the cells resuspended in the binding buffer (furnished by the commercial kit) with Annexin V-PE and incubated for 10' at RT, in the dark. In the end the apoptosis activation was measured by flow cytometric analysis.

4.4.3 Evaluation of Th17/Treg ratio

Th17 and Treg lymphocytes were identified by flow-cytometry among PBMC. The immunostaining was performed using $2x10^6$ PBMC using mAb obtained by Becton Dickinson (Europe, Milan, Italy) and R&D Systems (Minnealpolis, USA).

4.4.3.1 Th17 cells analysis

The immunostaing used for T17 lymphocytes is reported in table 8.

Table 8: mAb used to detect Th17 lymphocytes among PBMC.

Tubes	FITC	PE	PerCP-Cy5.5	APC	APC-Cy7
Control	CD161	/	/	/	CD4
Th17 tube	CD161	IL-17	CCR6	IL-23R	CD4

In order to properly detect the cellular population of interest, two tubes were prepared: one used as a negative control, which was stained with anti-CD4 and anti-CD161 and one used to detect the population of interest. The steps used were the following:

1) PBMC were immunostained with the mAb detecting surface antigens (CD161, CCR6, IL-23R e CD4) and incubated at RT for 20' in the dark at RT.
2) 100 µL of solution A was added in each tube (Fix and Perm, BD, Becton Dickinson Europe, Milan, Italy) and incubated at RT for 10' in the dark at RT.
3) The mAb in excess was washed with Staining Buffer (PBS + 10% FCS) and the cells centrifuged at 1600 rpm for 5' at RT.
4) The cells were then incubated with 100 µL of solution B (Fix and Perm, BD, Becton Dickinson Europe, Milan, Italy) and with anti-IL-17 at RT for 30' in the dark at RT.
5) A washing step was performed as reported above (point 3). The cells were in the end resuspened with PBS 1X and analysed by flow-cytometry using a FACS Canto II (BD, Becton Dickinson Europe, Milan, Italy) and the data processed by the Diva Software.
6) The gating strategy is reported in the figure 9.

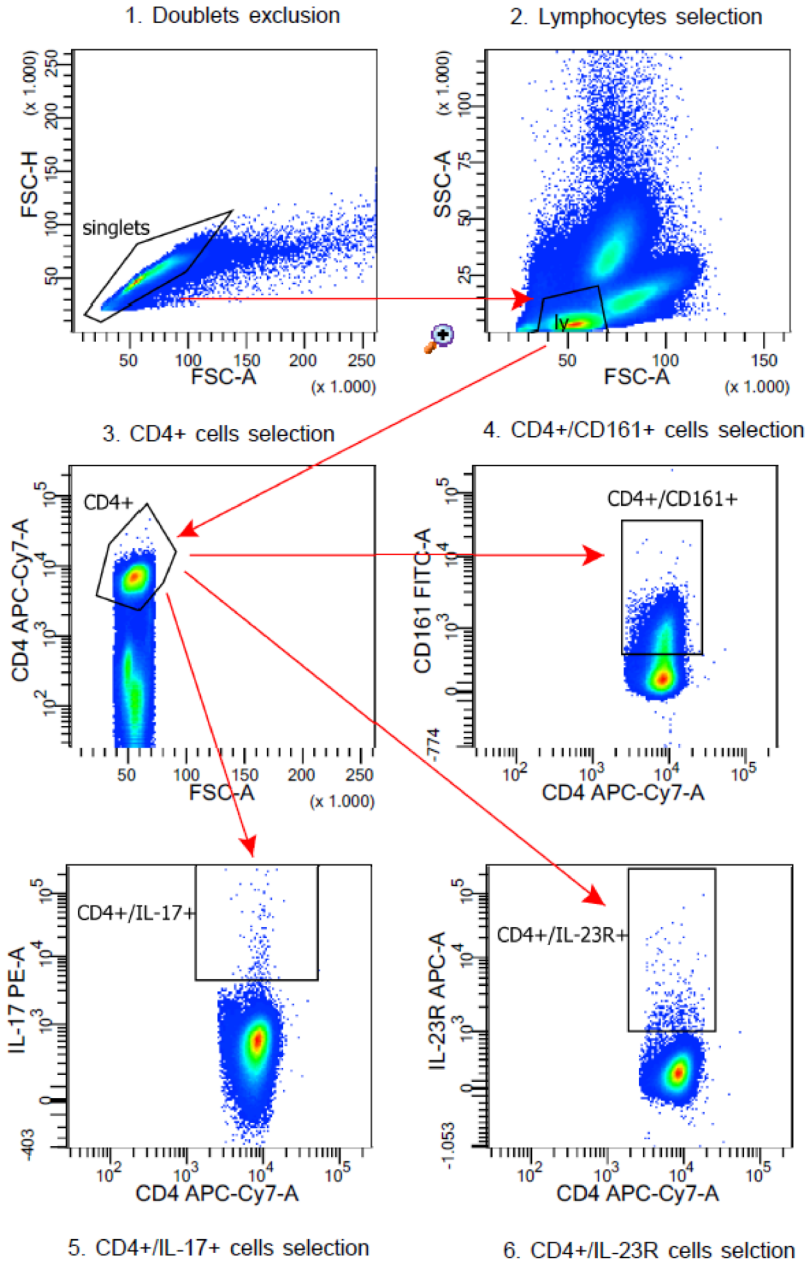

Figure 9: Gating strategy for Th17 cells identification. First of all, doublets were excluded through the selection of the population which was positioned at the bisector of the dot plot reporting the two FSC parameters [the relative pick height (H) on the y axis and amplitude (A) at the x]. To select lymphocytes based on their morphological features, SSC and FSC parameters were then reported in a dot plot. Lymphocytes gate was reported in a dot plot to select CD4+ lymphocytes based on the high intensity of this antigen expression. To identify Th17 cells, the positivity of CD4+ lymphocytes (on the x axis) and of one of the three antigens, CD161, IL-17 and IL-23R (on the y axis), was evaluated. Eventually, Th17 cells were defined as $CD4^+/CD161^+/IL\text{-}17^+/IL\text{-}23R^+$.

4.4.3.2 Treg cells analysis

The immunostaining used for Treg lymphocytes is reported in the table 9.

Table 9: mAb used to detect Treg lymphocytes among PBMC.

	PerCP-Cy5.5	PE-Cy7	APC-Cy7
FMO	/	CD25	CD4
Treg tube	FoxP3	CD25	CD4

In order to properly detect the cellular population of interest, a Fluorescence Minus One (FMO) sample was used, i.e. a tube in which every mAb, with the exception of the one necessary to identify Treg lymphocytes, was used. The steps performed were the following:

1) PBMC were immunostained with the mAb detecting surface antigens (CD25 and CD4) and incubated at RT for 20' in the dark.
2) All the solutions needed for the immunostaining were prepared as reported in the datasheet (Becton Dickinson Europe, Milan, Italy):

a. Buffer A: fixing solution;
b. Buffer B: permeabilization buffer.

3) The mAb in excess was washed with Staining Buffer (PBS + 10% FCS) and the cells centrifuged at 1600 rpm for 5' at RT.
4) The cells were incubated with 2 ml of Buffer A for 10' in the dark at RT.
5) The cells were then centrifuged 1600 rpm for 5' at RT.
6) A washing step was performed as reported in point 3.
7) 500 µl of Buffer B was added and incubated at RT 30' in the dark at RT.
8) A double washing step was performed as reported in point 3.
9) The Treg tube was incubated with anti-FoxP3 for 30' in the dark at RT.
10) A double washing step was performed as reported in point 3.
11) The cells are in the end resuspended with PBS 1X and analysed by flow-cytometry using a FACS Canto II (BD, Becton Dickinson Europe, Milan, Italy) and the data processed by the Diva Software.

The gating strategy is reported in the figure 10.

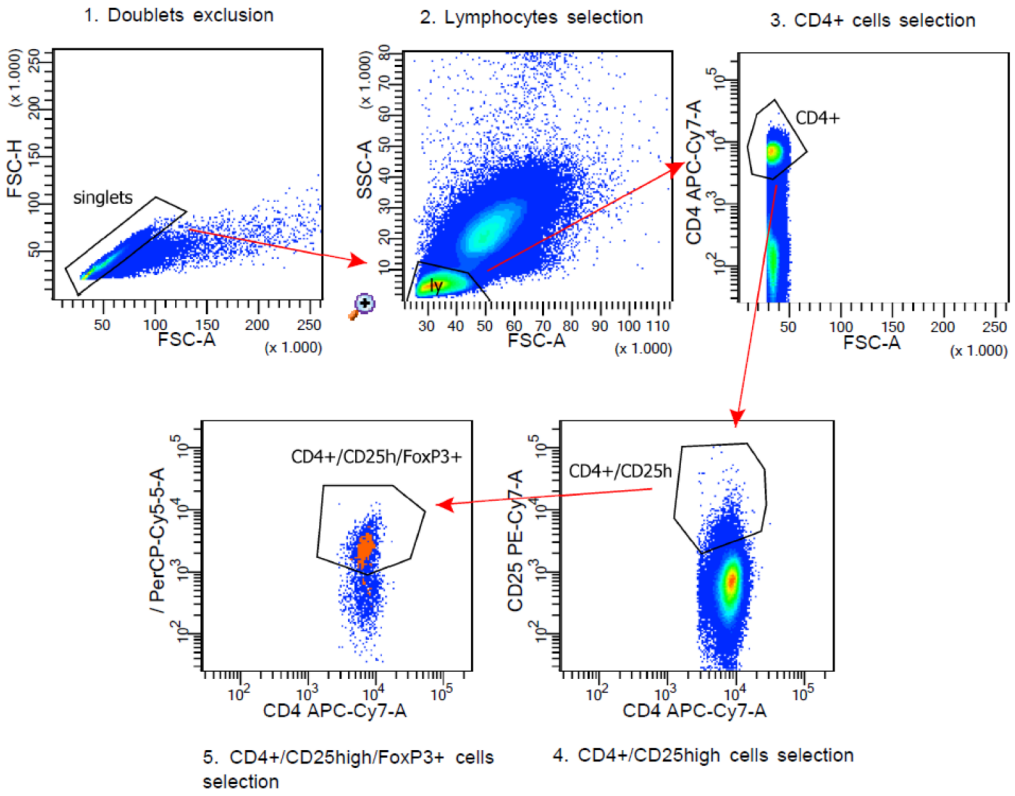

Figure 10: Gating strategy for Treg cells identification. First of all, doublets were excluded through the selection of the population which was positioned at the bisector of the dot plot reporting the two FSC parameters [the relative pick height (H) on the y axis and amplitude (A) at the x]. SSC and FSC parameters were reported in the following dot plot, in order to select lymphocytes based on their morphological features. Lymphocytes gate was reported in a dot plot to select CD4+ lymphocytes based on the high intensity of this antigen expression. Subsequently, Treg cells were selected by the identification of the CD4+ lymphocytes expressing high level of CD25 and the relative generated gate was then evaluated for intracellular FoxP3 expression.

4.4.4 Analysis of CD14 and CD16 distribution on monocytes

To evaluate the distribution of classic, intermediate and non-classical monocytes 50 µL of peripheral blood was immunostained with the following panel of mAb (table10). It was used to properly detect monocytes and to avoid contamination of other populations in the monocyte morphological gate:

- CD66b: defines granulocytes;
- CD19/CD3: defines lymphocytes;
- CD14/CD16: defines monocytes;
- HLA-DR: intermediate monocytes has the highest expression of this marker.

Table 10: mAb used to define monocytes distribution.

Tubes	FITC	PE	PerCP-Cy5.5	PeCy7	APC	APC-Cy7
Tube 1	CD66b	CD14	CD16	HLA-DR	CD19	CD3
Tube 2	CD66b	CD14	HLA-DR	CD16	CD19	CD3

The immunostaining was performed as follow:

1) The mAbs were added in the tube and the blood was incubated for 10' in the dark at RT.
2) Tubes were incubated for 5' at RT in the dark with red blood cells lysis solution to allow erythrocytes lysis.
3) The cells were centrifuged at 1300 rpm for 5' at RT.
4) The supernatant was discarded.
5) The cells were in the end resuspended with PBS 1X and analysed by flow-cytometry using a FACS Canto II (BD, Becton Dickinson Europe, Milan, Italy) and the data processed by the Diva Software.

The gating strategy was reported in the figure 11.

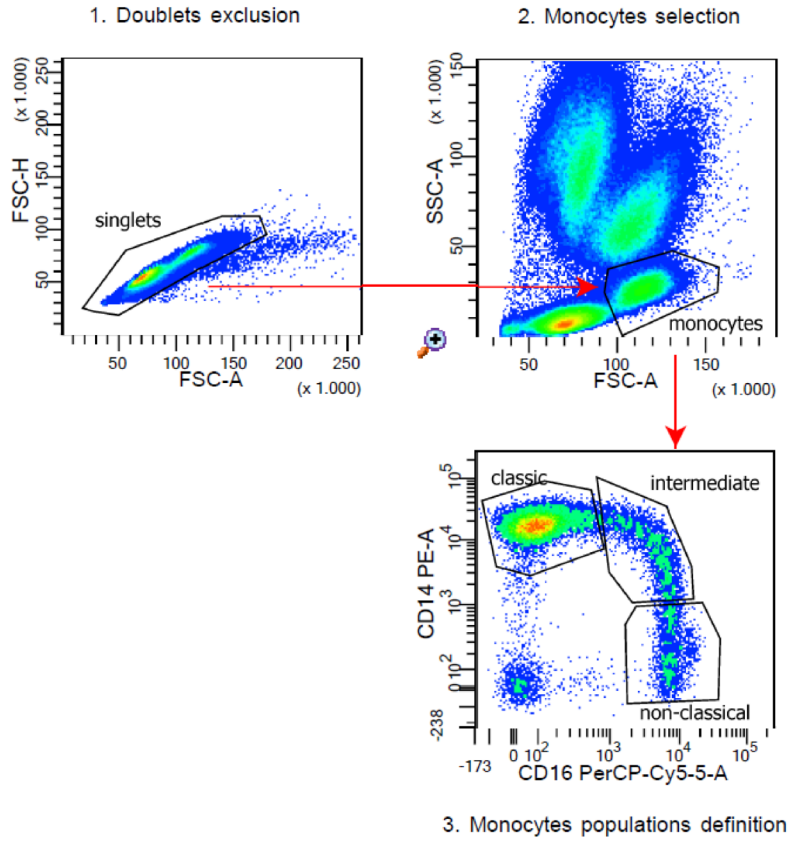

Figure 11: Gating strategy used to determine the three monocytes populations. First of all, doublets were excluded through the selection of the population which was positioned at the bisector of the dot plot reporting the two FSC parameters [the relative pick height (H) on the y axis and amplitude (A) on the x axis]. In the following dot plot were reported SSC and FSC parameters, in order to select monocytes based on their morphological features. Lastly monocytes gate was reported in the dot plot which harbours the fluorescence intensity given by the positivity, on the y axis, to CD14 and, on the x axis, to CD16. The three monocytic populations were then selected according to their immunophenotypical features: classic monocytes are defined by the $CD14^{high}/CD16^{-}$ phenotype, intermediate by the $CD14^{+}/CD16^{\pm}$ phenotype and non-classical by the $CD14^{\pm}/CD16^{+}$ phenotype.

4.5 Statistical analysis

Statistical evaluations were carried out using GraphPad (California, USA) and R software. Data were firstly analysed for normal distribution with Kolmogorov-Smirnov test or Shapiro-Wilk test. Statistical significance between two groups was assessed with t-test or Mann-Witney test, according to data distribution. Comparisons between groups were evaluated by one-way ANOVA or Kruskal-Wallis test, based on data distribution. For the analysis of more variable between groups two-way ANOVA test was used.

5 Results

5.1 Leukemic T-LGL survival depends on monocytes

The relevance of monocytes in favouring survival of pathological LGL has been evaluated in two different *in-vitro* culture systems: PBMC and PBMC deprived of CD14+ cells. The evaluation of LGL apoptosis was carried out using AnnexinV staining on LGL at different time points by flow cytometry. LGL were identified by fluorescently labelled monoclonal antibodies against CD57, CD56 or CD8. The analysis was performed on healthy controls (HC) and on T-LGLL patients and the results are reported in figure 12.

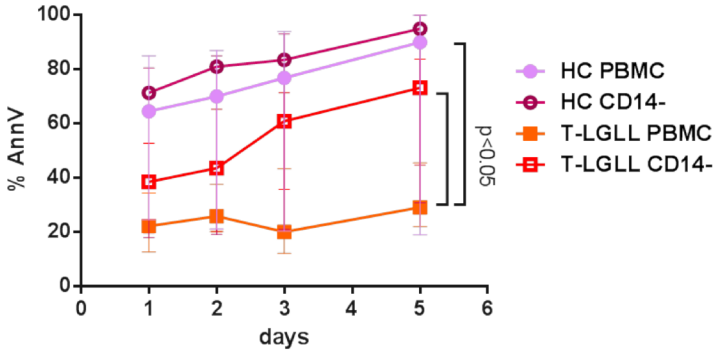

Figure 12: LGL apoptosis evaluation after *in-vitro* culture. LGL AnnexinV staining has been performed on 3 HC and 11 T-LGLL patients after *in-vitro* culture of PBMC or PBMC deprived of CD14+ cells. The level of apoptosis has been evaluated at 24, 48, 72 hours, 3 and 5 days by flow cytometry. The plot reports the median percentages and interquartile range (IQR) of LGL apoptosis for each group at the different time points. Data distribution has been evaluated by Kolmogorov-Smirnov test and statistical significance assessed with Kruskal-Wallis test.

LGL of T-LGLL patients were found to be more prone to survive *in-vitro* in comparison to LGL of HC. The data are reported as median percentage with first and third quartile (Q1; Q3). The median percentage of LGL apoptosis, over five days of PBMC culture, were significantly lower in patients than HC [27.48% (24.85%; 32.78%) against 61.52% (58.33%; 68.15%), $p<0.05$].

Two different behaviours were also observed in HC and patients when LGL apoptosis levels were compared among the two types of *in-vitro* culture. Within HC samples, LGL apoptosis was comparable in PBMC culture both with and without monocytes. In T-LGLL patients' PBMC culture, LGL were more apoptotic in the condition without CD14+ cells [51.35% (40.80%; 64.49%)] than with whole PBMC. The difference resulted to be significant after 3 and 5 days of culture, with a $p<0.05$. Taken together, a different CD14+ dependence and survival for normal LGL has been observed in comparison to leukemic LGL, for which monocytes were demonstrated to be crucial in maintaining survival.

5.2 Evaluation of T-LGL-monocytes interaction

5.2.1 CCL5 induces monocytes to produce IL-6

Several cytokines are known to be deregulated in patients' plasma, including IL-6 and CCL5[112]. The mechanism of action of IL-6 on LGL survival has been clarified, whereas the role of CCL5 in LGLL is still a matter of debate[113]. Interestingly, since CCR5, one of CCL5 receptors, is significantly down-regulated in leukemic T-LGL[115], the relationships between CCL5 and monocytes have been investigated. To this aim, immuno-magnetically purified monocytes and residual LGL negative fraction, were incubated for 12 hours with 100 ng/ml CCL5 in order to assess whether this chemokine might induce IL-6 expression. Results are reported in figure 13.

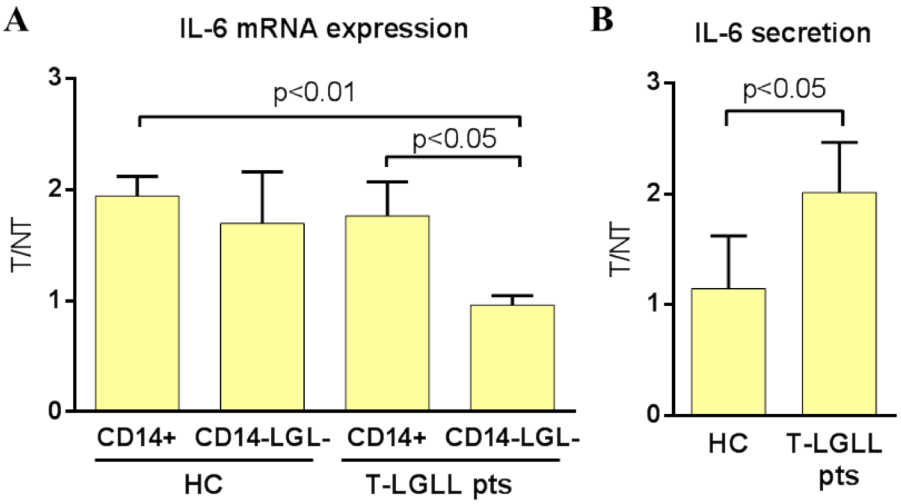

Figure 13: Panel A. Evaluation of IL-6 mRNA expression after CCL5 stimulation. Autologous monocytes (CD14+) and CD14-/LGL- fraction derived from 5 HC and 9 T-LGLL patients have been *in-vitro* stimulated for 12 hours with 100 ng/ml CCL5. IL-6 mRNA expression has been assessed by RT-pPCR and the relative expression of the treated condition has been normalized to the untreated one (T/NT). The bar plot reports the means (±SEM) of the T/NT for the different cell populations. Data distribution has been assessed by Kolmogorov-Smirnov test and statistical significance evaluated by unpaired t-test with Welch's correction. **Panel B: IL-6 monocytes secretion after CCL5 stimulation.** The level of IL-6 has been evaluated by ELISA assay on monocytes supernatants collected from the *in-vitro* cultures with or without CCL5 treatment. The IL-6 concentration of treated sample was normalized to the untreated one (T/NT). The bar plot reports the median and IQR of the T/NT. Data distribution has been assessed by Kolmogorov-Smirnov test and statistical significance evaluated by Mann-Witney test.

The results showed that CCL5 induced IL-6 mRNA expression on monocytes similarly in HC and patients, with mean fold increase (FI) of 1.941 (±0.180) and 1.763 (±0.398), respectively. On the other hand, different behaviours were observed for the relative negative fractions: a comparable IL-6 induction was observed in HC (FI=1.696 ±0.466), whereas no activity was detected in patients (FI=0.962 ±0.086). This lack of stimulation

resulted to be significantly different in comparison to the induction observed on HC' and patients' monocytes, with a $p<0.05$ (fig. 13A).
Interestingly, following CCL5 monocytes stimulation, the amount of IL-6 in the supernatant resulted to be increased only in patients as compared to HC (respective median FI: 1.146 (1.076; 1.619) and 2.012 (1.303; 2.462), $p<0.05$, fig. 13B).

These data indicate an increase of IL-6 production by patients' monocytes following CCL5 exposure, suggesting a possible mechanism of CCL5 action in T-LGLL. To gain insights on the pathways involved upon CCL5 stimulation, STAT3, p65 and ERK were analysed by Western Blot on patients' and healthy controls monocytes. Results are reported in figure 14.

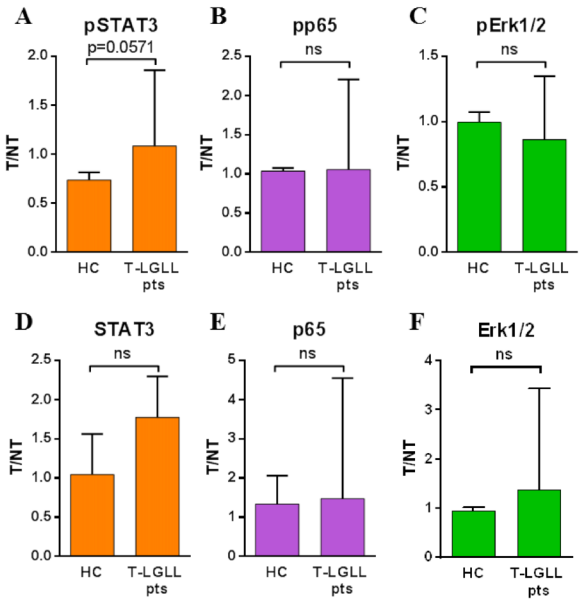

Figure 14: Evaluation of STAT3, p65 and ErK1/2 activation in monocytes after CCL5 stimulation. Monocytes derived from 3 HC and 4 T-LGLL pts have been *in-vitro* stimulated for 12 hours with 100 ng/ml CCL5. 10 µg of extracted proteins have been analysed through Western Blotting and the level of phosphorylation or expression determined by densitometric analysis. **Panel A, B, C: Evaluation of STAT3, p65 and Erk1/2 phosphorylation.** The bar plots report the median and IQR fold increase of phosphorylation in response to CCL5 treatment for HC and T-LGLL patients. The level of the phosphorylated protein has been normalized over the total amount of the relative protein and then the value obtained for the treated sample was normalized to its untreated condition (T/NT). The induction of pSTAT3 is reported in panel A, pp65 in B and pErk1/2 in C. **Panel D, E, F: Evaluation of STAT3, p65 and Erk expression.** The bar plots reported the median and IQR fold increase of expression in response to CCL5 treatment for HC and T-LGLL patients. The protein level has been normalized over GAPDH, as loading control, and then the value obtained for the treated sample has been normalized to its untreated condition. The induction of STAT3 expression is reported in panel D, p65 in E and Erk1/2 in F.

The downstream targets activation resulted to be similar between T-LGLL patients and HC. 12 hours treatment with CCL5 did not induce a strong p65 and Erk1/2 activation or expression, with a high variability being observed among patients. The large variability

after CCL5 stimulation was also evident for STAT3 activation: pSTAT3 resulted slightly downmodulated in healthy controls [0.737 (0.558; 0.816)] but not in patients [1.085 (0.982; 1.855)], the difference, however, was not statistically significant (p=0.0571). Similarly, the trend of STAT3 expression appears more easily induced in patients [1.772 (1.136; 2.296)] than HC [1.044 (0.7790; 1.561)]; more data are then necessary to assess the statistical significance.
Altogether these WB analyses evidenced that 12h CCL5 stimulation was able to partially induce STAT3 activation only in patients.

5.2.2 Leukemic CD8+ T-LGL are involved in monocytes IL-6 expression through CCL5

The PBMC expression of CCL5 in LGLL patients has been previously reported[113], but the precise cellular source of this chemokine was not defined. Therefore, RT-qPCR analysis of CCL5 mRNA expression was performed in immune-magnetically purified LGL and related negative fractions of HC and T-LGLL patients. As reported in figure 15A, CCL5 resulted to be mainly produced by T-LGL both in HC [mean arbitrary units (AU) of expression: 7.203 ±2.298)] and in patients (10.446 ±1.650) as compared to the relative negative fraction (2.497 ±1.490 and 4.196 ±0.546, respectively). Moreover, the high T-LGL CCL5 expression observed resulted to be significantly different with respect to the remaining fraction of the PBMC for patients, with a $p<0.01$.
To verify whether LGLL patients could express distinct CCL5 levels according to their different immunophenotype, patients were clustered as CD8+ and CD4+ T-LGLL and the results are plotted in fig. 15B. The increased CCL5 expression observed in T-LGLL patients was mainly related to CD8+ patients (15.050 ±2.347), significantly higher than HC ($p<0.05$) and CD4+ cases (6.500 ±0.744, $p<0.01$).
On the other hand, when the basal mRNA expression of IL-6 on CD8+ and CD4+ patients' and healthy controls' monocytes was compared, no significant differences among the groups were found (fig. 15C). Nevertheless, a high variability among patients, particularly for CD8+ cases, was reported; around 25% of them harboured also 10-fold increased expression, but further analysis might be necessary to uncover the molecular difference of the patients characterized by high IL-6 production.

Provided the role of CCL5 in inducing monocytes IL-6 expression and in view of the fact that CCL5 was mainly produced by T-LGL, a crosstalk between monocytes and T-LGL could be proposed through these two cytokines. Moreover, the significantly higher T-LGL CCL5 expression in CD8+ T-LGLL patients could suggest that this axis is likely to be more important for this group of patients in comparison to the CD4+ subset.

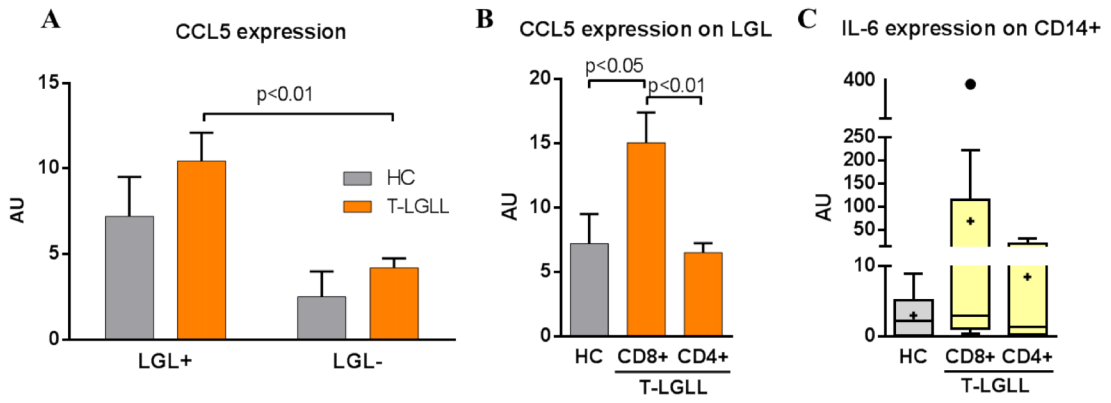

Figure 15: Evaluation of CCL5 and IL-6 basal expression. Panel A and B: CCL5 mRNA expression evaluation. CCL5 expression has been evaluated by RT-qPCR. Data are reported in a bar plot as the mean (±SEM) of the relative CCL5 expression, determined with the ddCt method and expressed as arbitrary units (AU). Normal distribution has been assessed by Kolmogorov-Smirnov test and statistical significance by two-way ANOVA test. **A.** Immune-magnetically purified LGL and the relative negative fraction were obtained from 3 HC and 13 T-LGLL patients. **B.** The expression data of the LGL fraction from the panel A is reported in panel B subdividing T-LGLL patients according to the immunophenotype in CD8+ (n=6) and CD4+ patients (n=7). **Panel C: IL-6 mRNA expression on monocytes.** Immuno-magnetically CD14+ cells were analysed for IL-6 expression by RT-qPCR. Seven HC, 9 CD8+ and 7 CD4+ T-LGLL patients were analysed. Data distribution was assessed by Kolmogorov-Smirnov test and statistical significance by Kruskal-Wallis test. ● identifies outliers and + represents the mean.

5.3 Monocytes characterization between T-LGLL groups

Since monocytes resulted to be important in mediating leukemic T-LGL survival, in order to dissect the different mechanisms behind the microenvironmental role in T-LGL lymphoproliferation sustainment, a phenotypical and molecular characterization of monocytes was performed.

5.3.1 Monocytes classes distribution is altered in T-LGLL

Recently different types of monocytes characterized according to CD14 and CD16 antigenic density have been identified, i.e. classic, intermediate and non-classical monocytes. Moreover, monocytes sub-types distribution was found altered in several pathological conditions as autoimmune diseases, often related to T-LGLL[27]. In order to analyse the distribution of the three group of monocytes, flow cytometric evaluations of CD14 and CD16 expression have been performed on monocytes collected from peripheral blood of the two T-LGLL groups of patients. The results obtained are reported in figure 16.

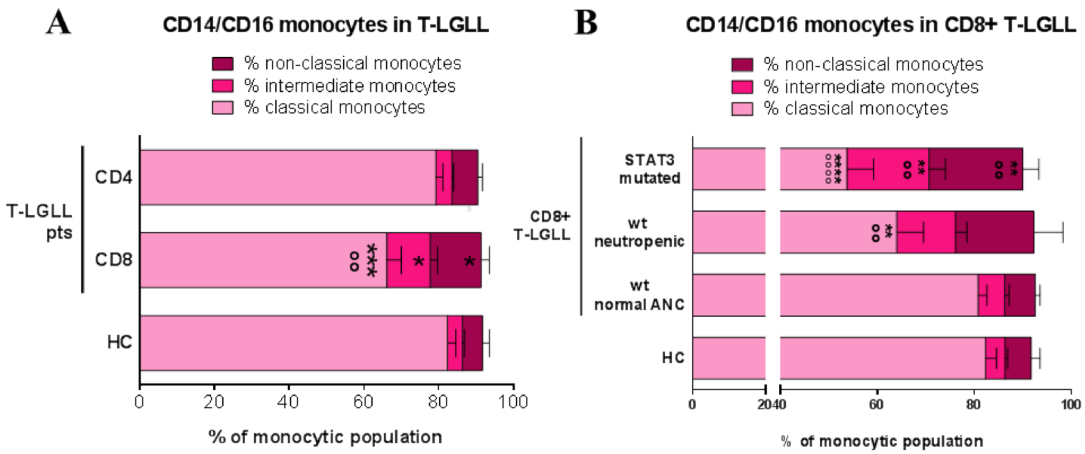

Figure 16: Evaluation of monocytes populations distribution in T-LGLL. Panel A: Evaluation of monocytes populations distribution in T-LGLL. Samples from peripheral blood of 5 HC, 20 CD8+ *STAT3* wt, and 16 CD4+ T-LGLL patients have been analysed. The bar plot reports the cumulative means (± SEM) of the 3 monocytes groups. Normal distribution was assessed by Kolmogorov-Smirnov test and statistical significance by two-way ANOVA test. The significance is reported as ○○=p<0.01 when CD8+ patients are compared to HC and ***=p<0.001 or *=p<0.05 when compared to CD4+ patients. **Panel B: Evaluation of monocytes populations distribution in CD8+ T-LGLL.** The bar plot reports the cumulative means (± SEM) of the 3 monocytes groups for 5 HC, 9 CD8+ *STAT3* mutated and 11 CD8+ *STAT3* wt patients which were selected for presence of neutropenia, i.e. ANC<1,500, (respectively n=8 non neutropenic and n=3 neutropenic). Statistical significance is represented in the plot as: ○○ or **=p<0.01 and ○○○○ or ****= p<0.0001. ○ indicates statistical significance against HC and * against CD8+ *STAT3* wt non-neutropenic patients.

The mean percentage of the three groups of monocytes for CD8+ patients resulted to be statistically different than in CD4+ cases. In particular, classical monocytes were significantly reduced in CD8+ cases (p<0.001) and the relative mean percentage was 66.152% ±3.844% whereas in CD4+ cases was 79.252% ±1.892%. This matched with a significant increase of intermediate (11.581% ±1.955) and non-classical (13.640%

±2.176%) monocytes in CD8+ patients as compared to CD4+ cases (4.314% ±0.414% and 6.924% ±1.170%, respectively; $p>0.05$). Moreover, classical monocytes from CD8+ patients also resulted to be significantly reduced as compared to healthy controls (82.340% ±2.214%, $p>0.01$), whereas monocytes population from CD4+ cases were consistent with that of healthy controls (fig. 16A).
Within CD8+ patients, both *STAT3* wt and *STAT3* mutated cases were included. The stringent correlation between *STAT3* mutation and neutropenia has been recently reported when the leukemic clone was phenotypically characterized by the expression of CD8 and CD16 with the absence of CD56[72]. However, some neutropenic CD8+/CD16+/CD56- *STAT3* wt patients have been also identified. Accordingly, the mean percentages of the three groups of monocytes within the CD8+ category have been clustered according to presence or absence of *STAT3* mutation and neutropenia. The analysis, reported in figure 16 Panel B, showed a characteristic pattern of monocytes subsets on CD8+ *STAT3* mutated patients, which was represented by 53.796% (±5.466%) classical, 16.884% (±3.363%) intermediate and 19.326% (±3.311%) non-classical monocytes, as compared with healthy controls and CD8+ *STAT3* wt non-neutropenic cases ($p<0.01$). On the contrary, the median percentages of monocytes in CD8+ *STAT3* wt non-neutropenic patients were comparable with those of healthy controls. Concerning CD8+ *STAT3* wt neutropenic patients a significant reduction of classical monocytes (64.067% ±5.488%) was observed in comparison to healthy controls and CD8+ *STAT3* wt non-neutropenic cases, $p<0.01$. In addition, a slight increase of intermediate (12.067% ±2.385%) and non-classical monocytes (16.167% ±5.984%) was detected, even if not statistically significant, probably as a consequence of the low number of cases.
A similar dissection of CD4+ patients was not performed because no changes in monocytes percentages within the group when compared to healthy controls had been identified.

The above results taken together, it was possible to establish an accumulation of intermediate and non-classical monocytes for CD8+ T-LGLL patients. In detail, the imbalance was evidenced for CD8+ *STAT*3 mutated patients, including all neutropenic cases, but also in other classes in relationship to neutropenia. This correlation between neutropenia and monocytes sub-populations disequilibrium deserves further investigation.

5.3.2 Analysis of monocytes transcriptional activity

Gene expression profiling studies of classic, intermediate and non-classical monocytes have described different patterns of transcriptional activity. Some genes involving NFkB machinery and pro-inflammatory cytokines production, as IL-23 and TNFα, resulted to be more expressed in intermediate or non-classical monocytes[20], whereas the expression of the anti-inflammatory IL-10 was higher in classic monocytes when compared to other classes. Regarding surface receptors CCR5, a receptor for the chemokine CCL5, was exclusively expressed by intermediate monocytes and the level of ADAM17 expression was higher for non-classical monocytes[20]. Therefore, in order to evaluate whether the expression of these genes was altered in T-LGLL patients' monocytes, the level of p65, NFkB1, IRF8, IL-23, TNFα, IL-10, CCR5 and ADAM17 expression in immuno-magnetically purified monocytes was evaluated by RT-qPCR.
Patients have been clustered according to the expression of CD8 or CD4 on the leukemic clone and the results were reported in figure 17. The levels of expression of the selected genes resulted to be conserved among the groups. However, a higher variability of the levels of expression for patients than healthy controls was detectable, possibly as a consequence of the presence of several outliers.

The two groups of patients were further subdivided according to *STAT3/5b* mutational status. Even if significant differences were not evidenced, some minimal changes among groups were detectable (fig. 18). In particular, despite the difference was not significant due to the high internal variability, a slight higher median expression of CCR5 was observed for CD8+ *STAT3* mutated patients [5.819 (1.023; 86.430)] in comparison to other groups. CCR5 expression for the other groups was 1.575 (0.3210; 2.751) for HC, 2.007 (0.185; 3.517) for CD8+ *STAT3* wt, 0.521 (0.409; 2.828) CD4+ *STAT5b* wt and 2.858 (0.506; 85.580) for CD4+ *STAT5b* mutated patients.
These data showed that the expression pattern of relevant inflammatory mediators in total monocytes was not significantly deregulated in T-LGLL patients in comparison to healthy controls. On CD4+ T-LGLL this result was expected since we observed that the monocyte classes distribution was similar to HC. On the other hand, in CD8+ T-LGLL (i.e. mostly CD8+ *STAT3* mutated cases) it was possible to observe that the increased percentage of intermediate and non-classical monocytes did not affect the monocytes overall gene expression. Anyway, differences in this group of patients could potentially be hidden by the percentage of classical monocytes, which still represented the mostly represented monocytes class.

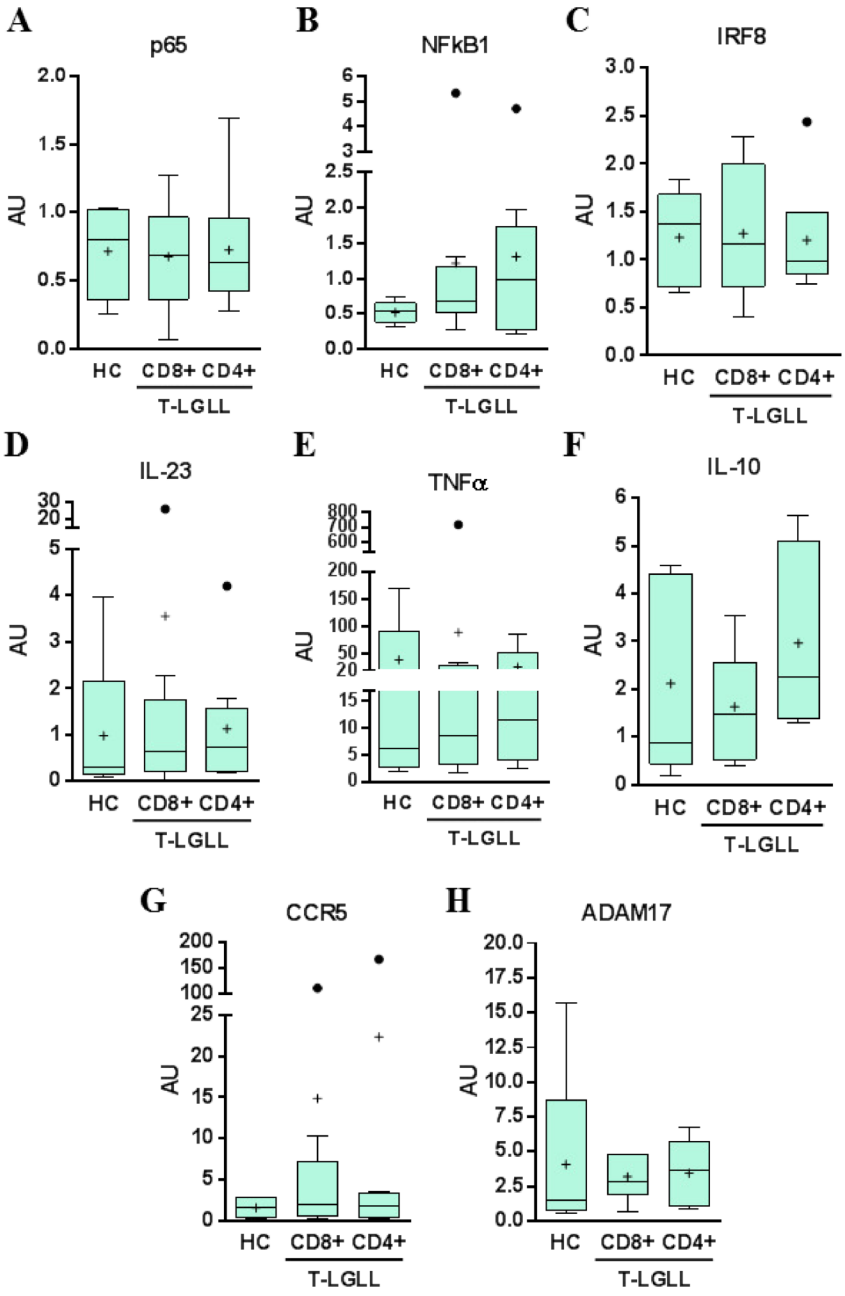

Figure 17: RT-qPCR analyses of different genes among classic, intermediate and non-classical monocytes. The level of mRNA expression was assessed in immuno-magnetically purified monocytes for 5 HC, 9 CD8+ and 10 CD4+ T-LGLL patients. p65, NFkB1, IRF8, IL-23, TNFα, IL-10, CCR5 and ADAM17 were evaluated and the related amount of expression was calculated by the ddCt method. Data distribution was evaluated by Kolmogorov-Smirnov test and statistical significance by one-way ANOVA or Kruskal-Wallis tests according to data distribution. Data are reported in box-plot as arbitrary units referred to the relative amount of expression. ● identifies outliers and + represents the mean.

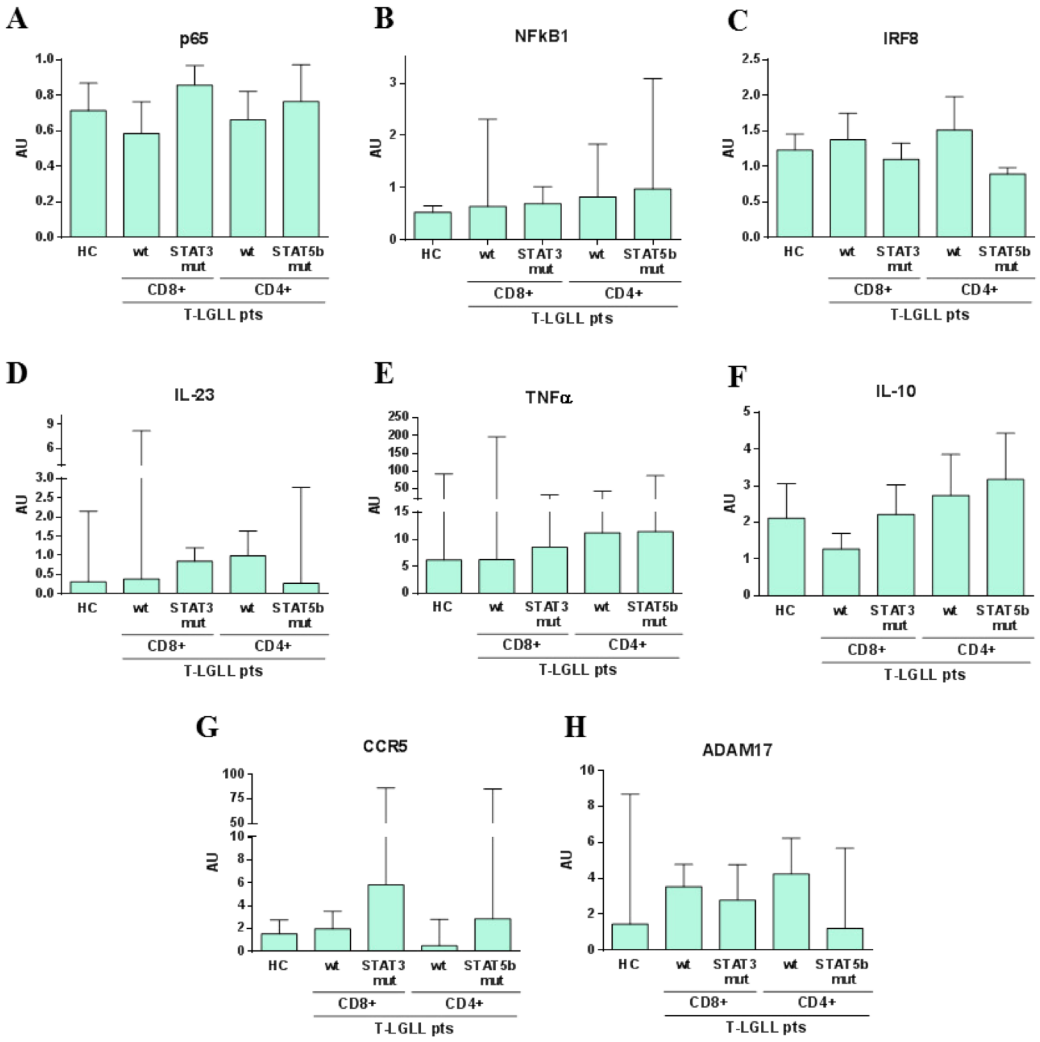

Figure 18: RT-qPCR analyses of differently expressed genes among classic, intermediate and non-classical monocytes in T-LGLL categories. The level of mRNA expression was assessed on immuno-magnetically purified monocytes for 5 HC, 6 CD8+ *STAT3* wt, 3 CD8+ *STAT3* mutated, 4 CD4+ *STAT5b* wt and 6 CD4+ *STAT5b* mutated T-LGL patients. p65, NFkB1, IRF8, IL-23, TNFα, IL-10, CCR5 and ADAM17 were evaluated and the related amount of expression was calculated by the ddCt method and reported in the plot as arbitrary units. Data distribution was evaluated by Kolmogorov-Smirnov test and statistical significance has been assessed with one-way ANOVA or Kruskal-Wallis tests according to data distribution. CD14+ cells immune-magnetically purified from 5 HC were analysed. RT-pPCR was performed and the related amount of expression was obtained by the DDct method and reported in the bar plots as arbitrary units (AU). **Panel A, C and F show the monocytes expression of p65, IRF8 and IL-10, respectively.** The means (±SEM) of the gene expression are reported in the bar plots. **Panel C, D, E, G and H show the monocytes expression of NFkB1, IL-23 and ADAM17, respectively.** The medians and IQR of the gene expression are reported in the bar plots.

5.3.3 Analysis of intracellular pathways activation in monocytes

Monocytes were known to play a role in cancer inflammation through several cellular pathways. NFkB and STAT3 signaling are the most important pathways reported in literature, which resulted to be activated and reciprocally linked. In fact, several cytokines and growth factors encoded by p65 were STAT3 activators[134]. Moreover, NFkB could interact also with MAPK to exert a pro-inflammatory stimulation on monocytes[135], which in turn could be addressed by cellular senescence by the activation of Erk[24].

To characterize the potential pro-inflammatory role then of T-LGLL patients' monocytes, the above mentioned cellular pathways were then evaluated in immune-magnetically purified CD14+ cells by Western Blotting analysis. The total protein expression has been evaluated and the pathways activation was assessed by the analysis of the phosphorylation of STAT3 (Y705), p65 (S536), Erk1/2 (T202/Y204) and p38 (Y180/182), in order to evaluate the activation of JAK/STAT, NFkB and MAPK axes, respectively. Patients have been divided according to the immunophenotype in CD8+ and CD4+ cases.

CD8+ T-LGLL patients' monocytes harboured a significant higher proteins expression when compared to healthy controls or CD4+ cases (fig. 19A, B, C and D). Mean STAT3 expression was 0.674 ±0.103 for CD8+ patients, which was significantly higher than HC (0.282 ±0.069, $p<0.01$) and CD4+ cases (0.397 ±0.040, $p<0.05$). Similarly, in CD8+ the mean expression of p65 (0.728 ±0.224) and Erk1/2 expression (2.067 ±0.271) was significant higher than HC and CD4+ cases (p65: 0.188 ±0.045 and 0.257 ±0.098, $p<0.05$; Erk1/2: 0.674 ±0.112 and 0.360 ±0.059, $p<0.001$). Only a slight, not significant, increase was detected for p38 in the CD8+ patient group as compared to the other two groups.

The increased expression levels above mentioned did not correlate with a higher protein activation. Indeed, only a slight increased phosphorylation of p65 for CD8+ cases (1.314 ±0.487) was observed when compared to HC (0.356 ±0.117) and CD4+ patients (0.973 ±0.293), but the difference did not result to be statistically significant (fig. 19F). The phosphorylation levels of STAT3 and p38 were not different among the studied groups (fig. 19E and H). Rather, a significant higher Erk1/2 phosphorylation was evidenced in CD4+ patients (1.863 ±0.439) than HC (0.457 ±0.099) and CD8+ cases (0.718 ±0.409), with a $p<0.05$ (fig 19G).

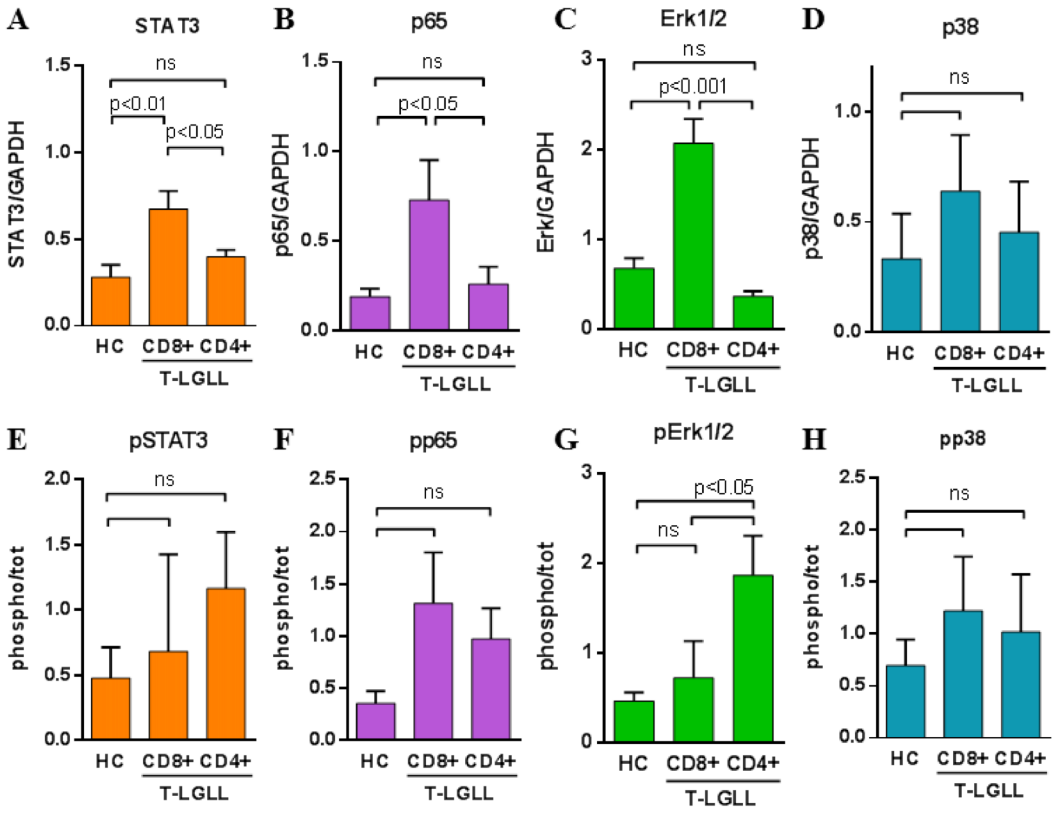

Figure 19: Evaluation of monocytes protein activation and expression in T-LGLL. Total protein lysate of immuno-magnetically purified monocytes from 6 HC, 6 CD8+ and 7 CD4+ T-LGLL patients has been analyzed through Western Blotting. The densitometric values of total protein expression were normalized over GAPDH. The four plots on the top of the figure report STAT3, p65, Erk1/2 and p38 protein expression. The four plots on the bottom of the figure report STAT3, p65, Erk1/2 and p38 phosphorylation, which was calculated normalizing the level of phosphorylation to the related amount of total proteins. Data distribution was evaluated by Kolmogorov-Smirnov test and then, according to data distribution, statistical significance was assessed with Kruskal-Wallis or one-way ANOVA test. **Panels A, B, C, F, G and H**. The means (±SEM) of the gene expression are reported in the bar plots. **Panels D and E**. In the bar plots the medians and IQR of the gene relative expression are shown.

Patients were further subdivided according to their mutational status, in order to identify whether the biological difference of the leukemic clone would influence also monocytes signaling.

The higher proteins expression previously identified in CD8+ patients was mostly restricted to *STAT3* mutated ones. Indeed, STAT3 expression (0.784 ±0.117) and p65 [0.780 (0.283; 1.566)] resulted significantly higher in CD8+ *STAT3* mutated patients than healthy controls ($p<0.001$ and $p<0.05$, respectively), CD8+ *STAT3* wt cases ($p<0.05$) and CD4+ cases, both *STAT5b* wt and *STAT5b* mutated ($p<0.01$) (fig 20A, 20C). Similarly, the slight increase of p38 above described in CD8+ patients was restricted to the *STAT3* mutated group (0.813 ±0.217), as the expression was significantly higher than healthy controls ($p<0.05$, fig. 20G). On the other hand, the higher Erk1/2 expression previously detected in CD8+ patients was found both in

STAT3 wt (1.868 ±0.225) and *STAT3* mutated (2.167 ±0.407) cases and resulted statistically significant when compared to the other groups (fig. 20E).
Concerning the levels of proteins activation, a significant increased p65 and Erk1/2 phosphorylation was detected for CD4+ *STAT5b* wt patients. In detail, the median phosphorylation levels for p65 was 1.222 (0.719; 2.259) and significantly higher than HC with $p<0.05$ (fig. 20D). The median phosphorylation levels for pErk1/2 was 2.657 (1.911; 3.908), which was significantly higher than HC ($p<0.01$) and CD8+ cases, both *STAT3* wt [0.459 (0.248; 0.669)] and mutated [0.288 (0.106; 2.150), $p<0.05$]; whereas the pErk was consistent with CD4+ *STAT5b* mutated patients [1.023 (0.608; 1.792), fig. 20F]. On the other hand, for STAT3 phosphorylation and p38 activation no statistically significant differences were detected (fig. 20B and H).

The evaluation of protein expression and activation showed different pattern in CD8+ and CD4+ T-LGLL patients. In CD8+ patients' monocytes, mostly in *STAT3* mutated cases, a higher expression of STAT3, p65, Erk1/2 and p38 was described in comparison to every other group. However, a significant increase in their phosphorylation levels was not detected. On the other hand, CD4+ patients' monocytes, precisely *STAT5b* wt cases, were characterized by a higher activation of Erk in comparison to healthy controls and CD8+ patients and of p65 with respect to healthy controls.

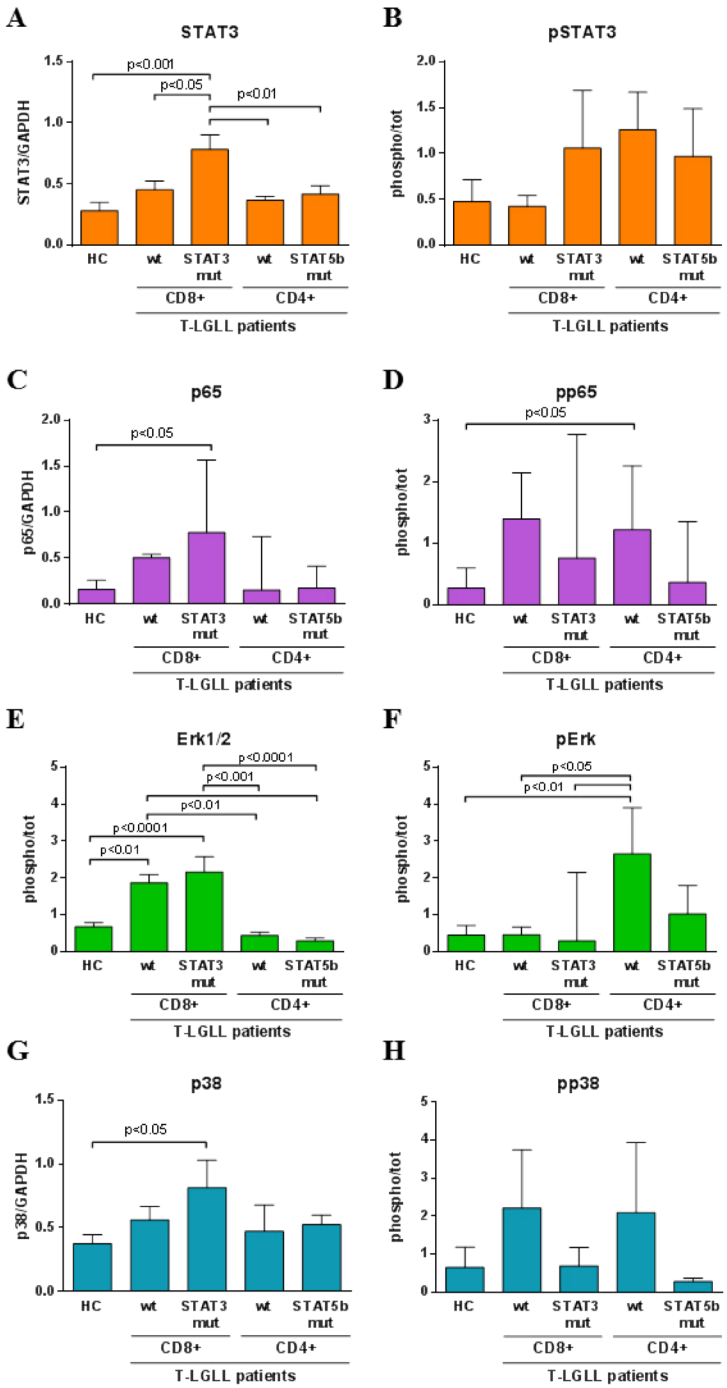

Figure 20: Evaluation of monocytes protein activation and expression in T-LGLL categories. Total protein lysate of immuno-magnetically purified monocytes from 6 HC, 3 CD8+ *STAT3* wt, 4 CD8+ *STAT3* mutated, 3 CD4+ *STAT5b* wt and 4 CD4+ *STAT5b* mutated T-LGLL patients has been analyzed through WB. The densitometric values of total protein expression were normalized over GAPDH. The four plots on the left of the figure report STAT3, p65, Erk1/2 and p38 protein expression. The four plots on the bottom of the figure report STAT3, p65, Erk1/2 and p38 phosphorylation, which was calculated normalizing the level of phosphorylation to the amount of total proteins. Data distribution was evaluated by Kolmogorov-Smirnov test and then, according to data distribution, statistical significance was assessed with Kruskal-Wallis or one-way ANOVA test. **Panels A, B, C, F, G and H.** In the bar plots the means (±SEM) of the gene relative expression are reported. **Panels D and E.** The medians and IQR of the gene relative expression are reported in the bar plots.

5.4 Th17 and Treg cells are altered in T-LGLL

A proper balance between Th17 and Treg populations was reported to be crucial for keeping immune response at a physiological level and a Th17/Treg ratio deregulation contributed to the pathogenesis of several autoimmune and oncological diseases[47]. Since T-LGLL has often been associated to autoimmune diseases, flow cytometric analyses have been performed to evaluate the percentage of Th17 cells and Treg lymphocytes on patients' and healthy controls' PBMC. Th17 population was identified according to the immunophenotype $CD4^+/CD161^+/IL\text{-}23R^+/IL\text{-}17^+$ and Treg cells were defined as $CD4^+/CD25^{high}/FoxP3^+$ cells. Subsequently, the ratio of Th17 and Treg cells percentages has been calculated for every sample. Patients were divided according to the expression of CD8 or CD4 and the results were reported in figure 21.
The percentage of Th17 resulted to be significantly higher in CD8+ patients (0.0329% ±0.008%) in comparison to CD4+ cases (0.012% ±0.003%, $p<0.01$) and healthy controls (0.006% ±0.001%, $p<0.05$). On the other hand, CD4+ patients harboured a significant reduction in Treg cells (0.597% ±0.119%) in comparison to CD8+ cases (1.657% ±0.230%, $p<0.001$) and healthy controls (1.455% ±0.380%, $p<0.05$). The calculated ratio between Th17 and Treg evidenced a significant deregulation, in favour of Th17 cells, either for CD8+ (0.018 ±0.005) or CD4+ patients (0.025 ±0.005) when compared to HC (0.006 ±0.002, $p<0.05$).

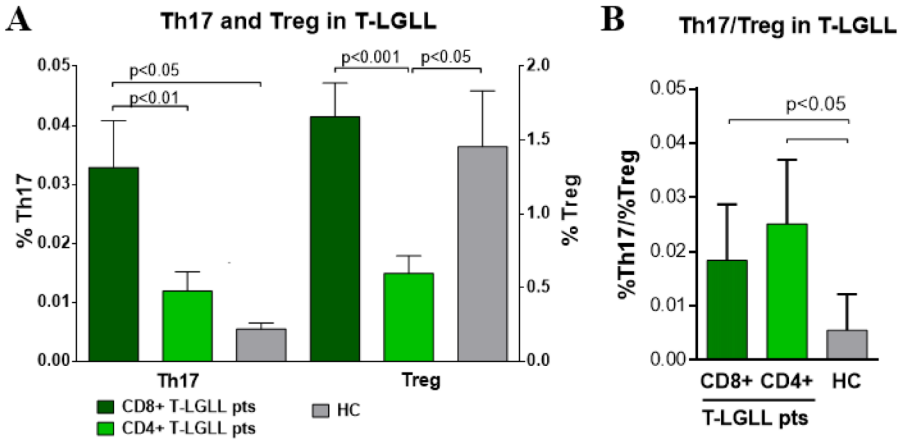

Figure 21: Evaluation of Th17 and Treg lymphocytes in T-LGLL PBMC. The percentages of Th17 and Treg cells were assessed by flow cytometric analyses in PBMC derived by 14 CD8+, 10 CD4+ T-LGLL cases and 4 HC. **Panel A: Th17 and Treg percentages evaluation.** The bar plot reports the mean percentages (±SEM) of Th17 cells (on the left) and Treg cells (on the right). The 3 groups analysed are distinguished by different bar colours, whose labels are reported on the legend on top of the graph. Data distribution was evaluated by Kolmogorov-Smirnov test and statistical significance by t-test. **Panel B: Th17/Treg ratio evaluation in T-LGLL.** The bar plot reports the mean Th17/Treg ratio (±SEM) calculated. Data distribution was evaluated by Kolmogorov-Smirnov test and statistical significance by Kruskal-Wallis test.

As for the characterization of monocytes, Th17/Treg balance was further evaluated subdividing the patients according to their mutational pattern. Th17 compartment resulted significantly higher in CD8+ *STAT3* mutated patients [0.036% (0.008%; 0.064%)] than CD4+ *STAT5b* wt cases [0.009% (0.003%; 0.037%), $p<0.05$, fig. 11A]. In addition, our data showed that CD4+ *STAT5b* mutated patients harboured the highest median ratio [0.049 (0.036; 0.054)] as compared to all other groups: CD8+ *STAT3* wt [0.008 (0.005; 0.037)], CD8+ *STAT3* mutated [0.017 (0.005; 0.033)], CD4+ *STAT5b* wt [0.016 (0.009; 0.022)] and healthy controls ($p<0.05$, fig. 22B).
Due to the high inner-group variability observed in CD8+ *STAT3* wt patients, they were sorted for the neutropenia status to dissect whether neutropenic cases would be characterized by a deregulation in Th17 and Treg cells, regardless the presence or absence of mutation. Our data showed that CD8+ *STAT3* wt neutropenic patients presented increased Th17 population [0.050% (0.030%; 0.091%)] with respect to healthy controls ($p<0.01$) and was consistent to what observed in CD8+ *STAT3* mutated patients. On the other hand, Th17 percentage resulted similar to HC for CD8+ *STAT3* wt non-neutropenic cases [0.009% (0.007%; 0.012%)] and was different from CD8+ *STAT3* mutated ($p<0.01$) and CD8+ *STAT3* wt neutropenic patients ($p=0.057$) (fig. 22C). As already described, the percentage of Treg cells resulted to be consistent with HC (fig. 22D). Moreover, the ratio between the two T cell populations was significantly increased in CD8+ *STAT3* wt neutropenic patients [0.047 (0.028; 0.077)] in comparison to every other group ($p<0.001$).

In summary, an overall deregulation of Th17/Treg lymphocytes in T-LGLL was observed. However, the mechanisms sustaining these features were different between CD8+ and CD4+ patients. For CD8+ patients, a direct boost of Th17 cells mainly in STAT3 mutated and neutropenic patients was detected. At variance, for CD4+ patients, either mutated and wt, the increase of Th17/Treg ratio was mostly related to the strong reduction in Treg cells.

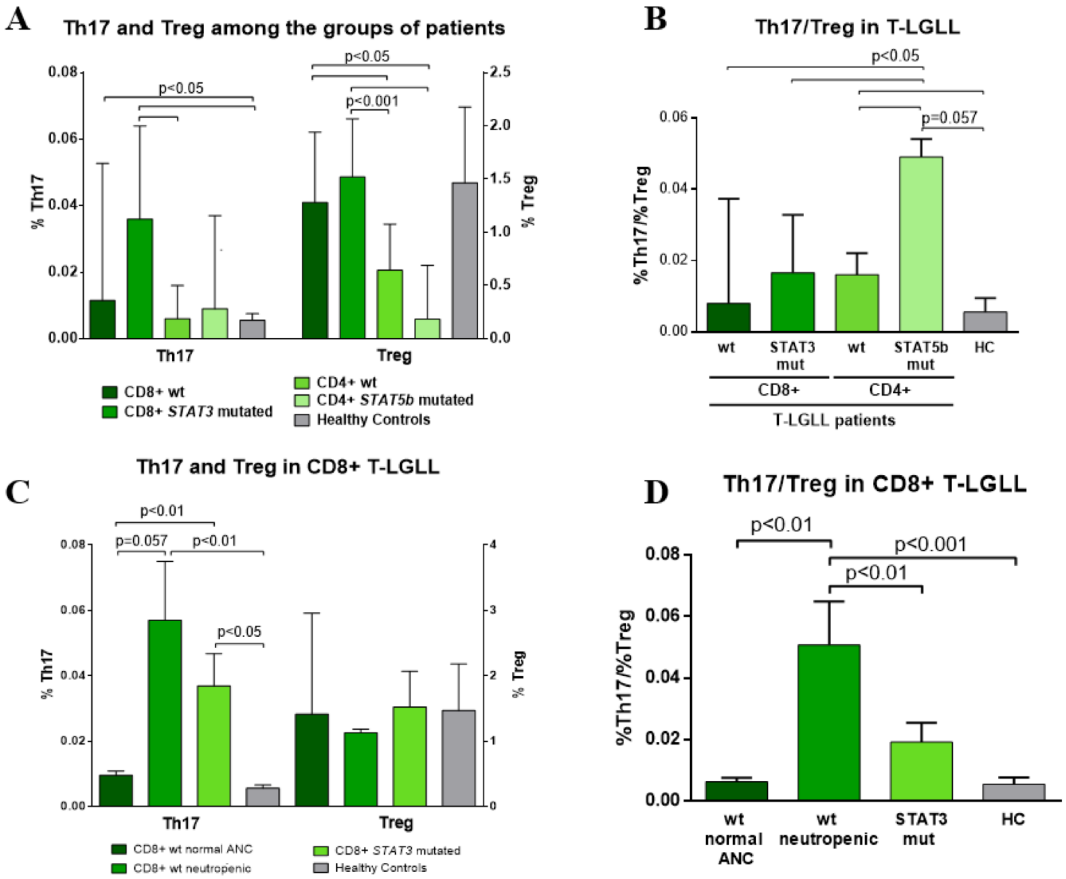

Figure 22: Evaluation of Th17 and Treg lymphocytes in T-LGLL categories. Panel A: Th17 and Treg in the different categories of T-LGLL. The bar plot reports the median percentages and IQR of Th17 cells (on the left) and Treg cells (on the right). The 5 groups analysed were distinguished by different bar colours, whose labels are reported on the legend at the bottom of the graph. Seven CD8+ *STAT3* wt, 7 CD8+ *STAT3* mutated, 7 CD4+ *STAT5b* wt and 3 CD4+ *STAT5b* mutated T-LGLL patients and 4 HC have been analysed. Data distribution was evaluated by Kolmogorov-Smirnov test and statistical significance by Mann-Whitney test. **Panel B: Th17/Treg ratio in T-LGLL.** The bar plot reports the median percentages and IQR of calculated Th17/Treg ratio for the group of patients evaluated in Panel A. Statistical evaluation was performed as for data in Panel A. **Panel C: Th17 and Treg in CD8+ T-LGLL.** The bar plot reports the Th17 cells mean (±SEM) percentages (on the left) and Treg cells median percentages and IQR (on the right). The 4 groups analysed were distinguished by different bar colours, whose labels are reported on the legend at the bottom of the graph. The 6 CD8+ *STAT3* wt cases were subdivided in non-neutropenic (normal ANC, n=4) and neutropenic (n=3). CD8+ *STAT3* mutated patients and HC are again reported for comparison. Statistical significance was assessed by one-way ANOVA or Kruskal-Wallis tests, according to the data distribution**. Panel D**: Th17/Treg ratio in CD8+ T-LGLL. The bar plot reports the mean Th17/Treg ratio (±SEM) calculated for the group of patients evaluated in Panel C. Statistical evaluation was performed by one-way ANOVA test.

5.5 Plasma cytokines concentration is differently represented in T-LGLL

Several secreted cytokines were reported to be deregulated and play a role for leukemic clone survival in T-LGLL, including CCL5 and IL-6[112,113]. For these reasons, a screening of 170 cytokines was performed in T-LGLL patients (n=14) and healthy controls' (n=4) plasma to identify possible new cytokines with a pathogenetic role in the disease. Plasma were incubated on commercially available arrays functionalized with antibodies specific for 170 soluble factors. The presence of each cytokine was evaluated by chemiluminescent reaction and the densitometric values were then compared among groups with one-way ANOVA or Kruskal-Wallis tests, according to data distribution. The statistical analyses were not definitively established yet, therefore, for this study, we reported the preliminary results obtained hitherto.
A first analysis was focused on the comparison between patients and healthy controls. Four cytokines resulted altered: three were increased in patients, namely Insulin Like Growth Factor Binding Protein 4 (IGFBP4), uPAR and MCSFR and IL-2Rγ was reduced, with $p<0.05$. An evaluation of the literature available for these deregulated soluble factors was performed in order to identify possible pathological roles. It turned out that they were involved in tumour growth, inflammation and immune system activation[136–139].
Since we previously demonstrated that CD8+ and CD4+ patients were characterized by different deregulation in TME cells, we compared the presence of soluble factors subdividing T-LGLL cases in CD4+ and CD8+ in order to define differences not only towards healthy controls but also between the two patients groups. The cytokines resulting altered from the groups comparison were listed in the table 11. Most of the differences we observed dealt with CD4+ patients.

Specific group comparison was performed according to data distribution. Of interest, we showed a higher concentration of soluble CD14 in CD4+ patients in comparison to CD8+ cases and healthy controls ($p<0.05$) and Lymphotactin was reduced than CD8+ patients, with $p<0.05$.

Taken together, this still preliminary analysis of patients secretome evidenced a peculiar deregulation in CD4+ patients. Future analyses are going to be performed to validate the differences on secretome between the groups of patients.

Table 11: Cytokines differently represented between healthy controls, CD8+ and CD4+ T-LGLL patients. Plasma obtained from 4 HC, 8 CD8+ and 6 CD4+ T-LGLL patients have been evaluated for soluble factors through a commercial cytokines array. Normalized densitometric data distribution have been assessed by Shapiro-Wilk test and have then been checked for group differences with one-way ANOVA or Kruskal-Wallis tests. The table reports the soluble factors, and related p-values, showing a significant difference between groups.

cytokine	p-value	cytokine	p-value
Agrp	0.016	IL-12p40	0.041
AR	0.039	IL-17A	0.029
BMP7	0.009	IL-1R2	0.028
CCL16	0.024	IL-21R	0.012
CCL27	0.011	IL-2Rγ	0.026
CCL28	0.050	IL-5Rα	0.016
CD102	0.021	IP10	0.032
CD105	0.002	LeptinR	0.005
CD31	0.045	LIF	0.008
CD80	0.037	Lymphotactin	0.031
CXCL16	0.045	MCSFR	0.012
DR6	0.019	MMP1	0.024
ErbB3	0.034	NGFR	0.003
IFNγ	0.042	PDGFRα	0.017
IGF2	0.005	PDGFRβ	0.032
IGFBP2	0.027	SDF1b	0.008
IGFBP4	0.009	TIMP2	0.041
IL-10Rβ	0.016	TIMP4	0.002
IL-11	0.023	VE-Cadherin	0.027

5.6 Effect of immunosuppressive therapy on monocytes, Th17 and Treg cells in treated T-LGLL patients

Although most T-LGLL patients presented with an indolent course of the disease, sometimes, due to neutropenia and/or recurrent infection, these patients require specific therapy, usually represented by immunosuppressive approach. In these cases, although neutropenia might disappear, the leukemic clone, even if in presence of complete response, often persists. Moreover, a description of drugs effects on non-leukemic peripheral blood cells is still lacking. To investigate this topic, patients at the end of the chemotherapy have been analysed to verify whether monocytes populations, Th17 and Treg cells were modulated by treatment. The patients evaluated received different immunomodulatory treatment, namely, Cyclosporine A, Cyclophosphamide and Methotrexate. All the patients reached at least partial response. Since almost only CD8+ T-LGLL patients need treatment, we performed the analysis only in this group subdividing treated and untreated patients, these latters being further subdivided in neutropenic and non-neutropenic cases, regardless the mutational status.

The evaluation of Th17 and Treg cells is reported in figure 23 A and B. Th17 cells from treated patients (0.022% ±0.013%) resulted to be slightly higher than non-neutropenic (0.010% ±0.001%) and healthy controls and slightly reduced as compared to neutropenic untreated cases (0.043% ±0.009%). Treg cells in treated patients resulted to be comparable among every other group, indicating that the treatment did not affect Treg population. The relative ratio between the two populations reflected what observed for Th17 cells: the mean Th17/Treg ratio for treated patients (0.016 ±0.011) was increased as compared to healthy controls and non-neutropenic cases (0.006 ±0.002) and reduced as compared to neutropenic patients (0.030 ±0.008), although statistical significance was not yet reached likely for the low number of treated cases that have been considered.
Also monocytes population distribution resulted changed in treated patients similarly to the Th17 percentage modulation (fig 23C). In treated patients the mean percentage of classical monocytes (70.625% ±2.617%) was significantly higher in comparison to neutropenic cases (56.364% ±4.412%, $p<0.01$) and comparable to healthy controls and non-neutropenic patients (80.833% ±1.759%). Intermediate monocytes (5.575% ±1.845%) resulted reduced as compared to neutropenic cases (15.680% ±2.612%, $p<0.05$) and comparable to non-neutropenic patients (5.433% ±0.930%) and healthy controls. In treated patients even non-classical monocytes were slightly reduced (9.500% ±3.174%) despite the difference was not significant in comparison to neutropenic patients (18.536% ±2.789%), being comparable to non-neutropenic (5.460% ±0.854%) cases and healthy controls.

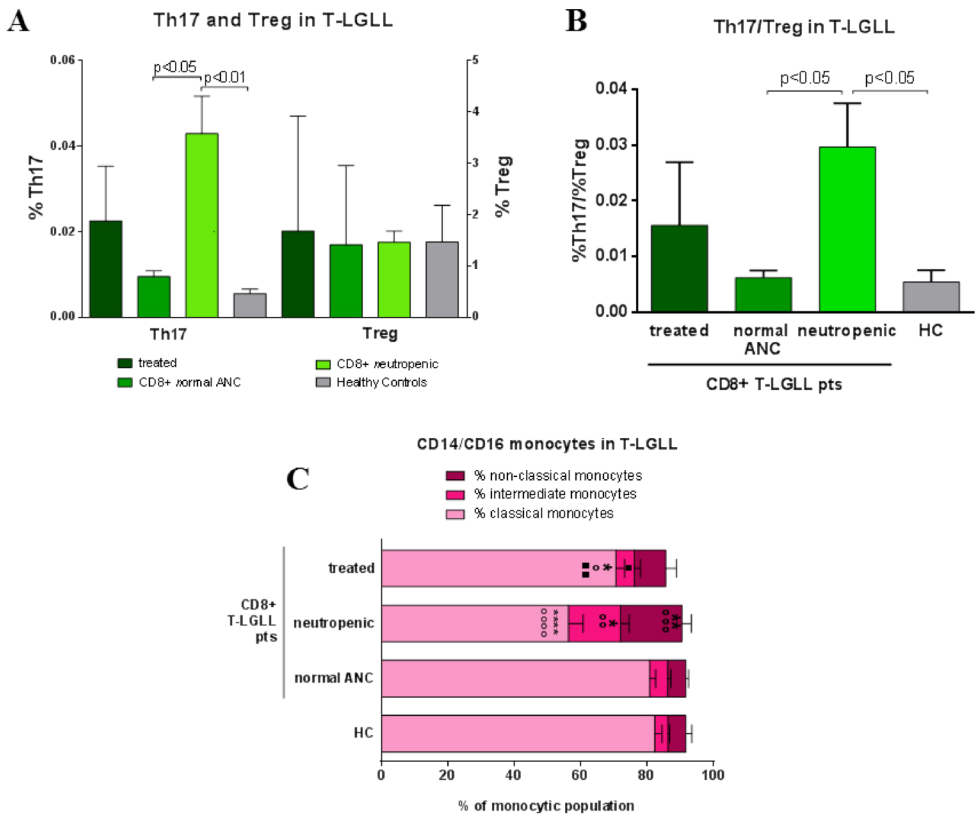

Figure 23: Evaluation of Th17 and Treg cells and monocytes populations distribution in treated and untreated patients. Panel A: Th17 and Treg cells evaluation. The bar plot reports the mean percentages (±SEM) of Th17 cells (on the left) and the median percentages and IQR of Treg cells (on the right). The 3 groups analysed are distinguished by different bar colours, whose labels are reported on the legend at the bottom of the graph. Three treated, 4 non-neutropenic, 10 neutropenic CD8+ T-LGLL patients and 4 HC have been analysed. Data distribution was evaluated by Kolmogorov-Smirnov test and statistical significance by one-way ANOVA or Kruskal-Wallis test. **Panel B: Th17/Treg ratio analysis.** The bar plot reports the mean (±SEM) of calculated Th17/Treg ratio for the groups of patients evaluated in Panel A. Statistical evaluation was performed as for data in Panel A. **Panel C: monocytes evaluation.** Samples from peripheral blood of the cases reported in panel A and B have been analysed. The bar plot reports the cumulative means (±SEM) of the 3 monocytes groups. Normal distribution was assessed by Kolmogorov-Smirnov test and statistical significance by two-way ANOVA test. Statistical significance is represented in the plot as: ○ or * or □=p<0.05, ○○ or ** or □□=p<0.01, ○○○=p<0.001 and ○○○○ or ****= p<0.0001. ○ indicates statistical significance against HC, * against CD8+ non-neutropenic patients, and □ against CD8+ neutropenic cases.

Taken together, these analyses suggest that the immunosuppressive drugs are active in the leukemic microenvironment, in particular reshaping the altered phenotype towards the physiological one. Indeed, both Th17 and monocytes populations were unbalanced in CD8+ neutropenic patients, who usually are more symptomatic thus requiring therapy, and the deregulation resulted partially reverted after treatment. Further evaluations in a larger cohort is needed to confirm this trend and to possibly separate patients reaching a response, either complete or only partial, to those who are refractory.

6 Discussion

In the present study we demonstrated an alteration of different subsets of the immune system in T-LGLL. It has already been described that a pro-inflammatory microenvironment is needed for the leukemic LGL proliferation. For the first time, here we demonstrated a strong relationship between leukemic LGL and other immune cells, particularly, monocytes, Th17 and Treg lymphocytes, which were involved in the pathogenesis of several oncological and autoimmune diseases[47].

We demonstrated that monocytes were mandatory to sustain LGL survival. So far, the role of monocytes was only suggested for their role in the inflammatory response and secretion of important T-LGLL pro-survival cytokines, including IL-6 and IL-15[113,101]. In this study, we identified that IL-6 was produced by monocytes in T-LGLL patients and that some T-LGLL cases were characterized by a very high IL-6 expression. We also demonstrated that CCL5, a monocyte chemoattractant reported to be increased in patients' plasma[112], was specifically released by leukemic LGL and able to induce the production of IL-6 by patients' monocytes. This property was not observed in healthy controls, suggesting a disease specificity. According to these results, we hypothesize that monocytes and leukemic LGL could interact each other.

T-LGLL is a heterogeneous disease, as defined according to different CD4+/CD8+ phenotypes and the mutational status[72]. The leukemic biological features, that contribute to discriminates among T-LGLL sub-types, were also reflected in microenvironment heterogeneity among groups. In fact, we found that the significant increase of CCL5 expression was restricted to CD8+ T-LGL. This latter subset is also characterized by a high IL-6 expression in monocytes. Provided the above reported findings and the peculiar expression of IL-6 and CCL5 in CD8+ patients, we can speculate that the crosstalk between LGL and monocytes *via* CCL5 and IL-6 is likely to be more relevant for this subset of patients.

We observed that monocytes-mediated LGL survival was a common feature for both CD8+ and CD4+ T-LGLL patients, but monocytes exert pro-survival actions with different mechanisms in the two disease entities. Consistently, a different alteration was observed not only on monocytes, but also on Th17 and Treg lymphocyte subsets in PB among CD4+ and CD8+ patients.

CD8+ T-LGLL patients were characterized by an accumulation of intermediate and non-classical monocytes together with an increase of Th17 lymphocytes. These features are characteristic of an inflammatory environment and were also reported to be one of the pathogenetic mechanism of RA development[47], a disease that is often associated to T-LGLL[59]. Moreover, we identified a correlation between monocytes, Th17 cells deregulation and T-LGLL severity. As a matter of fact, monocytes and Th17/Treg ratio alterations were mostly detected in CD8+ *STAT3* mutated cases, a T-LGLL subset that is characterized by neutropenia.

The identification of a consistent pattern of TME alterations present also in *STAT3* wt neutropenic patients suggested a correlation between unbalanced TME cells and

neutropenia. Interestingly, the unbalanced Th17/Treg ratio demonstrated in neutropenic cases was mostly sustained by an increase of Th17 population. Since Th17 cells can stimulate T lymphocyte to secrete CCL5, this feature could explain LGL production of this cytokine[140]. Literature data suggest that also leukemic LGL, derived from CD8+ *STAT3* mutated cases, might induce Th17 differentiation; in particular, IL-23 was found to be more expressed in a small cohort of these patients[55]. As a future perspective, considering that IL-23 is mandatory for pathogenetic Th17 differentiation[36], we will evaluate IL-23 expression in T-LGL in our cohort of patients to verify the hypothesis of a putative interaction between leukemic clone and TME cells. Moreover, we speculate that patients' monocytes in this disorder are also involved in Th17 differentiation, since we provided evidence that they were able to produce high level of IL-6, a cytokine necessary for Th17 maturation[46].

Different gene expression profiles between monocytes classes have been also reported[20]. In this study, we evaluated some of those factors involved in inflammation, including CCR5 and IL-23, which are more expressed in intermediate monocytes. However, we did not detect any significant modification of these genes in bulk monocytes, concluding that an imbalance on monocytes classes did not affect the overall monocytes gene expression. Nevertheless, we observed a slight higher CCR5 expression in *STAT3* mutated patients' monocytes. We suggest that this increase might be interpreted as an effect of the high intermediate monocytes percentage in this group of patients, since these monocytes were defined as the only monocyte class to express CCR5[24]. This might lead to an increase of monocytes avidity to CCL5, produced by the leukemic clone. Taken these data together, a tentative network between leukemic LGL, monocytes and Th17 cells in CD8+ T-LGLL can be suggested, as summarized in figure 24.

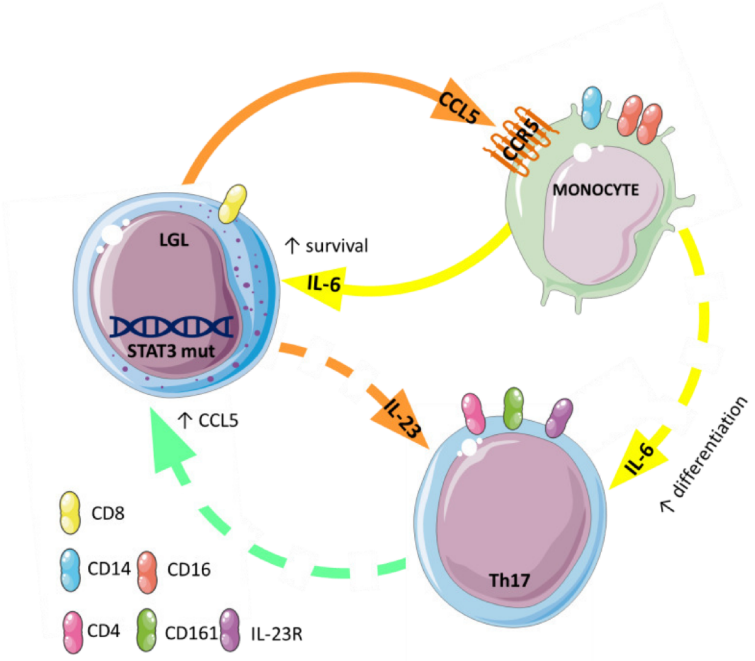

Figure 24: TME cellular network proposed for CD8+ T-LGLL neutropenic patients. The full arrows identify verified interactions; dashed arrows identify hypothesized interactions.

In detail, we hypothesize that the high levels of CCL5 produced by leukemic LGL, through CCR5, stimulate monocytes to produce IL-6, which favours both leukemic clone survival and Th17 cells differentiation. Moreover, pathogenic differentiation of Th17 cells could be induced by leukemic T-LGL through IL-23 and these cells, in turn, can potentially induce LGL to express more CCL5. This network was mostly functional in CD8+ T-LGLL neutropenic patients, although we cannot yet exclude that it might be relevant also for the other disease groups. Studies are still ongoing and future plans are aimed to completely characterize this system, with the ultimate purpose of identifying new potential therapeutic targets.

Monocytes derived from CD8+ *STAT3* mutated patients were altered not only phenotypically, but also in their intracellular activation. A high protein expression of important signaling mediators, as STAT3, p65 and Erk, was identified in monocytes, even if not correlated with their increased activation, indicating that there was high amount of un-phosphorylated (u-) proteins. Interestingly, also u-proteins have reported to provide signaling capacity[140]. In particular, u-STAT3 and u-Erk were found to translocate into the nucleus where they are able to induce the expression of several pro-survival genes[140]. Moreover, u-STAT3 can also interact with u-p65 to trigger the secretion of inflammatory cytokines, i.e. CCL5 and IL-6[141]. According to our results, studies are in progress to evaluate whether these intracellular processes might be active in CD8+ *STAT3* mutated T-LGLL patients in order to define whether STAT3 might act as a potential pro-leukemic factor even by modulating the TME cells.

CD8+ *STAT3* mutated patients require treatment for symptomatic neutropenia and, to date, the approved therapeutic strategies are immunosuppressive drugs[57]. In several haematological malignancies, the role of TME in mediating drug resistance has been reported and also drugs targeting microenvironment have been exploited as anticancer therapeutic strategy[143]. Even if immunosuppressive drugs were reported to give not satisfactory responses in these disorders[57], our data demonstrated a potential mechanism of action of these drugs in T-LGLL as TME modifiers. In fact, patients who underwent this type of treatment showed a partial recovery of altered monocytes and Th17 populations distribution, e.g. features that characterize neutropenic cases. Future studies will be focused to evaluate whether this observation might be useful as a prognostic marker of patients' treatment response.

Apart from the results obtained in CD8+ T-LGLL patients, we provided evidence that alterations in monocytes physiology and Th17/Treg ratio have been detected also in CD4+ T-LGLL cases. Interestingly, in CD4+ T-LGLL we observed that the mechanism leading to these deregulations was different from that shown in CD8+ T-LGLL. In particular, we found a decrease in Treg cells, that led to an imbalance of Th17/Treg ratio and a strong pErk activation on monocytes. These two features differently characterize *STAT5b* wt and mutated patients: the unbalanced Th17/Treg ratio has been identified in mutated ones, whereas monocytes activation has been associated to wt cases. We could speculate that *STAT5b* mutations might lead the leukemic clone to differently influence the TME and further analyses are in progress to unravel possible differences between the two groups of patients. Nevertheless, from ongoing studies on patients' plasma secretome, some cytokines resulted to be differently represented in CD4+ patients. In particular, Lymphotactin was one of the few soluble factors that was reduced in CD4+ patients, as they were characterized by an overall increased level of plasma cytokines than healthy controls and CD8+ cases. Interestingly, Lymphotactin has been reported to be involved in Treg dysfunction when it is reduced[144], suggesting its possible role in the decrease of Treg cells observed in these patients. On the other hand, among the soluble factors that have been found to be increased in CD4+ T-LGLL patients, we detected the soluble form of CD14, which has been regarded as an indicator of monocytes activation[145]. Together with the identification of a strong Erk activation on monocytes, this finding suggests that also CD4+ T-LGLL patients' monocytes might be altered. In particular, Erk activation has been used as a marker of monocytes senescence, characterized by a peculiar pro-inflammatory senescence associated secretory phenotype (SASP)[27]. This observation can be linked to the higher presence of soluble factors in CD4+ patients' plasma than in healthy controls and CD8+ cases. Taken our data together, we demonstrated that also CD4+ T-LGLL patients were characterized by an inflammatory microenvironment, although with different features as compared to CD8+ LGLL patients.

In conclusion, T-LGLL has often been referred as a heterogeneous disease. In the present study we provided new information on the T-LGLL inflammatory events

showing that TME is different according to the biological features of the leukemic clone and the clinical setting. We unravelled, in this way, the differential role of monocytes, Th17 and Treg cells in the T-LGLL subsets. Moreover, we identified a potential network ongoing between leukemic clone and cells of TME in neutropenic patients, then contributing to better define the pathogenetic mechanisms leading to neutropenia development in this disorder.

7 References

1. Zambello R, Semenzato G. Large granular lymphocytosis. *Haematologica*. 1998;83:936–942.
2. Zhang D, Loughran TP. Large granular lymphocytic leukemia: molecular pathogenesis, clinical manifestations, and treatment. *Hematol. Am. Soc. Hematol. Educ. Progr.* 2012;2012:652–9.
3. Semenzato G, Zambello R, Starkebaum G, Oshimi K, Loughran TP. The lymphoproliferative disease of granular lymphocytes: Updated criteria for diagnosis. *Blood*. 1997;89:256–260.
4. Sokol L, Loughran TP. Large Granular Lymphocyte Leukemia. *The Oncologist.* 2006;11:263–273.
5. Wlodarski MW, Schade AE, Maciejewski JP. T-large granular lymphocyte leukemia: Current molecular concepts. *Hematology*. 2006;11:245–256.
6. Shah MV, Zhang R, Loughran TP. Never say die: survival signaling in large granular lymphocyte leukemia. *Clin. Lymphoma Myeloma*. 2009;9:244–253.
7. Rose MG, Berliner N. T-Cell Large Granular Lymphocyte Leukemia and Related Disorders. *Oncologist*. 2004;9:247–258.
8. Guilliams M, Mildner A, Yona S. Review Developmental and Functional Heterogeneity of Monocytes. *Immunity*. 2018;49:595–613.
9. Passlick B, Flieger D, Ziegler-Heitbrock HW. Identification and characterization of a novel monocyte subpopulation in human peripheral blood. *Blood*. 1989;74:2527–2534.
10. Ziegler-Heitbrock L, Ancuta P, Crowe S, et al. Nomenclature of monocytes and dendritic cells in blood. *Blood*. 2010;116:5–7.
11. Wong KL, Tai JJ, Wong W, et al. Gene expression profiling reveals the defining features of the classical, intermediaten and nonclassical human monocyte subsets. *Blood*. 2011;118:16–32.
12. Boyette LB, Macedo C, Hadi K, Elinoff BD, Walters JT. Phenotype, function and differentiation potential of human monocyte subsets. *PLoS ONE*. 2017; 12:1–20.
13. Cignarella A, Tedesco S, Cappellari R, Fadini GP. The continuum of monocyte phenotypes : Experimental evidence and prognostic utility in assessing cardiovascular risk. *J. Leukoc. Biol.* 2018;1–8.
14. Patel AA, Zhang Y, Fullerton JN, et al. The fate and lifespan of human monocyte subsets in steady state and systemic inflammation. *J. Exp. Med.* 2017;214:1913–1923.
15. Villani A, Satija R, Reynolds G, et al. Single-cell RNA-seq reveals new types of human blood dendritic cells, monocytes, and progenitors. *Science.* 2017;356:1-12.
16. Patel VK, Williams H, Li SCH, Fletcher JP, Medbury HJ. Monocyte inflammatory profile is specific for individuals and associated with altered blood lipid levels. *Atherosclerosis*. 2017;263:15–23.
17. Weber C, Belge KU, Von Hundelshausen P, et al. Differential chemokine receptor expression and function in human monocyte subpopulations. *J. Leukoc. Biol.* 2000;67:699–704.
18. Shi C, Pamer EG. Monocyte recruitment during infection and inflammation. *Nat. Rev. Immunol.* 2011;11:762.
19. Metcalf TU, Wilkinson PA, Cameron MJ, et al. Human Monocyte Subsets Are Transcriptionally and Functionally Altered in Aging in Response to Pattern Recognition Receptor Agonists. *J. Immunol.* 2017;199:1-13.
20. Gren ST, Rasmussen TB, Janciauskiene S. A Single-Cell Gene-Expression Profile Reveals Inter-Cellular Heterogeneity within Human Monocyte Subsets. *PLoS ONE.* 2015;12:1–20.
21. Anbazhagan K, Duroux-richard I, Jorgensen C, Anbazhagan K, Duroux-Richard i. Transcriptomic Network Support Distinct Roles of Classical and Non-Classical

Monocytes in Human. *Int. Rev. Immunol*. 2014;33:470-489.
22. Segura V, Valero M, Cantero L, et al. In-Depth Proteomic Characterization of Classical and Non-Classical Monocyte Subsets. *Proteomes*. 2018;6:1-13.
23. Buscher K, Marcovecchio P, Hedrick CC, Ley K. Patrolling Mechanics of Non-Classical Monocytes in Vascular Inflammation. *Front. Cardiovasc. Med.* 2017;4:1–10.
24. Ong S, Hadadi E, Dang T, et al. The pro-inflammatory phenotype of the human non-classical monocyte subset is attributed to senescence. *Cell Death Dis.* 2018;9:1–12.
25. Stansfield BK, Ingram DA. Clinical significance of monocyte heterogeneity. *Clin. Transl. Med.* 2015;4:1-20.
26. Cappellari R, D'Anna M, Bonora BM, et al. Shift of monocyte subsets along their continuum predicts cardiovascular outcomes. *Atherosclerosis*. 2017;266:95–102.
27. Radwan WM, Khalifa KA, Esaily HA, Lashin NA. CD14++CD16+ monocyte subset expansion in rheumatoid arthritis patients: Relation to disease activity and interleukin-17. *Egypt. Rheumatol.* 2016;38:161–169.
28. Selimoglu-Buet S, Wagner-Ballon O, Saada V, et al. Characteristic repartition of monocyte subsets as a diagnostic signature of chronic myelomonocytic leukemia.*Blood.* 2015;125:3618–3627.
29. Franceschi C, Capri M, Monti D, et al. Inflammaging and anti-inflammaging: A systemic perspective on aging and longevity emerged from studies in humans. *Mech. Ageing Dev.* 2007;128:92–105.
30. Langrish CL, Chen Y, Blumenschein WM, et al. IL-23 drives a pathogenic T cell population that induces autoimmune inflammation. *J. Exp. Med.* 2005;201:233–240.
31. Harrington LE, Hatton RD, Mangan PR, et al. Interleukin 17-producing CD4 + effector T cells develop via a lineage distinct from the T helper type 1 and 2 lineages. *Nat. Immunol.* 2005;6:1123–1132.
32. Park H, Li Z, Yang XO, et al. A distinct lineage of CD4 T cells regulates tissue inflammation by producing interleukin 17. *Nat. Immunol.* 2005;6:1133–1141.
33. Annunziato F, Cosmi L, Liotta F, Maggi E, Romagnani S. Defining the human T helper 17 cell phenotype. *Trends Immunol.* 2012;33:505–512.
34. Ciofani M, Madar A, Galan C, et al. A validated regulatory network for Th17 cell specification. *Cell*. 2012;151:289–303.
35. Stockinger B, Omenetti S. The dichotomous nature of T helper 17 cells. *Nat. Rev. Immunol.* 2017;17:535–544.
36. Lee Y, Awasthi A, Yosef N, et al. Induction and molecular signature of pathogenic TH17 cells. *Nat. Immunol.* 2012;13:991–999.
37. Kimura A, Kishimoto T. IL-6: Regulator of Treg/Th17 balance. *Eur. J. Immunol.* 2010;40:1830–1835.
38. Plitas G, Rudensky AY. Regulatory T Cells: Differentiation and Function. *Cancer Immunol. Res.* 2016;4:721–725.
39. Li MO, Rudensky AY. T cell receptor signalling in the control of regulatory T cell differentiation and function. *Nat. Rev. Immunol.* 2016;16:220–233.
40. Vignali DAA, Collison LW, Workman CJ. How regulatory T cells work. *Nat. Rev. Immunol.* 2008;8:523–532.
41. Ohkura N, Kitagawa Y, Sakaguchi S. Development and Maintenance of Regulatory T cells. *Immunity*. 2013;38:414–423.
42. Li X, Zheng Y. Regulatory T cell identity: Formation and maintenance. *Trends Immunol.* 2015;36:344–353.
43. Josefowicz SZ, Lu L-F, Rudensky AY. Regulatory T Cells: Mechanisms of Differentiation and Function. *Annu. Rev. Immunol.* 2012;30:531–564.
44. Wang J, Ke XY. The Four types of Tregs in malignant lymphomas. *J. Hematol. Oncol.* 2011;4:50.
45. Diller ML, Kudchadkar RR, Delman KA, Lawson DH, Ford ML. Balancing inflammation: The link between Th17 and regulatory T cells. *Mediators Inflamm.*

2016;2016:1-8.
46. Zheng SG. Regulatory T cells versus Th17: Differentiation of Th17 versus treg, are they mutually exclusive? *Am. J. Clin. Exp. Immunol.* 2013;2:91–107.
47. Gaafar T, Farid R. The TH17/Treg Imbalance in Rheumatoid Arthritis and Relation to Disease Activity. *J. Clin. Cell. Immunol.* 2015;06:1-7.
48. Fasching P, Stradner M, Graninger W, Dejaco C, Fessler J. Therapeutic potential of targeting the Th17/Treg axis in autoimmune disorders. *Molecules*. 2017;22:1-24
49. Semenzato G, Zambello R, Starkebaum G, Oshimi K, Loughran TP. The lymphoproliferative disease of granular lymphocytes: updated criteria for diagnosis. *Blood*. 1997;89:256–260.
50. Swerdlow SH, Campo E, Pileri SA, et al. The 2016 revision of the World Health Organization classification of lymphoid neoplasms. *Blood*. 2016;127:2375–90.
51. Loughran TPJ. Clonal diseases of large granular lymphocytes. *Blood*. 1993;82:1–14.
52. Dinmohamed AG, Brink M, Visser O, Jongen-Lavrencic M. Population-based analyses among 184 patients diagnosed with large granular lymphocyte leukemia in the Netherlands between 2001 and 2013. *Leukemia*. 2016;30:1449–1451.
53. Shah M V., Hook CC, Call TG, Go RS. A population-based study of large granular lymphocyte leukemia. *Blood Cancer J.* 2016;6:e455.
54. Zambello R, Teramo A, Gattazzo C, Semenzato G. Are T-LGL Leukemia and NK-Chronic Lymphoproliferative Disorder really two distinct diseases? *Transl. Med. @ UniSa*. 2014;8:4–11.
55. Jerez A, Clemente MJ, Makishima H, et al. STAT3 mutations unify the pathogenesis of chronic lymphoproliferative disorders of NK cells and T-cell large granular lymphocyte leukemia. *Blood*. 2012;120:3048–57.
56. Suzuki R, Suzumiya J, Nakamura S, et al. Aggressive natural killer-cell leukemia revisited: Large granular lymphocyte leukemia of cytotoxic NK cells. *Leukemia*. 2004;18:763–770.
57. Barilà G, Calabretto G, Teramo A, et al. T cell large granular lymphocyte leukemia and chronic NK lymphocytosis. *Best Pract. Res. Clin. Haematol.* 2019;32:207-216.
58. Semenzato G, Pandolfi F, Chiesi T, et al. The lymphoproliferative disease of granular lymphocytes. A heterogeneous disorder ranging from indolent to aggressive conditions. *Cancer*. 1987;60:2971–2978.
59. Moignet A, Lamy T. Latest Advances in the Diagnosis and Treatment of Large Granular Lymphocytic Leukemia. *Am. Soc. Clin. Oncol. Educ. B.* 2018;38:616–625.
60. Lamy T, Moignet A, Loughran TP. LGL leukemia: From pathogenesis to treatment. *Blood*. 2017;129:1082–1094.
61. Bigouret V, Hoffmann T, Arlettaz L, et al. Monoclonal T-cell expansions in asymptomatic individuals and in patients with large granular leukemia consist of cytotoxic effector T cells expressing the activating CD94:NKG2C/E and NKD2D killer cell receptors. *Blood*. 2003;101:3198–3204.
62. Gentile TC, Uner AH, Hutchison RE, et al. CD3+, CD56+ aggressive variant of large granular lymphocyte leukemia. *Hematol. Oncol.* 1994;84:2315–2321.
63. Lima M, Almeida J, Dos Anjos Teixeira M, et al. TCRαβ+/CD4+ large granular lymphocytosis: A new clonal T-cell lymphoproliferative disorder. *Am. J. Pathol.* 2003;163:763–771.
64. Garrido P, Ruiz-Cabello F, Bárcena P, et al. Monoclonal TCR-Vβ13.1+/CD4+/NKa+/CD8−/+dim T-LGL lymphocytosis: evidence for an antigen-driven chronic T-cell stimulation origin. *Blood*. 2007;109:4890–4898.
65. Rodríguez-Caballero A, García-montero C, Ba P, et al. Expanded cells in monoclonal TCR-alfa-beta+/CD4+/NKa+/CD8dim-neg/ T-LGL lymphocytosis recognize hCMV antigens. *Hematology*. 2008;112:4609–4616.
66. Sandberg Y, Almeida J, Gonzalez M, et al. TCRγδ+ large granular lymphocyte leukemias reflect the spectrum of normal antigen-selected TCRγδ+ T-cells. *Leukemia*.

2006;20:505–513.
67. Bourgault-Rouxel AS, Loughran TP, Zambello R, et al. Clinical spectrum of γδ+ T cell LGL leukemia: Analysis of 20 cases. *Leuk. Res.* 2008;32:45–48.
68. Clemente MJ, Przychodzen B, Jerez A, et al. Deep sequencing of the T-cell receptor repertoire in CD8+ T-large granular lymphocyte leukemia identifies signature landscapes. *Blood*. 2013;122:4077–4085.
69. Langerak AW, Beemd R Van Den, Wolverstettero ILM, et al. Molecular and flow cytometric analysis of the Vβ repertoire for clonality assessment in mature TCR α β T-cell proliferations *Blood.* 2001;98:165–173.
70. Clemente MJ, Wlodarski MW, Makishima H, et al. Clonal drift demonstrates unexpected dynamics of the T-cell repertoire in T-large granular lymphocyte leukemia. *Blood.* 2011;118:4383–4393.
71. Dearden C. Large granular lymphocytic leukaemia pathogenesis and management. *Br. J. Haematol.* 2011;152:273–283.
72. Teramo A, Barilà G, Calabretto G, et al. STAT3 mutation impacts biological and clinical features of T-LGL leukemia. *Oncotarget*. 2017;8:61876-61889.
73. Alekshun TJ, Sokol L. Diseases of large granular lymphocytes. *Cancer Control*. 2007;14:141–150.
74. Lamy T, Loughran TP. Clinical features of large granular lymphocyte leukemia. *Semin. Hematol.* 2003;40:185–95.
75. Viny A, Lichtin A, Pohlman B, Loughran T, Maciejewski J. Chronic B-cell dyscrasias are an important clinical feature of T-LGL leukemia. *Leuk. Lymphoma*. 2008;49:932–938.
76. Zhang X, Sokol L, Bennett JM, et al. T-cell large granular lymphocyte proliferation in myelodysplastic syndromes: Clinicopathological features and prognostic significance. *Leuk. Res.* 2016;43:18–23.
77. Go RS, Lust JA, Phyliky RL. Aplastic anemia and pure red cell aplasia associated with large granular lymphocyte leukemia. *Semin. Hematol.* 2003;40:196–200.
78. Garrido P, Ruiz-cabello F, Ba P, et al. Monoclonal TCR-Vβ13.1^{+}/CD4^{+}/NKa^{+}/CD8$^{-/+dim}$ T-LGL lymphocytosis: Evidence for an antigen-driven chronic T-cell stimulation origin. *Blood.* 2006;109:4890–4899.
79. Poullot E, Bouscary D, Guyader D, et al. Large granular lymphocyte leukemia associated with hepatitis C virus infection and B cell lymphoma: Improvement after antiviral therapy. *Leuk. Lymphoma*. 2013;54:1797–1799.
80. Kimura H, Ito Y, Kawabe S, et al. EBV-associated T/NK-cell lymphoproliferative diseases in nonimmunocompromised hosts: Prospective analysis of 108 cases. *Blood*. 2012;119:673–686.
81. Starkebaum G, Kalyanaraman VS, Kidd P, et al. Serum reactivity to human t-cell leukaemia/lymphoma virus type i proteins in patients with large granular lymphocytic leukaemia. *Lancet*. 1987;329:596–599.
82. Zambello R, Berno T, Cannas G, et al. Phenotypic and functional analyses of dendritic cells in patients with lymphoproliferative disease of granular lymphocytes (LDGL). *Mol. Med.* 2005;106:3926–3931.
83. Lamy T, Liu JH, Landowski TH, Dalton WS, Loughran TP. Dysregulation of CD95/CD95 ligand-apoptotic pathway in CD3+ large granular lymphocyte leukemia. *Blood*. 1998;92:4771–4777.
84. Liu JH, Wei S, Lamy T, et al. Blockade of Fas-dependent apoptosis by soluble Fas in LGL leukemia Blockade of Fas-dependent apoptosis by soluble Fas in LGL leukemia. *Blood.* 2002;100:1449–1453.
85. Yang J, Painter JS, Zou J, et al. Antigen activation and impaired Fas-induced death-inducing signaling complex formation in T-large-granular lymphocyte leukemia. *Blood.* 2008;111:1610–1616.

86. LeBlanc F, Zhang D, Liu X, Loughran TPJ. Large granular lymphocyte leukemia: from dysregulated pathways to therapeutic targets. *Future Oncol.* 2012;8:787–801.
87. Shah MV, Zhang R, Loughran TP. Never say die: survival signaling in large granular lymphocyte leukemia. *Clin. Lymphoma Myeloma*. 2009;9:S244–S253.
88. Schade AE, Wlodarski MW, Maciejewski JP. Pathophysiology defined by altered signal transduction pathways: The role of JAK-STAT and PI3K signaling in leukemic large granular lymphocytes. *Cell Cycle*. 2006;5:2571–2574.
89. Epling-Burnette PK, Liu JH, Catlett-Falcone R, et al. Inhibition of STAT3 signaling leads to apoptosis of leukemic large granular lymphocytes and decreased Mcl-1 expression. *J. Clin. Invest.* 2001;107:351–62.
90. Koskela HLM, Eldfors S, Ellonen P, et al. Somatic STAT3 mutations in large granular lymphocytic leukemia. *N. Engl. J. Med.* 2012;366:1905–13.
91. Andersson E, Kuusanmäki H, Bortoluzzi S, et al. Activating somatic mutations outside the SH2-domain of STAT3 in LGL leukemia. *Leukemia*. 2016;30:1204-1208
92. Dutta A, Yan D, Hutchison RE, Mohi G. STAT3 mutations are not sufficient to induce large granular lymphocytic leukaemia in mice. *Br. J. Haematol.* 2018;180:911-915
93. Kerr CM, Clemente MJ, Chomczynski PW, et al. Subclonal STAT3 mutations solidify clonal dominance. *Blood Adv.* 2019;3:917-921
94. Andersson EI, Rajala HLM, Eldfors S, et al. Novel somatic mutations in large granular lymphocytic leukemia affecting the STAT-pathway and T-cell activation. *Blood Cancer J.* 2013;3:e168.
95. Coppe A, Andersson EI, Binatti A, et al. Genomic landscape characterization of large granular lymphocyte leukemia with a systems genetics approach. *Leukemia*. 2017;31:1243–1246.
96. Rajala HLM, Olson T, Clemente MJ, et al. The analysis of clonal diversity and therapy responses using STAT3 mutations as a molecular marker in large granular lymphocytic leukemia. *Haematologica*. 2015;100:91–9.
97. Jerez A, Clemente MJ, Makishima H, et al. STAT3 mutations indicate the presence of subclinical T-cell clones in a subset of aplastic anemia and myelodysplastic syndrome patients. *Blood*. 2013;122:2453-2459.
98. Rajala HLM, Eldfors S, Kuusanmäki H, et al. Discovery of somatic STAT5b mutations in large granular lymphocytic leukemia. *Blood*. 2013;121:4541–50.
99. Andersson EI, Tanahashi T, Sekiguchi N, et al. High incidence of activating STAT5B mutations in CD4-positive T-cell large granular lymphocyte leukemia. *Blood*. 2016;128:2465–2468.
100. Zhang R, Shah M V., Yang J, et al. Network model of survival signaling in large granular lymphocyte leukemia. *Proc. Natl. Acad. Sci.* 2008;105:16308–16313.
101. Zambello R, Facco M, Trentin L, et al. Interleukin-15 triggers the proliferation and cytotoxicity of granular lymphocytes in patients with lymphoproliferative disease of granular lymphocytes. *Blood*. 1997;89:201–211.
102. Tsudo M, Goldman CK, Bongiovanni KF, et al. The p75 peptide is the receptor for interleukin 2 expressed on large granular lymphocytes and is responsible for the interleukin 2 activation of these cells. *Proc. Natl. Acad. Sci.* 2006;84:5394–5398.
103. Hodge DL, Yang J, Buschman MD, et al. Interleukin-15 enhances proteasomal degradation of bid in normal lymphocytes: implications for large granular lymphocyte leukemias. *Cancer Res.* 2009;69:3986–94.
104. Mishra A, Liu S, Sams GH, et al. Aberrant overexpression of IL-15 initiates large granular lymphocyte leukemia through chromosomal instability and DNA hypermethylation. *Cancer Cell*. 2012;22:645–55.
105. Fehniger TA, Suzuki K, Ponnappan A, et al. Fatal leukemia in interleukin 15 transgenic mice follows early expansions in natural killer and memory phenotype CD8+ T cells. *J Exp Med*. 2001;193:219–31.
106. Hodge DL, Yang J, Buschman MD, et al. Interleukin-15 enhances proteasomal

degradation of Bid In normal lymphocytes:implications for Large granular lymphocyte leukemias. *Cancer Res.* 2009;69:3986–3994.
107. Sato N, Sabzevari H, Fu S, et al. Development of transgenic mice requires the cis expression of IL-15R α and IL-15–autocrine CD8 T-cell leukemia in IL-15–transgenic mice requires the cis expression of IL-15Rα. *Blood*. 2011;117:4032–4040.
108. Chen J, Petrus M, Bamford R, et al. Increased serum soluble IL-15Rα levels in T-cell large granular lymphocyte leukemia. *Blood*. 2012;119:137–43.
109. Waldmann TA, Conlon KC, Stewart DM, et al. Phase 1 trial of IL-15 trans presentation blockade using humanized Mik-Beta-1 mAb in patients with T-cell large granular lymphocytic leukemia. *Blood*. 2013;121:476–485.
110. Wang TT, Yang J, Zhang Y, et al. IL-2 and IL-15 blockade by BNZ-1, an inhibitor of selective γ-chain cytokines, decreases leukemic T-cell viability. *Leukemia*. 2019;33:1243–1255.
111. Makishima H, Ishida F, Ito T, et al. DNA microarray analysis of T cell-type lymphoproliferative disease of granular lymphocytes. *Br J Haematol*. 2002;118:462–469.
112. Kothapalli R, Nyland S, Kusmartseva I, et al. Constitutive production of proinflammatory cytokines RANTES, MIP-1β and IL-18 characterizes LGL leukemia. *Int. J. Oncol.* 2005;26:529-535
113. Teramo A, Gattazzo C, Passeri F, et al. Intrinsic and extrinsic mechanisms contribute to maintain the JAK/STAT pathway aberrantly activated in T-type large granular lymphocyte leukemia *Blood*. 2013;121:3843–3854.
114. Zambello R, Trentin L, Facco M, et al. Upregulation of CXCR1 by proliferating cells in patients with lymphoproliferative disease of granular lymphocytes. *Br. J. Haematol.* 2003;120:765–73.
115. Moura J, Rodrigues J, Santos A, et al. Chemokine receptor repertoire reflects mature T-cell lymphoproliferative disorder clinical presentation. *Blood Cells, Mol. Dis.* 2009;42:57–63.
116. Momose K, Makishima H, Ito T, et al. Close Resemblance between Chemokine Receptor Expression Profiles of Lymphoproliferative Disease of Granular Lymphocytes and Their Normal Counterparts in Association with Elevated Serum Concentrations of IP-10 and MIG. *Int. J. Hematol.* 2007;86:174–179.
117. Morice WG, Kurtin PJ, Tefferi A, Hanson CA. Distinct bone marrow findings in T-cell granular lymphocytic leukemia revealed by paraffin section immunoperoxidase stains for CD8, TIA-1, and granzyme B. *Blood*. 2002;99:268–274.
118. Evans HL, Burks E, Viswanatha D, Larson RS. Utility of immunohistochemistry in bone marrow evaluation of T-lineage large granular lymphocyte leukemia. *Hum. Pathol.* 2000;31:1266–1273.
119. Mailloux AW, Zhang L, Moscinski L, et al. Fibrosis and subsequent cytopenias are associated with basic fibroblast growth factor-deficient pluripotent mesenchymal stromal cells in large granular lymphocyte leukemia. *J. Immunol.* 2013;191:3578–93.
120. Loughran TP, Kidd PG, Starkebaum G. Treatment of large granular lymphocyte leukemia with oral low-dose methotrexate. *Blood*. 1994;84:2164-2170.
121. Moignet A, Hasanali Z, Zambello R, et al. Cyclophosphamide as a first-line therapy in LGL leukemia. *Leukemia*. 2014;28:1134-1136
122. Bareau B, Rey J, Hamidou M, et al. Analysis of a French cohort of patients with large granular lymphocyte leukemia: A report on 229 cases. *Haematologica*. 2010;95:1534-1541.
123. Sanikommu SR, Clemente MJ, Chomczynski P, et al. Clinical features and treatment outcomes in large granular lymphocytic leukemia (LGLL). *Leuk. Lymphoma*. 2018;59:416–422.
124. Qiu ZY, Fan L, Wang R, et al. Methotrexate therapy of T-cell large granular lymphocytic leukemia impact of STAT3 mutation. *Oncotarget*. 2016;7:61419–61425.

125. Loughran TP, Zickl L, Olson TL, et al. Immunosuppressive therapy of LGL leukemia: Prospective multicenter phase II study by the Eastern Cooperative Oncology Group (E5998). *Leukemia*. 2015;29:886-894.
126. Battiwalla M, Melenhorst J, Sauntharajah Y, et al. HLA-DR4 predicts haematological response to cyclosporine in T-large granular lymphocyte lymphoproliferative disorders. *Br. J. Haematol.* 2003;123:449-453.
127. Dumitriu B, Ito S, Feng X, et al. Alemtuzumab in T-cell large granular lymphocytic leukaemia: interim results from a single-arm, open-label, phase 2 study. *Lancet Haematol.* 2016;3:e22-9.
128. Ma SY, Au WY, Chim CS, et al. Fludarabine, mitoxantrone and dexamethasone in the treatment of indolent B- and T-cell lymphoid malignancies in Chinese patients. *Br. J. Haematol.* 2004;124:754-761.
129. Zaja F, Baldini L, Ferreri AJM, et al. Bendamustine salvage therapy for T cell neoplasms. *Ann. Hematol.* 2013;92:1249-1254.
130. Cornec D, Devauchelle-Pensec V, Jousse-Joulin S, et al. Long-term remission of T-cell large granular lymphocyte leukemia associated with rheumatoid arthritis after rituximab therapy. *Blood*. 2013;122:1583-1586.
131. Bilori B, Thota S, Clemente MJ, et al. Tofacitinib as a novel salvage therapy for refractory T-cell large granular lymphocytic leukemia. *Leukemia*. 2015;29:2427-2429.
132. Bustin S a. Absolute quantification of mrna using real-time reverse transcription polymerase chain reaction assays. *J. Mol. Endocrinol.* 2000;25:169–193.
133. Livak KJ, Schmittgen TD. Analysis of Relative Gene Expression Data Using Real- Time Quantitative PCR and the 2 delta-delta CT Method. *Methods*. 2001;408:402–408.
134. Yu H, Pardoll D, Jove R. STATs in cancer inflammation and immunity: A leading role for STAT3. *Nat. Rev. Cancer*. 2009;9:798–809.
135. Liu HS, Pan CE, Liu QG, Yang W, Liu XM. Effect of NF-κB and p38 MAPK in activated monocytes/macrophages on pro-inflammatory cytokines of rats with acute pancreatitis. *World J. Gastroenterol.* 2003;9:2513–2518.
136. Erkut N, Menteşe A, Özbaş HM, et al. The Prognostic Significance of Soluble Urokinase Plasminogen Activator Receptor in Acute Myeloid Leukemia. *Turkish J. Hematol.* 2016;33:135–140.
137. Damon SE, Maddison L, Ware JL, Plymate SR. Overexpression of an inhibitory insulin-like growth factor binding protein (IGFBP), IGFBP-4, delays onset of prostate tumor formation. *Endocrinology*. 1998;139:3456–3464.
138. Liao J, Feng W, Wang R, et al. Diverse in vivo effects of soluble and membrane-bound M-CSF on tumor-associated macrophages in lymphoma xenograft model. *Oncotarget*. 2016;7:1354–1366.
139. Hong C, Luckey MA, Ligons DL, et al. Activated T cells secrete an alternatively spliced form of γc that inhibits cytokine signaling and exacerbates inflammatory autoimmune disease. *Immunity*. 2014;40:910–923.
140. Peng X, Xiao Z, Zhang J, et al. IL-17A produced by both γδ T and Th17 cells promotes renal fibrosis via RANTES-mediated leukocyte infiltration after renal obstruction. *J. Pathol.* 2015;235:79–89.
141. Khokhlatchev A V, Canagarajah B, Wilsbacher J, et al. Phosphorylation of the MAP Kinase ERK2 Promotes Its Homodimerization and Nuclear Translocation complex factors and helix-loop-helix proteins. *Cell*. 1998;93:605–615.
142. Yang J, Liao X, Agarwal MK, et al. Unphosphorylated STAT3 accumulates in response to IL-6 and activates transcription by binding to NFκB. *Genes Dev.* 2007;21:1396–1408.
143. Casagrande N, Borghese C, Visser L, et al. CCR5 antagonism by maraviroc inhibits Hodgkin lymphoma microenvironment interactions and xenograft growth. *Hematologica.* 2019; 104:564-575.
144. Nguyen KD, Fohner A, Booker JD, et al. XCL1 Enhances Regulatory Activities of CD4+/CD25/CD127low/− T Cells in Human Allergic Asthma. *J. Immunol.*

2008;181:5386–5395.
145. Shive CL, Jiang W, Anthony DD, Lederman MM. Soluble CD14 is a nonspecific marker of monocyte activation. *AIDS*. 2015;29:1263–1265.